Alma Mater Studiorum – Università di Bologna

DOTTORATO DI RICERCA

In Automatica e Ricerca Operativa

Ciclo XXI

Settore scientifico disciplinare di afferenza: ING-INF/04

TITOLO TESI

Internal Model Principle:
extension to the switching case and applications

Presentata da: **Toniato Manuel**

Coordinatore Dottorato

Prof. Claudio Melchiorri

Relatore

Prof. Carlo Rossi

Esame finale anno 2009

Alma Mater Studiorum - University of Bologna

PhD School in Information Engineering
Doctorate in Control System Engineering
and Operational Research

Manuel Toniato

Internal Model Principle:
extension to the switching case and applications

PhD Thesis

A Luca e Silvia

Contents

Introduction

Advantages of Internal-model-based control

The Internal-model-based control (IMC) is one of the best techniques to control the output of a dynamical system so as to asymptotically track prescribed trajectories.

Since the birth of modern Control Theory, the problem of asymptotic tracking of predetermined references has been one of its central themes. In the last century many authors tackled this problem both for linear and nonlinear systems and three different main approaches have been explored: besides the above mentioned internal-model-based approach, also tracking by dynamic inversion and adaptive tracking have been considered.

The first and simpler solution that has been taken into account is the so-called *Dynamic Inversion*. Under a "perfect knowledge" of the plant and of the reference to be tracked, a suitable precise initial state x_0 and a suitable precise control input $u^*(t)$ are calculated: if the system is initialized to x_0 and driven by $u^*(t)$, its output exactly reproduces the reference signal. The requirement of perfect knowledge of both the plant and the reference makes this approach unsuitable for many real world applications.

Adaptive tracking still needs the perfect knowledge of the reference to be tracked but can achieve the asymptotic tracking even in presence of uncertainties on the plant by automatically tuning the parameters of a controller calculated via Dynamic Inversion.

Differently from Dynamic inversion and Adaptive tracking, the control schemes based on the *Internal Model Principle* can successfully achieve the asymptotic tracking in presence of uncertainties on both reference and plant. Instead of considering one single reference, the IMC takes into account the class of all the references that can be generated by a fixed dynamical system (usually referred to as *exogenous system* or *exosystem*). It has been demonstrated that, if the controller includes an Internal Model of the exosystem, it can ensure the asymptotic tracking of all the references of the class despite of the parameter uncertainties of the plant. This features make the IMC very appealing for many real world applications where the plant is not perfectly known, as for example Aircraft control, and/or where high precisions are required such the applications in high energy physics.

After its introduction in mid 70's for LTI plants and LTI exosystems ([DAVISON 1976], [FRANCIS 1975], [BASILE 1992]), the Internal Model Principle has proved to be an effective control approach also for more complex systems. In particular the case of nonlinear systems, which was first considered by Isidori and Byrnes ([ISIDORI 1990]), has been extensively studied in the last decade ([SERRANI 2001], [BYRNES 2005]) and its solution has been used in advanced control applications ([ISIDORI 2003], [MARCONI 2008]). More recently, many authors addressed the problem of extending the class of exosystems that can be considered for IMC, including, among the others, special classes of nonlinear systems ([BYRNES 2004]) and the linear periodic systems ([ZHANG 2006], [ZHANG 2009]). Following this path, the aim of this thesis is to extend the IMP to a special class of exosystems capable to generate periodic references having a infinite number of harmonics.

Internal Model Principle for references with an infinite number of harmonics

The asymptotic tracking of periodic references is one of the more common applications of Internal Model approach. If the spectrum of the reference comprehends only a finite number N of harmonics, a simple finite-dimensional LTI exosystem with N oscillators can be considered. However, many "real world" applications requires to track periodic references with an infinite number of harmonics such as triangular waves or more complicate references as in CNAO Storage Ring Dipole Magnet Power Converter $3000A\,/\,\pm 1600V$ ([CARROZZA 2006]) where the current reference is a set of ramps and constant references connected by 5th order polynomial curves. In this cases a finite-dimensional LTI exosystem allows to achieve only a practical regulation: an upper bound on the norm of tracking error can be guaranteed but not its convergence to zero and, above all, good performances can be reached only by taking into account a large number of oscillators (high order exosystems). If for some applications this could be an acceptable compromise, when high precisions are required as in many power electronics applications, different approaches have to be considered.

Since the Nonlinear Output Regulation has a well-established and powerful theoretical assessment, one Internal-model-based possibility for the asymptotic tracking of infinite-harmonics references is to consider *Nonlinear Internal Model Units*. The main difficulty of such approach is to find a structure for the internal model units which can generate the control inputs needed for tracking and, at the same time, is manageable for stabilization. This has usually required to adopt the so-called *immersion assumption*, which limits the applicability of the method to a restricted class of reference/disturbance signals. Recently, this constraint has been removed ([BYRNES 2005]) allowing to cope

with every infinite-harmonics or even more complex reference but the solution could be very involved even for simple cases and even considering practical regulation.

A second Internal-model-based solution for the asymptotic tracking of infinite-harmonics references is the *Repetitive Learning Control*, which is widespread in the world of automotive and power electronics ([HARA 1988], [CUIYAN 2004b]). This method exploits a closed-loop time-delay system with delay T as Internal Model Unit thus obtaining the asymptotic tracking of any T-periodic signal. A relevant drawback in the practical application of this approach is the large sensitivity to some non-T-periodic disturbances. As a matter of fact, owing to the constraint imposed by Bode's sensitivity integral (see for example [GOODWIN 2000, Ch. 9]), the null values ($-\infty$ dB) of the sensitivity at any frequency multiple of $f = \frac{1}{T}$ lead to very large sensitivity values at some other frequencies.

The sensitivity problem that afflicts the Repetitive Learning Control is actually one of the main critical issues shared by all the IMP-based methods. At steady state, an Internal-model-based control guarantees the perfect tracking of all the references of the class generated by the Internal model unit and the perfect rejection of all the external disturbances belonging to the same class. This fact reflects in a relevant sensitivity to disturbances not "captured" by the internal model, due to Bode's integral constraint on sensitivity. The phenomenon is particularly problematic in Repetitive Learning Control since its Internal Model Unit is capable to generate *all* the periodic reference of given period T but a similar behavior is expected also for more sophisticated methodologies as the above-mentioned ones. Potentially some adaptation mechanism could be added to deal with "strange" disturbances, but at the cost of a relevant complexity increasing.

The Switched Linear Internal Model control

Motivated by the fact that, in many practical applications (especially in high energy physics), the references to be tracked are sequences of curves which can be generated by different LTI systems, the basic idea underlying the novel control approach proposed in this thesis is to extend the Internal Model Principle to the case of free periodic switched exosystems. In this way, by restricting the class of infinite-harmonics references that is generated by the Internal Model Unit, the novel approach called *Swiched Linear Internal Model* (SLIM) is expected on one hand, to exhibit a considerably better sensitivity behaviour with respect to Repetitive Learning Control and, on the other hand, to be simpler to manage with respect to the control approach based on Nonlinear Internal Model units.

Differently form many classic works on Internal Model Principle, in this thesis great emphasis has been placed on the problem of the synthesis of a generator for a given reference. If for LTI systems the theory of realization is well-established and the no-

tions of realization and minimal realization have been extensively studied and related with the structural properties of the system (observability, controllability), in the world of switched linear systems many different structures for the generator of the same reference can be considered. The choice of the exosystem structure definitely affects the design of the Internal-model-based control and, in particular, of the stabilization unit.

The problem of the stabilization of the Switched Linear Internal Model controller has been the other important issue that has been tackled in this thesis. The exoststem structure that has been considered intrinsically exhibits observability properties that change at switching times. Since in standard results on Internal-model-based control, the observability (or at least the detectability) of the exosystem is one of the basic requirements for the solution of the Output Regulation problem, the fact of considering periodic systems that, inside a period, switch from observable phases to possibly undetectable phases represented a considerable hurdle in the path towards a general design pattern of the stabilization unit. For this reason the problem of stabilization has not been directly addressed but it has been tackled step by step by first considering the problem of the *asymptotic observer* for the exosystem and then by trying to extend the obtained results to the general case.

Outline of the thesis

This thesis, which gathers the work carried out by the author in the last three years of research, is subdivided in two main parts.

The first part (chapters 1-5) contains the main topics about the Switched Linear Internal Model control.

In chapter 1 the class of exosystems that has been considered for the SLIM approach is described. In particular the problem of synthesizing a free switched linear generator for a given periodic reference is addressed. A parallel solution is presented and the problem of the minimal solution is briefly discussed. Since a parallel solution can always be found independently from the reference, it is adopted as the model for the class of exosystems considered for the SLIM approach.

As a preliminary stabilization result, the problem of asymptotic observer for the chosen exosystem models is presented in chapter 2. The structure of the asymptotic observer for switched systems is recalled and two different sufficient conditions for asymptotic convergence are provided. The feasibility of both condition is analyzed and, while the unfeasibility of the first condition is demonstrated, a design procedure for an asymptotically convergent observer is derived from the second condition.

An interesting extension of the results of chapter 2 is presented in chapter 3 where the asymptotic observer structure is revised and updated in order to achieve convergence in

finite time. Taking inspiration form the recent results on finite time observers that employ two asymptotic observer to obtain the exact estimation in finite time, the design procedure for a single switched impulsive finite-time observer is presented. As a subsidiary result, a non-impulsive alternative is shown.

The stabilization results presented in chapter 2 are exploited in two different control schemes presented in chapter 4. The first control schemes that is considered is a mixed feedforward-feedback control scheme in which the estimation produced by an asymptotic observer of exosystem state is used to generate a reference for the plant state that guarantees the asymptotic tracking. Recalling the comparison between Dynamic Inversion tracking and Internal Model control, this scheme can be considered halfway between the two control approaches since it is robust with respect to uncertainties on the reference, it does not need the exact knowledge of the initial state of the plant but, on the other hand, it needs a perfect knowledge of plant parameters. Within the problem of state trajectory generation, the extension of the regulator equations to the switching case is considered and the problem of convergence of Differential Sylvester Equation is briefly discussed. The problems of robustness that characterize the first control scheme are partially overcome in the second that is actually a preliminary version of the SLIM control. The controller is represented by an asymptotic observer of exosystem state and the stabilization is achieved only for simple plants that are "sufficiently fast" with respect to the reference by means of singular perturbations-like arguments.

The last chapter of the first part presents a preliminary analysis on the sensitivity of SLIM control. A comparison between the performances of a Repetitive Learning Control and that of the SLIM control presented in chapter 4 is carried out on a simple case study by using simulations. Being the SLIM control a time-varying system, a special sensitivity function based on the infinity-norm and representing a worst-case estimation is defined.

In the second part two applications of the internal model control coming from the world of high energy physics are presented.

In chapter 6 the control of the power supply of a booster quadrupole for a Synchrotron Light Source is considered. Since the current reference to be tracked is a sinusoid bounded within $2A$ and $200A$ and the precision to be guaranteed is very high ($\pm 10ppm$), a classic Internal-model-based control with LTI exosystem has proved to be a very effective solution. Besides the high precision requirement, a second issue has been taken into account in the control, that is, a Power Factor as much close to the unit as possible and low distortion of mains current. This control objective has been fulfilled by means of a cascade control structure that regulates both the voltage on the DC-Link and the Booster current. Simulations results concludes the chapter.

The application presented in chapter 7 is not actually based on the Internal Model Principle, however it has been included in this thesis for it is the application that inspired

the Switched Linear Internal model control. In order to accomplish the cycle that drives the particles to the required energy, the power supply of CNAO dipole has to track a set of complex references which are sequences of constant and ramps connected by fifth order polynomial curves with a precision of 5ppm with respect to the full scale. The controller structure that has been chosen to fulfill these requirements is a three-level cascade structure, each level consisting in a traditional LTI controller. The main problem of this control structure is that the tracking error drastically increase when the reference switches from constants to ramps and back by means of polynomial curves. The reduction of this phenomenon has been the primary motivation of the development of Switching Internal Model Control. Simulations of the current control structure end the chapter.

In the last chapter of thesis, the obtained results are summarized and the guidelines for future developments are reported.

Finally some basic results on switched systems that are useful to better understand the results of this thesis, in particular those regarding the Switched Linear internal model control, are presented in Appendix A.

The topics of this thesis have been presented in [ROSSI 2008a], [ROSSI 2008b], [ROSSI 2009b], [ROSSI 2009a], [**?**] and [CARROZZA 2006].

Part I

The Switched Linear Internal Model approach

Chapter 1

Structure of the exosystem

In this chapter the formal definition of the class of periodic signals considered for the SLIM approach is presented. Some possible structures for a free switched linear system capable to generate a given signal of the class are explored.

THE structure of an Internal Model Controller heavily depends on the class of references that has to be tracked and the exosystem adopted to model them. The reference signals considered for the Switched Linear Internal Model control are smooth periodic signals that are piecewise outputs of LTI systems. Except for trivial cases where the reference is the output of a single LTI system, the main characteristic of these signals is that their spectrum contains an infinite number of harmonics.

Many different structures for dynamical systems capable to generate these trajectories may be considered as, for instance, special nonlinear systems or systems that involve a memory unit recording the trajectory within a period (as in *Repetitive Learning Control*). Being the reference piecewise defined, the more natural choice is to consider a *switched linear system*. As a matter of fact, the switched linear system is not required to be periodic to generate periodic references. Anyway, since a periodic switched linear system is generally simpler to stabilize and to implement on a controller, in the following only periodic switched linear systems having the same period T of the reference to be synthesized will be considered as generators.

A final consideration has to be done: without additional conditions, in general, a periodic switched system does not generate periodic trajectories. Therefore, besides satisfying the periodicity condition on the system matrices, some additional boundary condition have to be considered.

The chapter is organized as follows. In section 1.1 the synthesis problem is formulated and discussed. In section 1.2 a solution is proposed and in section 1.3 some considerations on minimization of the generating system are presented. The chapter ends with

section 1.4 where the class of signals which can be generated with the proposed solutions is considered; particular attention is paid to the effects of the initial conditions of the generating systems.

1.1 The problem formulation

Let $y_d(t) : \mathbb{R}_0^+ \to \mathbb{R}$ be a T–periodic function defined over the positive time axis (i.e. $y_d(t_0) = y_d(t_0 + T)$, $\forall t_0 \in \mathbb{R}_0^+$), with the following properties.

- *Smoothness*: the r-th derivative $\dfrac{d^r y_d(t)}{dt^r}$ is continuous or at least piecewise continuous for $t \geqslant 0$;

- *LTI-Sys Concatenation*: $y_d(t)$ is piecewise output of different LTI systems or equivalently:

$$y_d(t) = \begin{cases} y_{d1}(t) & t_0 = 0 \leqslant t < t_1 \\ y_{d2}(t) & t_1 \leqslant t < t_2 \\ \vdots & \\ y_{dN}(t) & t_{N-1} \leqslant t < t_N = T \end{cases} \tag{1.1}$$

$$y_{di}(t) = \sum_{k=0}^{m_i} A_{ik} t^{a_{ik}} e^{b_{ik} t} \sin\left(\omega_{ik} t + \varphi_{ik}\right)$$

The problem to be solved is to find N matrix pairs

$$(S_1, q_1), (S_2, q_2), \ldots, (S_N, q_N),$$

a T-periodic piecewise constant function $\sigma(t)$

$$\sigma(t) : \mathbb{R}_0^+ \to \{1, 2, \ldots, N\}, \qquad \sigma(t + T) = \sigma(t),$$

and a vector w_0, such that:

$$\Sigma : \begin{cases} \dot{w}(t) = S_{\sigma(t)} w(t) & w(0) = w_0 \\ y_d(t) = q_{\sigma(t)} w(t) \end{cases} \tag{1.2}$$

Remark According to (1.2), the class of possible system generating y_d is restricted to linear systems with switching parameters and *continuous state solution*. A more general model that may be considered includes *impulsive actions* (*jumps* on the state) occurring at

switching instants (*impulsive switched linear system*).

$$\Sigma : \begin{cases} \dot{w}(t) = S_{\sigma(t)} w(t) & \text{if } \sigma(t_j^-) = \sigma(t_j) \\ w(t_j) = E_{\sigma(t_j)} w(t_j^-) & \text{if } \sigma(t_j^-) \neq \sigma(t_j) \\ y_d(t) = q_{\sigma(t)} w(t) \end{cases} \tag{1.3}$$

The non-impulsive solution has been preferred because, as it was stated in section A.2.2, the results on stability of impulsive systems tend to be more conservative and few results on stabilization of these systems are available.

Remark In order to guarantee that $y_d(t)$ is periodic, the state trajectory has to be periodic too. Therefore, the system has to perform during every period a sort of "reset" to guarantee that $w(t_0) = w(t_0 + T)$. This could be done adding additional boundary conditions on matrices S_is or, in the case of *impulsive switched system*, by an instantaneous reset of the state performed at the switching on instant.

In the following a quite straightforward solution based on a parallel structure is presented, proving the solubility of the synthesis problem. Afterwards, a different solution with reduced system order is briefly discussed.

1.2 Parallel synthesis

The main idea of the "parallel synthesis" is to use N parallel-connected subsystems, each one representing a linear piece according to (1.1). By changing the dynamical matrix of the overall system, each subsystem is "turned on", during suitable time-intervals, "rewound" and "frozen" during the rest of time, while it is not observable.

As a matter of fact, for each of $y_{d1}(t)$,..., $y_{dN}(t)$, defined according to (1.1), an observable realization (Ω_i, Θ_i) of dimension $n_i \geqslant m_i$, suitably initialized with state w_{0i}, can be found in order to obtain:

$$\Sigma_i : \begin{cases} \dot{w}_i(t) = \Omega_i w_i(t) & w_i(t_{i-1}) = w_{0i} \\ y_{di}(t) = \Theta_i w_i(t) & \forall t \in [t_{i-1}, t_i[\end{cases} \tag{1.4}$$

Hence a solution for the problem defined in section 1.1, can be obtained by a suitable parallel connection of the N subsystems Σ_i as reported in the following.

The matrix pairs (S_i, q_i) have the form:

$$
\begin{aligned}
S_1 &= \begin{bmatrix} \Omega_1 & 0 & \dots & 0 \\ 0 & 0 & \dots & 0 \\ \vdots & \vdots & \ddots & \vdots \\ 0 & 0 & \dots & -\alpha_N \Omega_N \end{bmatrix} \\
q_1 &= \begin{bmatrix} \Theta_i & 0 & \dots & 0 & 0 & 0 & \dots & 0 \end{bmatrix} \\
S_i &= \begin{bmatrix} 0 & \dots & \dots & \dots & \dots & \dots & \dots & 0 \\ \vdots & \ddots & \dots & \dots & \dots & \dots & \dots & \vdots \\ \vdots & \dots & 0 & 0 & 0 & 0 & \dots & \vdots \\ \vdots & \dots & 0 & -\alpha_{i-1}\Omega_{i-1} & 0 & 0 & \dots & \vdots \\ \vdots & \dots & 0 & 0 & \Omega_i & 0 & \dots & \vdots \\ \vdots & \dots & 0 & 0 & 0 & 0 & \dots & \vdots \\ \vdots & \dots & \dots & \dots & \dots & \dots & \ddots & \vdots \\ 0 & \dots & \dots & \dots & \dots & \dots & \dots & 0 \end{bmatrix} \\
q_i &= \begin{bmatrix} 0 & \dots & 0 & 0 & \Theta_i & 0 & \dots & 0 \end{bmatrix} \quad i = 2 \dots N.
\end{aligned}
\tag{1.5}
$$

where the α_i are coefficients for time normalization and are defined as:

$$\alpha_i = \frac{t_i - t_{i-1}}{t_{i+1} - t_i} = \frac{\tau_i}{\tau_{i+1}} \tag{1.6}$$

($\tau_i = t_i - t_{i-1}$ is the duration of the time interval in which the i-th subsystem is "turned on ").

The switching function $\sigma(t)$ has the simple form:

$$\sigma(t) = j \qquad \text{for } t_{j-1} \leqslant t < t_j \tag{1.7}$$

The initial condition w_0 is defined as follows:

$$w(0) = w_0 = \begin{bmatrix} w_{01} \\ w_{02} \\ \vdots \\ w_{0N-1} \\ w_{fN} \end{bmatrix} \tag{1.8}$$

where w_{0i}, $i = 1 \dots N$ denote the initial conditions of the subsystems Σ_i according to (1.4) and w_{fi} the corresponding "*final conditions*", i.e. $w_{fi} = e^{\Omega_i (t_i - t_{i-1})} w_{0i}$.

For any time instant $t \geqslant 0$, each subsystem Σ_i can be in one and only one of the

following "states" depending on the particular time interval the actual time t belongs to:

- *turned on* ($t \in \left[t_{i-1} + kT, t_i + kT\right[$): the evolution of the subsystem state $w_i(t)$ is determined by dynamical matrix Ω_i; the system is connected to the output by matrix Θ_i; $w_i(t)$ is the only observable part of the overall state $w(t)$ from the output $y_d(t)$.

- *rewinding* ($t \in \left[t_i + kT, t_{i+1} + kT\right[$): the subsystem Σ_i is not connected to the output and its state is then unobservable; Σ_i is "rewinding" the state trajectory $w_i(t)$ from the state reached at $t_i + kT$ (w_{fi}) to its initial state ($w_i(t_{i-1} + kT)$) by adopting a dynamic matrix $-\alpha_i\Omega_i$;

- *turned off* ($t \in \left[t_{i+1} + kT, t_{i-1} + (k+1)T\right[$): the subsystem Σ_i is not connected to the output and its state is "frozen" at the state $w_i(t_{i+1} + kT)$

For the sake of clarity, in Figure 1.1 the state evolution of a case with $N = 4$ is depicted. The orders of subsystems Σ_1, Σ_2, Σ_3 and Σ_4 are equal to 3, 2, 3 and 3 respectively.

1.3 Minimal synthesis

The solution presented in previous section is characterized by a very large system dimension ($\sum n_i$, with n_i defined just before (1.4)). Hence the main purpose of this part is to present some considerations toward minimization of the system generating y_d.
Clearly, the dimension of a system Σ solving the problem stated in section 1.1 cannot be lower than $\max n_i$. In the following, the realization of a system generating y_d and having dimension $\max n_i$ is considered.

Starting from the N subsystems Σ_i, defined in (1.4) for the parallel solution, it is always possible to homogenize the order of each subsystem to $\max n_i$ by extending the matrices Ω_i and vectors Θ_i and w_{0i} without modifying the output behavior, that is by adding unobservable dynamics to the system. This operation can be simply done, for instance, by appending zeros to the above mentioned matrices and vectors. Hence, denoting with $\bar{\Omega}_i$, $\bar{\Theta}_i$ and $\bar{w}_{0i}$ the "extended elements" and introducing N non-singular matrices T_i with dimension $\max n_i$, it can be easily proved that

$$\begin{aligned} S_i &= T_i\bar{\Omega}_i T_i^{-1},\ q_i = \bar{\Theta}_i T_i^{-1},\ i = 1 \dots N \\ \sigma(t) &= j \quad \text{for } t_{j-1} \leqslant t < t_j \\ w(0) &= T_1\bar{w}_{01} \end{aligned} \tag{1.9}$$

is a solution with dimension $\max n_i$ for the problem defined in section 1.1 if and only if

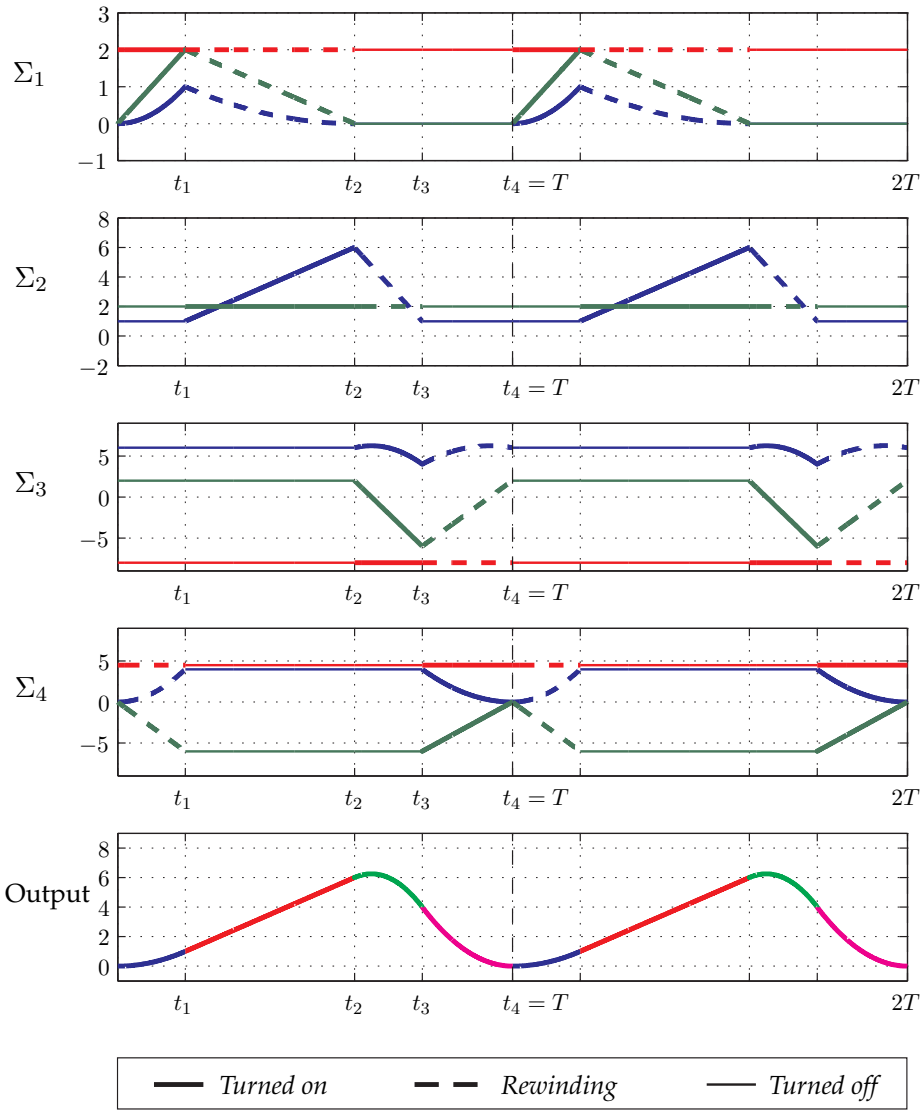

Figure 1.1: Parallel solution. The resulting system has order 11 and is made up of 4 subsystems.

the following condition is satisfied

$$\begin{cases} T_1 w_1(t_1^-) = T_2 w_2(t_1^+) \\ T_2 w_2(t_2^-) = T_3 w_3(t_2^+) \\ \vdots \\ T_N w_N(t_N^-) = T_1 w_1(t_0^+) \end{cases} . \tag{1.10}$$

The general idea underlying the proposed minimal solution is to substitute the parallelization of system Σ_i of (1.4) with a "true" commutation, but preserving continuity of the state evolution by means of suitable coordinate transformations (if possible). Condition (1.10) represents this requirement.
From a operative viewpoint, solving the equation (1.10) with respect to T_i under the constraint of non-singularity, will give a direct way to build a minimal solution from a given parallel one.

Remark There could be parallel solutions for which the linear system (1.10) is unsolvable, i.e. a minimal solution with the proposed structure need not to exist. On the other hand, it is worth noting that solvability of (1.10) could depend also on the way the elements Ω_i, Θ_i, w_{0i} are extended to $\bar{\Omega}_i$, $\bar{\Theta}_i$, $\bar{w}_{0i}$.

In figure 1.2 two generators for the same reference, one obtained with parallel solution and one with minimal solution, are compared. The reference is made up of two concatenated parabolic arcs. As a consequence there are $N = 2$ subsystems Σ_i, both of order $n_1 = n_2 = 3$. The parallel solution, which is depicted in 1.2(a), results of order $n_1 + n_2 = 6$ whilst the minimal solution is of order 3.

1.4 Class of output signals generated by the proposed systems

After considering the synthesis problem for an assigned y_d, it is quite natural wondering what class of functions can be generated with the proposed systems structures by simply varying the initial condition.
Clearly, for the parallel solution of section 1.2 the initial condition is crucial to guarantee the smoothness of the solution. It is easy to prove that, using a generic initial state, the generated output is T–periodic, complies the *LTI–Sys Concatenation* condition, but, in general, does not satisfy the *Smoothness* property. An important class of references that satisfies the smoothness property is that generated by systems initialized at $w(0) = kw_0, k \in \mathbb{R}$.

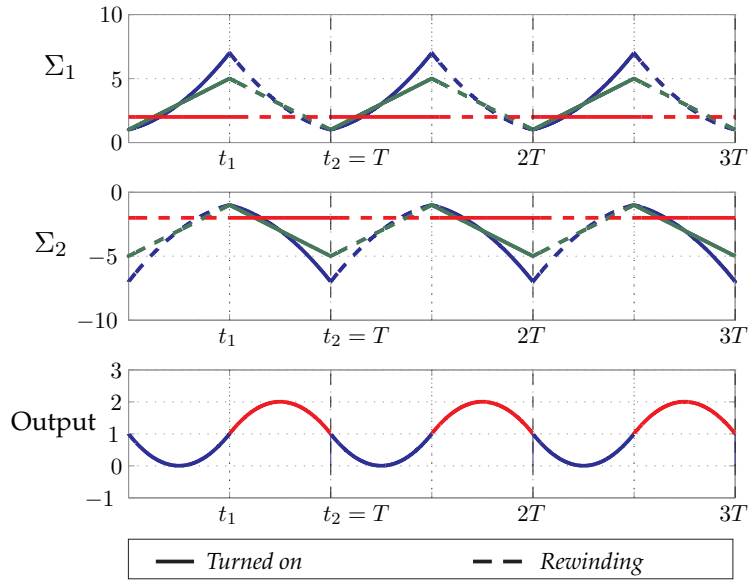

(a) Parallel Solution

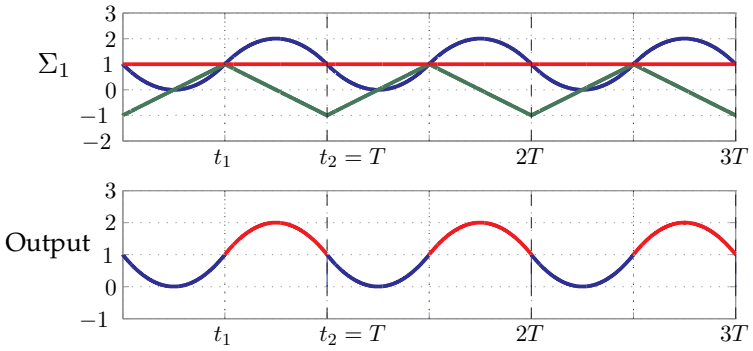

(b) Minimal Solution

Figure 1.2: Comparison of parallel and minimal solution when the reference is made up of two concatenated arcs of parabola.

Differently, for the minimal solution proposed in section 1.3, setting a generic initial state, also T–periodicity property is not guaranteed, beside the *Smoothness* property violation. A T–periodic behavior can be imposed for every $w(0)$ if the following additional condition on the non-singular matrices $T_1, \ldots, T_N$ is satisfied:

$$e^{(t_{N-1}-t_{N-2})T_N^{-1}\Omega_N T_N} \cdot e^{(t_{N-1}-t_{N-2})T_{N-1}^{-1}\Omega_{N-1}T_{N-1}} \cdot \ldots \cdot e^{(t_2-t_1)T_2^{-1}\Omega_2 T_2} e^{(t_1-t_0)T_1^{-1}\Omega_1 T_1} = I \tag{1.11}$$

This condition comes directly from composition of the evolutions of the different LTI systems.

A final consideration on the trajectories that can be generated by the proposed exosys-

tem structures is required by the *Internal Model Principle*. Let consider a plant P having a well-defined relative degree r_P: are the structures that has been examinated (parallel or minimal) capable to generate the input $u(t)$ that guarantees the exact tracking on P of reference $y_d(t)$? In other words could similar structures satisfy the Internal Model Principle and, consequently, could them be used as Internal Model Units? If the plant to be controlled is LTI and if the well known *reproducibility constraint* is satisfied, i.e. the r_P-th derivative of y_d is at least piecewise continuous, the answer is affirmative for both the structures. This fact directly follows from the Internal Model Principle for LTI systems applied to the single subsystems Σ_i.

Chapter 2

Asymptotic observer

As a preliminary step towards a general theory of the stabilization of the SLIM approach, the problem of the asymptotic observer for the parallel structure presented in chapter 1 is considered. In this chapter the structure of the asymptotic observer is explored and two different sufficient conditions for the asymptotic convergence are examined.

A controller structure based on the Internal Model Principle may be subdivided in two main components. The Internal Model Unit capable to generate the signal that guarantee the exact tracking and a Stabilization unit that stabilize this trajectory depending on the plant that has to be controlled. In chapter 1 two possible models for the exosystems have been explored and, in the last consideration, it has been shown how both these structures can be used as Internal Model Unit when the plant to be controlled is LTI. Despite the minimal solution would be preferable for is reduced dimension and for its observability properties, the fact that, for a given reference, a parallel solution is always available tips the scale in favour of this solution.

If on one hand the choice of parallel solution simplifies the synthesis of the Internal Model Unit, on the other the problem of stabilization complicates due to the inherent partial observability of parallel solution. For this reason, as a preliminary step towards a general stabilization procedure, the problem of designing an asymptotic observer for an exosystem that exhibits the parallel structure of equations (1.5) has been considered. The existing results on switched observer ([CHENG 2005]) has been extended by removing the hypothesis that all the subsystems are observable or at least detectable.

The chapter is organized as follows. In section 2.1 the structure of the proposed observer for parallel solution is reported and the related design problem is formulated. In Section 2.2 a first condition based on the ideas of Ezzine and Haddad (see proposition 1.3 is examined. Although this condition can be applied to general periodic switched linear system, the particular symmetric structure of the exosystem adopted in SLIM ap-

proach (journey there and back) makes it unfeasible. A second condition that revises the first condition by introducing some results coming from [CHENG 2005] is enunciated and demonstrated in section 2.3. The results of simulations on the example of figure 1.1 are reported in section 2.4.

2.1 Structure of the asymptotic observer

The observer considered to estimate the state of the parallel structure is inspired by the classic Luenberger observers for linear switched systems (see A.3).

$$\dot{\hat{w}}(t) = S_{\sigma(t)}\hat{w}(t) + G_{\sigma(t)}(y_d - q_{\sigma(t)}\hat{w}) \qquad \hat{w}(0) = \hat{w}_0 \tag{2.1}$$

The structure of the observer matrices $G_1, \ldots, G_N$ is similar to the structure of the output matrices $q_1, \ldots, q_N$ and is presented in equation (2.2).

$$G_i = \begin{pmatrix} 0 & \ldots & 0 & \Gamma_i^T & 0 & \ldots & 0 \end{pmatrix}^T \tag{2.2}$$

The parallel structure of the exosystem is thus extended to the observer and the problem of the stabilization of estimate $\hat{w}(t)$ reduces to the stabilization of the N estimates $\hat{w}_i(t)$ of the states $w_i(t)$. The evolution of each estimation error $\tilde{w}_i(t) = w_i(t) - \hat{w}_i(t)$ is described by the following equation.

$$\begin{cases} \dot{\tilde{w}}_i(t) = (\Omega_i + \Gamma_i\Theta_i)\tilde{w}(t) & \text{for } t_{i-1} + kT \leqslant t < t_i + kT \\ \dot{\tilde{w}}_i(t) = -\alpha_i\Omega_i\tilde{w}(t) & \text{for } t_i + kT \leqslant t < t_{i+1} + kT \\ \dot{\tilde{w}}_i(t) = 0 & \text{otherwise} \end{cases} \tag{2.3}$$

The problem of the stabilization of the estimates $\hat{w}_i(t)$ can be further simplified by normalizing the time-intervals and by omitting the time intervals in which the system is frozen.

Proposition 2.1 *Let the symbol τ_i denote the difference $t_i - t_{i-1}$. The asymptotic observer design problem, related to the structure of eq.* (A.15)*, is equivalent to find N matrices Γ_i such that the N periodic systems of equation* (2.4) *are asymptotically stable ($k \in \mathbb{N}$).*

$$\begin{cases} \dot{\tilde{w}}_i(t) = (\Omega_i + \Gamma_i\Theta_i)\tilde{w}_i(t) & \textit{for } 2k\tau_i \leqslant t < (2k+1)\tau_i \\ \dot{\tilde{w}}_i(t) = -\Omega_i\tilde{w}_i(t) & \textit{for } (2k+1)\tau_i \leqslant t < (2k+2)\tau_i \end{cases} \tag{2.4}$$

This asymptotic observer design problem is not a straightforward extension of the classic observer problem for LTI systems. The main issue to be tackled is that in the "rewind phase" every subsystem Σ_i is not observable and, if the dynamics to be observed

is unstable, the subsystem turns out to be *not detectable*. Therefore it is not sufficient to simply require that for every i the matrix $\Omega_i+\Gamma_i\Theta_i$ is Hurwitz to guarantee the asymptotic stability of the observer. A more restrictive condition is required and will be the object of investigations and results reported in the next two sections.

The asymptotic observer problem for the SLIM approach in the form of Proposition 2.1 can be partitioned in two distinct problems: first of all, to find a condition that the matrices Γ_i have to satisfy in order to guarantee the asymptotic stability and then to define an algorithm to find the matrices Γ_i satisfying the condition.

2.2 First sufficient condition

The first sufficient condition for the asymptotic stability employs the result on stability of periodically switched systems of proposition 1.3 and, in particular, the Coppel Inequality (see proposition 1.10). It has been presented in [ROSSI 2008a] and extensively studied in [ROSSI 2009b].

2.2.1 Statement and proof

Proposition 2.2 (*first stability condition*) *A matrix Γ_i guarantees the asymptotic stability of the observer* (2.4) *if:*

$$\mu_2\left(\Omega_i + \Gamma_i\Theta_i\right) + \mu_2\left(-\Omega_i\right) < 0 \tag{2.5}$$

where the symbol $\mu_2(A)$ represents the measure of the real matrix A w.r.t. euclidean norm, i.e.

$$\mu_2(A) = \lim_{\theta\to 0}\frac{\|I-\theta A\|_2 - 1}{\theta} = \frac{1}{2}\Big(\lambda_{max}\left\{A + A^T\right\}\Big)$$

.

Proof By applying the proposition 1.10 to a general linear system $\dot{x}(t) = Ax(t)$, the following relation is obtained $\forall t \geqslant t_0$:

$$\|x(t)\| \leqslant e^{\mu_2(A)(t-t_0)}\,\|x(t_0)\| \tag{2.6}$$

Applying the bound of equation 2.6 to the evolution of the i-th estimation error $\tilde{w}_i(t) = w_i(t) - \hat{w}_i(t)$, it follows that:

$$\|\tilde{w}_i(t_0+T)\| \leqslant m_{2i}m_{1i}\,\|\tilde{w}_i(t_0)\| \tag{2.7}$$

where the scalars m_{1i} and m_{2i} are defined as:

$$m_{1i} = e^{\mu_2(\Omega_i+\Gamma_i\Theta_i)(t_i-t_{i-1})}$$
$$m_{2i} = e^{\alpha_i\mu_2(-\Omega_i)(t_{i+1}-t_i)} = e^{\mu_2(-\Omega_i)(t_i-t_{i-1})}$$

If the matrix Γ_i is chosen such that $\mu_2\left(\Omega_i + \Gamma_i\Theta_i\right) + \mu_2\left(-\Omega_i\right) < 0$ it follows that:

$$\|\tilde{w}_i(t_0 + T)\| < \|\tilde{w}_i(t_0)\|$$

then proposition 1.2 holds and the periodic switched system (2.4) is *uniformly asymptotically stable*. □

2.2.2 Unfeasibility of the first condition

The condition of Proposition 2.2 can be rewritten as a *linear matrix inequality* by exploiting the following basic results of the matrix theory.

1. Let $\lambda\{A\} = \{\lambda_1, \lambda_2, \ldots, \lambda_n\}$ be the spectrum of a matrix $A \in \mathbb{R}^{n\times n}$. The spectrum of the matrix $A + \gamma I$, $\gamma \in \mathbb{R}$ is $\lambda\{A + \gamma I_n\} = \{\lambda_1 + \gamma, \lambda_2 + \gamma, \ldots, \lambda_n + \gamma\}$ and, consequently, it holds that

$$\lambda_{max}\{A\} + \gamma = \lambda_{max}\{A + \gamma I_n\}.$$

2. A symmetric matrix A is negative-definite if and only if $\lambda_{max}\{A\} < 0$.

Therefore, the condition of the first sufficient condition becomes:

$$\Omega_i + \Omega_i^T - \lambda_{min}\left\{\Omega_i + \Omega_i^T\right\} I_n + \Gamma_i\Theta_i + \Theta_i^T\Gamma_i^T < 0 \tag{2.8}$$

The symmetric matrix $\Omega_i+\Omega_i^T-\lambda_{min}\left\{\Omega_i + \Omega_i^T\right\} I_n$ proves to be positive-semidefinite. Therefore the condition of Proposition 2.2 can be satisfied only if the matrix $\Gamma_i\Theta_i + \Theta_i^T\Gamma_i^T$ is negative-definite. The negative definiteness of matrix $\Gamma_i\Theta_i - \Theta_i^T\Gamma_i^T$ can be tested by applying the *Sylvester criterion* for positive definiteness to the matrix $-\Gamma_i\Theta_i - \Theta_i^T\Gamma_i^T$. In order to analyze more easily the minors of that matrix, let introduce the auxiliary matrices M_{ij} defined as

$$M_{ij} = (e_j\Theta_i) + (e_j\Theta_i)^T \tag{2.9}$$

where e_j is the j-th element of the canonical base of $\mathbb{R}^n$. The matrix $\Gamma_i\Theta_i + \Theta_i^T\Gamma_i^T$ can be written as

$$\Gamma_i\Theta_i + \Theta_i^T\Gamma_i^T = \gamma_{i1}M_{i1} + \gamma_{i2}M_{i2} + \ldots + \gamma_{in}M_{in} \tag{2.10}$$

where γ_{ij} are the elements of Γ_i.

The first principal minor of $-\Gamma_i\Theta_i - \Theta_i^T\Gamma_i^T$ is $-2\gamma_{i1}\theta_{i1}$ that is positive iff $\text{sign}(\gamma_{i1}) \neq \text{sign}(\theta_{i1})$.
The second principal minor is

$$\begin{aligned}
&\begin{vmatrix} -2\gamma_{i1}\theta_{i1} & -\gamma_{i1}\theta_{i2} - \gamma_{i2}\theta_{i1} \\ -\gamma_{i1}\theta_{i2} - \gamma_{i2}\theta_{i1} & -2\gamma_{i2}\theta_{i2} \end{vmatrix} = \\
&\quad = 4\gamma_{i1}\gamma_{i2}\theta_{i1}\theta_{i2} - \gamma_{i1}^2\theta_{i2}^2 - 2\gamma_{i1}\gamma_{i2}\theta_{i1}\theta_{i2} - \gamma_{i2}^2\theta_{i1}^2 = \\
&\quad = -(\gamma_{i1}^2\theta_{i2}^2 - 2\gamma_{i1}\gamma_{i2}\theta_{i1}\theta_{i2} + \gamma_{i2}^2\theta_{i1}^2)
\end{aligned} \tag{2.11}$$

The result is a *quadratic form*:

$$\begin{pmatrix} \gamma_i & \gamma_2 \end{pmatrix} \begin{pmatrix} -\theta_2^2 & \theta_i\theta_2 \\ \theta_i\theta_2 & -\theta_i^2 \end{pmatrix} \begin{pmatrix} \gamma_i \\ \gamma_2 \end{pmatrix}$$

The characteristic polynomial $P(\xi)$ of the quadratic form is

$$(\xi + \theta_2^2)(\xi + \theta_i^2) - \theta_i^2\theta_2^2 = \xi\Big(\xi + (\theta_i^2 + \theta_2^2)\Big)$$

The eigenvalues are $\xi = 0$ and $\xi = -(\theta_i^2 + \theta_2^2) \leqslant 0$. The second principal minor cannot be strictly positive for any Θ_i and any Γ_i. Consequently, the matrix $-(\Gamma_i\Theta_i + \Theta_i^T\Gamma_i^T)$ cannot be positive definite and it is not possible to find a matrix Γ_i that satisfies the condition of proposition 2.2.

2.3 Second sufficient condition

One of the reasons for which the first sufficient condition is unfeasible is that the bound given by the Coppel Inequality is used both for observable and unobservable phase and results too conservative for the observable phase. Considering that, in that phase, the matrix $\Omega_i + \Gamma_i\Theta_i$ can be made Hurwitz and diagonalizable, the bound of proposition A.12 can be used instead (see for example [BALLUCHI 2002] or [CHEN 2004]).

2.3.1 Statement and proof

Proposition 2.3 (*second stability condition*) *A matrix Γ_i guarantees the asymptotic stability of the observer* (2.4) *if for $i = 1, \ldots, N$ it holds that:*

$$\kappa(T_{Ji})e^{\left(\beta_i^- + \mu_2(-\Omega_i)\right)\tau_i} < 1 \tag{2.12}$$

where T_{Ji} is the matrix of generalized eigenvectors of matrix $\Omega_i + \Gamma_i\Theta_i$ and $\beta_i^- = \max_j \left(\text{Re}\left(\lambda_j\left\{\Omega_i + \Gamma_i\Theta_i\right\}\right)\right)$

Proof The estimation error $\tilde{w}_i\left((2n+2)\tau_i\right)$ can be written as a function $\tilde{w}_i\left((2n)\tau_i\right)$ as:

$$\tilde{w}_i\left((2n+2)\tau_i\right) = e^{\Omega_i\tau_i}e^{(\Omega_i+\Gamma_i\Theta_i)\tau_i}\tilde{w}_i\left(2n\tau_i\right) \tag{2.13}$$

Considering the norms and applying the Coppel Inequality and the bound of proposition A.12, it follows that:

$$\begin{aligned}\left\|\tilde{w}_i\left((2n+2)\tau_i\right)\right\| &= \left\|e^{-\Omega_i\tau_i}e^{(\Omega_i+\Gamma_i\Theta_i)\tau_i}\tilde{w}_i\left(2n\tau_i\right)\right\| \leqslant \\ &\leqslant e^{\mu_2(-\Omega_i)\tau_i}\left\|e^{(\Omega_i+\Gamma_i\Theta_i)\tau_i}\tilde{w}_i\left(2n\tau_i\right)\right\| \leqslant \\ &\leqslant e^{\mu_2(-\Omega_i)\tau_i}\left\|e^{(\Omega_i+\Gamma_i\Theta_i)\tau_i}\right\| \cdot \left\|\tilde{w}_i\left(2n\tau_i\right)\right\| \leqslant \\ &\leqslant \kappa(T_{Ji})e^{\mu_2(-\Omega_i)\tau_i}e^{\beta_i^-\tau_i}\left\|\tilde{w}_i\left(2n\tau_i\right)\right\|\end{aligned} \tag{2.14}$$

If $\kappa(T_{Ji})e^{\left(\beta_i^- + \mu_2(-\Omega_i)\right)\tau_i} < 1$, the condition of proposition 1.2 is satisfied and the system of equation (2.4) is asymptotically stable.

□

Remark In [BALLUCHI 2002] and [CHEN 2004] the asymptotic stability of the observer is proved by exploiting the bound of proposition A.12 for all the subsystems. In the case of SLIM exosystems a "mixed condition" has to be used since in the rewind phase the subsystem is unobservable and, possibly, not detectable.

2.3.2 Feasibility of the second condition

In order to prove the feasibility of the second condition, an algorithm to build a set of Γ_i satisfying the condition will be provided. The key point of the algorithm is the fact that the coefficient $\kappa(T_{Ji})$ is (at least asymptotically) a polynomial function of β_i^- as it is stated in proposition 1.11.

The algorithm presented in the following will use a proof based on a different path. The alternative proof is based on the estimation of condition numbers given by Guggenheimer et al. ([GUGGENHEIMER 1995]) and on a theorem by Fahmy and O'Reilly about the eigenstructure of a linear feedback system ([FAHMY 1982]).

Lemma 2.4 *Given a non singular square matrix T_J, the following relation on condition number $\kappa(T_J)$ holds:*

$$\kappa(T_J) < \frac{2}{|\det(T_J)|}\left(\frac{\sum\sum t_{ij}}{n}\right)^{\frac{n}{2}} \tag{2.15}$$

Lemma 2.5 *Consider an observable matrix pair (Ω, Θ) and an observer matrix Γ. Let $S_0 = \{\lambda_{01}, \lambda_{02}, \ldots, \lambda_{0n}\}$ be the spectrum of Ω and $S = \{\lambda_1, \lambda_2, \ldots, \lambda_n\}$ be the spectrum of $(\Omega + \Gamma\Theta)$.*

Let T_J and T_J^{-1} such that

$$T_J^{-1}(\Omega + \Gamma\Theta)T_J = \begin{pmatrix} \lambda_1 & 0 & \dots & 0 \\ 0 & \lambda_2 & \dots & 0 \\ \dots & \dots & \dots & \dots \\ 0 & 0 & \dots & \lambda_n \end{pmatrix} \tag{2.16}$$

If Γ is chosen such that $S \cap S_0 = \varnothing$, the matrix T_J^{-1} has the following form

$$T_J^{-1} = \begin{pmatrix} \Theta\left(\lambda_1 I - \Omega\right)^{-1} \\ \Theta\left(\lambda_2 I - \Omega\right)^{-1} \\ \dots \\ \Theta\left(\lambda_n I - \Omega\right)^{-1} \end{pmatrix} \tag{2.17}$$

Algorithm 2.6 *The algorithm for finding the set of Γ_i is made up of the following steps that have to be executed for all $i = 1, \dots, N$:*

1. *Consider $n-1$* distinct *positive numbers $\{\alpha_1, \alpha_2, \dots, \alpha_{n-1}\}$ with $\alpha_j > 1$.*
2. *Set $\beta_i^- = -\beta_i^+$*
3. *Choose Γ_i such that the spectrum of $\Omega_i + \Gamma_i\Theta_i$ is $\left\{\beta_i^-, \alpha_1\beta_i^-, \alpha_2\beta_i^-, \dots, \alpha_{n-1}\beta_i^-\right\}$.*
4. *Test if sufficient condition (2.12) is verified. If it is verified return Γ_i; if not, set $\beta_i^- = 2\beta_i^-$.*

Proposition 2.7 *For any given observable pair (Ω_i, Θ_i) the Algorithm 2.6 will always return a matrix Γ_i that satisfies the condition (2.12) of Proposition 2.3.*

Proof Exploiting the results of Lemma 2.4, the following bound on the condition of proposition 2.3 can be stated.

$$\begin{aligned} &\kappa(T_{Ji})e^{\left(\beta_i^- + \beta_i^+\right)\tau_i} < \\ &< \frac{2}{|\det(T_{Ji}^{-1})|}\left(\frac{\operatorname{tr}\left(\left(T_{Ji}^{-1}\right)^T T_{Ji}^{-1}\right)}{n}\right)^{\frac{n_i}{2}} \cdot e^{\left(\beta_i^- + \beta_i^+\right)\tau_i} \end{aligned} \tag{2.18}$$

where

$$\beta_i^+ = \mu_2(-\Omega_i)$$

The parameters τ_i, β_i^+ and n_i are fixed. Consider the expression for T_{Ji}^{-1} of Lemma 2.5 and the spectrum of $\Omega_i + \Gamma_i\Theta_i$ obtained at step 3. It follows that T_{Ji}^{-1} is a *proper rational matrix* in the real variable β_i^-. All the entries of T_{Ji}^{-1} are proper rational functions $\frac{n(\beta_i^-)}{d(\beta_i^-)}$ and the poles of each entry are a subset of the spectrum of the original matrix Ω_i.

Therefore $|\det(T_{Ji}^{-1})|$ and $\operatorname{tr}\left(\left(T_{Ji}^{-1}\right)^T T_{Ji}^{-1}\right)$ are proper rational functions too and $\kappa(T_{Ji}) = O\left(\left(\beta_i^-\right)^{\frac{n_i^2}{2}}\right)$. From standard analytical results it follows that

$$\lim_{\beta_i^- \to -\infty} \kappa\left(T_{Ji}(\beta_i^-)\right) e^{\left(\beta_i^- + \beta_i^+\right)\tau_i} = 0 \tag{2.19}$$

and consequently there will exists a sufficiently negative $\bar{\beta}_i^-$ to guarantee that the coefficient of Proposition 2.3 is less than one. Since the set $\mathbb{R}$ is an Archimedean Field, the algorithm will always return a suitable Γ_i. □

Remark At a first glance, this result could appear equivalent to the results on the stability of switched systems with stable and unstable subsystems (see for example [ZHAI 2000]). In these papers the stability of the overall system is obtained by extending the activation time of the stable phase. Actually, the considered case is different since the switching instants are fixed. The only available degree of freedom is the observer pole placement (in the "turned on" phase), and differently from the case of free switching intervals it has a side effect on the coefficients $\kappa(T_{Ji})$, hence further considerations on the eigenstructure are needed, as reported in Proposition 2.7.

From the above results it is straightforward to derive a procedure to select Γ_i for a given instance of the observer design problem. Selecting the eigenvalues of $\Omega_i + \Gamma_i\Theta_i$ according to the proof of Proposition 2.7, the value β_i^- can be rendered more and more negative until the condition (2.12) is verified (Proposition 2.7 guarantees that this procedure ends with a finite β_i^-).

2.4 Simulations

The second sufficient condition has been applied to the case study depicted in figure 1.1 that has been used in chapter 1 to present the parallel solution.

The parameters of the case study are presented in the following:

- the matrices $\Omega_1, \ldots, \Omega_4$ and $\Theta_1, \ldots, \Theta_4$:

$$\begin{aligned} \Omega_1 = \Omega_3 = \Omega_4 &= \begin{pmatrix} 0 & 1 & 0 \\ 0 & 0 & 1 \\ 0 & 0 & 0 \end{pmatrix} \qquad \Omega_2 = \begin{pmatrix} 0 & 1 \\ 0 & 0 \end{pmatrix} \\ \Theta_1 = \Theta_3 = \Theta_4 &= \begin{pmatrix} 1 & 0 & 0 \end{pmatrix} \qquad \Theta_2 = \begin{pmatrix} 1 & 0 \end{pmatrix} \end{aligned} \tag{2.20}$$

- initialization of the exosystem:

$$\begin{aligned} w_{01} &= \begin{pmatrix} 0 & 0 & 2 \end{pmatrix}^T & w_{02} &= \begin{pmatrix} 1 & 2 \end{pmatrix}^T \\ w_{03} &= \begin{pmatrix} 6 & 2 & -8 \end{pmatrix}^T & w_{04} &= \begin{pmatrix} 0 & 0 & 4.5 \end{pmatrix}^T \end{aligned} \tag{2.21}$$

- the switching instants t_i:

$$t_1 = 1s \qquad t_2 = 3.5s \qquad t_3 = 4.5s \qquad t_4 = 5.83s \tag{2.22}$$

- the exponents β_i^+, calculated from Ω_i:

$$\beta_1^+ = \beta_3^+ = \beta_4^+ = \sqrt{2} \qquad \beta_2^+ = 0 \tag{2.23}$$

- the initialization of the observer substates $\hat{w}_i$

$$\hat{w}_{01} = \hat{w}_{02} = \hat{w}_{03} = \hat{w}_{04} = 0 \tag{2.24}$$

Choosing $\alpha_1 = 2, \alpha_2 = 3$, the following observer matrices guarantees that the second sufficient condition is satisfied for $i = 1, \ldots, 4$.

$$\begin{aligned} \Gamma_1 = \Gamma_3 &= \begin{pmatrix} -60 & -1100 & -6000 \end{pmatrix}^T & \beta_1^- &= \beta_3^- - 10 \\ \Gamma_2 &= \begin{pmatrix} -6 & -8 \end{pmatrix}^T & \beta_2^- &= -2 \\ \Gamma_4 &= \begin{pmatrix} -42 & -539 & -2058 \end{pmatrix}^T & \beta_4^- &= -7 \end{aligned} \tag{2.25}$$

In fact the coefficients of the second sufficient condition turn out to be:

$$\begin{aligned} \kappa(T_{J1})e^{\beta_1^- + \beta_1^+} = \kappa(T_{J3})e^{\beta_3^- + \beta_3^+} &= 0.50 < 1 \\ \kappa(T_{J2})e^{\beta_2^- + \beta_2^+} &= 0.75 < 1 \\ \kappa(T_{J4})e^{\beta_4^- + \beta_4^+} &= 0.77 < 1 \end{aligned} \tag{2.26}$$

The resulting evolution of the estimation errors $\tilde{w}_i$ is depicted in figure 2.1. The system turns out to be very fast and after two periods the estimation error is negligible.

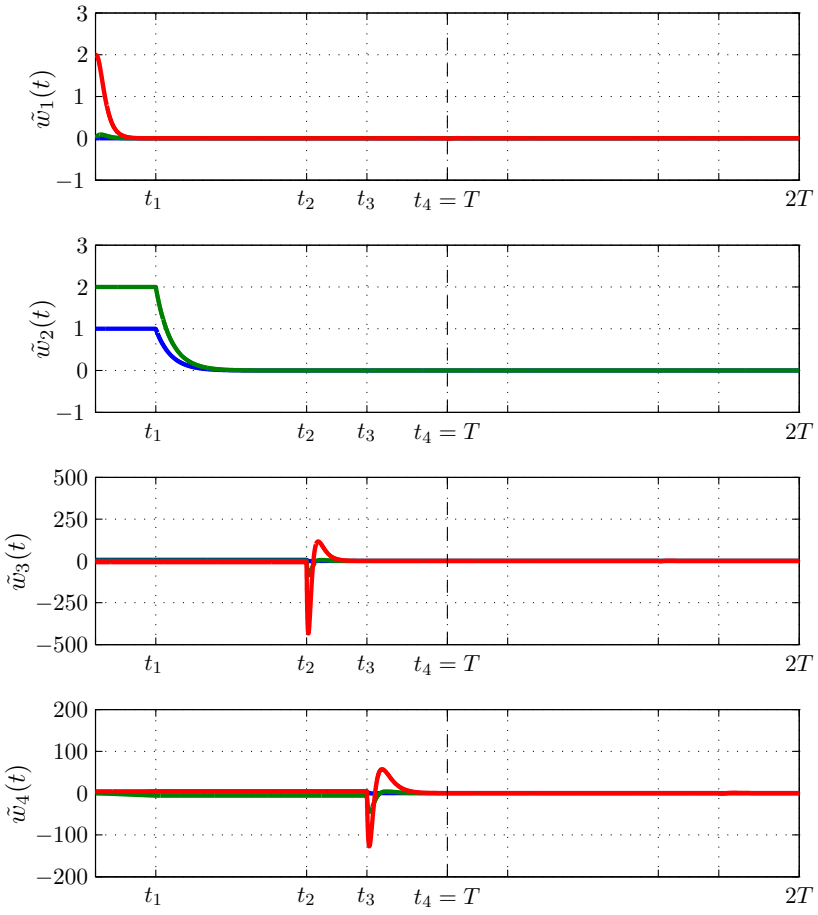

Figure 2.1: Evolution of the four estimation errors $\tilde{w}_i(t)$

Chapter 3

Finite-time Observer

Recently a novel approach to design finite state observers has been proposed. This approach, which in its original formulation involves two different observers working at the same time and an impulsive action, can be successfully applied to the SLIM exosystem by using a single switching observer.

Most observer design techniques for continuous-time systems and, among them, all the results about observers for switched systems that are cited in section A.3 share a common property, namely, the system state is estimated in an asymptotic fashion. However, from the work of James ([JAMES 1991]) onwards, many approaches have been proposed to achieve the exact state estimation in predetermined time both for linear and nonlinear (continuous-time) systems. The principal techniques involve probabilistic-variational methods ([JAMES 1991]), sliding mode observers ([DRAKUNOV 1995], [HASKARA 1998]), moving horizon observers ([MICHALSKA 1995], [ZIMMER 1994]). In recent years a novel method that involves two different asymptotic observers working at the same time has been elaborated ([ENGEL 2002], [MENOLD 2003], [RAFF 2007a]). The exact estimation of initial state is achieved in finite time by means of an impulsive action that is calculated from the outputs of the two asymptotic observers.

In this chapter it is shown how the "double-observer" technique can profitably be applied to the the case of switched exosystems of the SLIM approach and how the finite time exact estimation can be obtained by using a *single* switched linear impulsive observer. The organization of the chapter is similar to that of chapter 2. In section 3.1 the structure of the impulsive observer is derived from the structure of the asymptotic observer. The conditions for finite time convergence are enunciated and proved in 3.2. An non-impulsive alternative is explained in section 3.3 and some ideas on its possible use for the estimation of unknown inputs are presented. Simulations on both observer schemes (impulsive and non-impulsive) are illustrated in section 3.4.

3.1 Structure of the impulsive observer

In order to obtain the finite time state estimation for the exosystem of chapter 1 by using the "Double Observer" technique, the observer have to provide an impulsive action at predetermined time instants. The structure of the impulsive observer is derived from the structure of the asymptotic observer that has been presented in chapter 2 (see equations 2.1 and 2.2).

Following the conceptual line of [RAFF 2007a], the structure of the impulsive observer, which is depicted in equation (3.1), is obtained from equation (2.1) by adding a second equation that regulates the update of the state at the switching times beginning from the second period.

$$\begin{cases} \dot{\hat{w}}(t) = S_{\sigma(t)}\hat{w}(t) - G_{\sigma(t)}(y_d - q_{\sigma(t)}\hat{w}) & \text{for } t \neq t_{i-1} + (k+1)T \\ \hat{w}(t^+) = \hat{w}(t) + F_{\sigma(t)}(\hat{w}(\cdot), t) & \text{for } t = t_{i-1} + (k+1)T \\ \hat{w}(t_0^+) = \hat{w}_0 & i = 1, \ldots, N, k \in \mathbb{Z}^+ \end{cases} \tag{3.1}$$

The correction terms $F_1(\hat{w}(\cdot), t)$,...,$F_N(\hat{w}(\cdot), t)$, are matrices with the following structure

$$F_i = \begin{pmatrix} 0 & \ldots & \ldots & \ldots & \ldots & \ldots & 0 \\ \vdots & \ddots & \ldots & \ldots & \ldots & \ldots & \vdots \\ \vdots & \ldots & 0 & 0 & 0 & \ldots & \vdots \\ \vdots & \ldots & 0 & f_i^T(\hat{w}(\cdot), t) & 0 & \ldots & \vdots \\ \vdots & \ldots & 0 & 0 & 0 & \ldots & \vdots \\ \vdots & \ldots & \ldots & \ldots & \ldots & \ddots & \vdots \\ 0 & \ldots & \ldots & \ldots & \ldots & \ldots & \ldots \quad 0 \end{pmatrix} \tag{3.2}$$

From the structure imposed to the correction terms, it results that in the time instants $t_{i-1} + kT$ the matrix F_i leaves unchanged all the states $\hat{w}_j, j \neq i$: only the state $\hat{w}_i$ is updated. The relations describing f_i as functions of $\hat{w}(\cdot)$ and t are not specified, they have to be suitably designed in order to obtain finite-time convergence.

Due to its parallel structure, the design of observer (3.1) reduces to the design of the N observers $\hat{w}_i(t)$ of the states $w_i(t)$ described in equation (3.3).

$$\begin{cases} \dot{\hat{w}}_i(t) = \Omega_i \hat{w}(t) - \Gamma_i \Theta_i (w_i(t) - \hat{w}(t)) & \text{for } t \in (t_{i-1} + kT, t_i + kT) \\ \dot{\hat{w}}_i(t) = -\alpha_i \Omega_i \hat{w}(t) & \text{for } t \in [t_i + kT, t_{i+1} + kT) \\ \dot{\hat{w}}_i(t) = 0 & \text{for } t \in [t_{i+1} + kT, t_{i-1} + (k+1)T) \\ \hat{w}_i(t^+) = \hat{w}_i(t) + f_i(\hat{w}(\cdot), t) & \text{for } t = t_{i-1} + (k+1)T \\ \hat{w}_i(t_{i-1}^+) = \hat{w}_{i0} & i = 1, \dots, N, \quad k \in \mathbb{Z}^+ \end{cases} \tag{3.3}$$

Hence the problem of designing a Finite Time Observer for system (1.5) has been translated in the search of N matrices Γ_i and N correction terms $f_i(\hat{w}(\cdot))$. In the next section a sufficient condition on these items that guarantees the finite time convergence is provided.

3.2 Condition for Finite Time Convergence

Consider the evolution of the i-th estimate error $\tilde{w}_i = w_i(t) - \hat{w}_i(t)$ in the interval $[t_{i-1}, t_{i-1} + T)$ which is described by equation (3.4).

$$\begin{cases} \dot{\tilde{w}}_i(t) = (\Omega_i + \Gamma_i \Theta_i) \tilde{w}(t) & \text{for } t \in (t_{i-1}, t_i) \\ \dot{\tilde{w}}_i(t) = -\alpha_i \Omega_i \tilde{w}(t) & \text{for } t \in [t_i, t_{i+1}) \\ \dot{\tilde{w}}_i(t) = 0 & \text{for } t \in [t_{i+1}, t_{i-1} + T) \\ \tilde{w}_i(t_{i-1}^+) = \tilde{w}_{i0} & i = 1, \dots, N \end{cases} \tag{3.4}$$

Being (3.4) a free linear system, the estimation error $\tilde{w}_i(t)$ at time $t_{i+1} + T$ can be calculated from $\tilde{w}_i(t_{i-1})$ as:

$$\tilde{w}_i(t_{i-1} + T) = \Phi_i(t_{i-1}, t_{i-1} + T) \tilde{w}_i(t_{i-1}) \tag{3.5}$$

where $\Phi_i(t_{i-1}, t_{i-1} + T)$ is the *transition matrix* from t_{i-i} to $t_{i-1} + T$

$$\begin{aligned} \Phi_i(t_{i-1}, t_{i-1} + T) &= e^{-\alpha_i \Omega_i \tau_{i+1}} e^{(\Omega_i + \Gamma_i \Theta_i)\tau_i} = \\ &= e^{-\Omega_i \tau_i} e^{(\Omega_i + \Gamma_i \Theta_i)\tau_i} \end{aligned} \tag{3.6}$$

In order to simplify the notation, in the following the matrix $\Phi_i(t_{i-1}, t_{i-1} + T)$ will be denoted as Φ_i.

Proposition 3.1 *Suppose that, for $i = 1, \dots N$, the matrix Γ_i is such that the matrix $(I - \Phi_i)$ is* non-singular. *Then, define the correction terms f_i, of equation* (3.2) *as:*

$$f_i(\hat{w}(\cdot), t) = \kappa_i(\hat{w}(t^-) - \hat{w}((t - T)^+)) \text{ with } \kappa_i = \Phi_i (I - \Phi_i)^{-1}$$

Under these hypotheses the observer (3.1) *estimates the exact state of system* (1.5) *in predetermined finite time* $t_{N-1} + T$.

Proof Consider the difference $\hat{w}_i(t_{i-1} + T) - \hat{w}_i(t_{i-1})$. From the periodicity of the exosystem state $w_i(t)$ it follows that (omitting $^+$, $^-$ for the sake of readability):

$$\begin{aligned}
&\hat{w}_i(t_{i-1} + T) - \hat{w}_i(t_{i-1}) = \\
&\quad = \hat{w}_i(t_{i-1} + T) - w_i(t_{i-1} + T) + w_i(t_{i-1} + T) - \hat{w}_i(t_{i-1}) = \\
&\quad = \hat{w}_i(t_{i-1} + T) - w_i(t_{i-1} + T) + w_i(t_{i-1}) - \hat{w}_i(t_{i-1}) = \\
&\quad = -\tilde{w}_i(t_{i-1} + T) + \tilde{w}_i(t_{i-1})
\end{aligned} \tag{3.7}$$

Combining equations (3.7) and (3.5) the estimation error at time $t_{i-1} + T$ may be calculated from the difference $\hat{w}_i(t_{i-1} + T) - \hat{w}_i(t_{i-1})$.

$$\tilde{w}_i(t_{i-1} + T) = -\Phi_i(I - \Phi_i)^{-1}(\hat{w}_i(t_{i-1} + T) - \hat{w}_i(t_{i-1})) \tag{3.8}$$

The exosystem state $w_i(t)$ at time $t_{i-1} + T$ result to be

$$w_i(t_{i-1} + T) = \hat{w}_i(t_{i-1} + T) + \Phi_i(I - \Phi_i)^{-1}(\hat{w}_i(t_{i-1} + T) - \hat{w}_i(t_{i-1})) \tag{3.9}$$

By choosing $\kappa_i = \Phi_i(I-\Phi_i)^{-1}$, the impulsive action at time t_i+T exactly resets $\hat{w}_i(t)$ to $w_i(t)$. The last reset to be performed is the reset of the N-th subsystem which happens at time $t_{N-1} + T$. After that, the estimate $\hat{w}(t)$ produced by observer (3.1) will track exactly the state $w(t)$. All the subsequent resets happening at time instants $t_i + kT, k = 2, 3, \ldots$ will not have any effect since for $t \geqslant t_{N-1} + T$ it holds that $\hat{w}(t) - w(t) = 0$. □

Remark Except for the condition about the invertibility of $(I - \Phi_i)$, there are no other requirements on matrices Γ_i. In particular it is not required that the matrices $\Omega_i + \Gamma_i$ are Hurwitz.

Remark In [ENGEL 2002] a simple sufficient condition to find matrices Γ_i such that the matrices $(I - \Phi_i)$ are non-singular is provided.

3.3 An non-impulsive alternative for finite time convergence

Once that the estimation error has been exactly identified (according to the result of Section 3.2), $\tilde{w}_i(t_{i-1}+T) = \kappa_i(\hat{w}(t_{i-1}+T)-\hat{w}(t_{i-1})))$, the employment of an impulsive action is not the only choice to obtain the estimation convergence in finite time. For example the

exact state estimation can be reached by adding suitable inputs $u_i(t)$ to the asymptotic observer.

$$\begin{cases} \dot{\hat{w}}_i(t) = \Omega_i \hat{w}(t) - \Gamma_i \Theta_i (w_i(t) - \hat{w}(t)) + u_i(t) & \text{for } t \in (t_{i-1} + kT, t_i + kT) \\ \dot{\hat{w}}_i(t) = -\alpha_i \Omega_i \hat{w}(t) & \text{for } t \in [t_i + kT, t_{i+1} + kT) \\ \hat{w}_i(t_{i-1}^+) = \hat{w}_{i0} & i = 1, \dots, N, \quad k \in \mathbb{Z}^+ \end{cases} \tag{3.10}$$

A suitable $u_i(t)$ is for instance a signal that is constant and not zero only in the interval $[t_{i-1} + T, t_i + T]$, with

$$u_i(t) = \begin{cases} \Psi_i \tilde{w}_i(t_{i-1} + T) & \text{for } t \in [t_{i-1} + T, t_i + T] \\ 0 & \text{otherwise} \end{cases} \tag{3.11}$$

where Ψ_i is:

$$\Psi_i = \left(\int_{t_{i-1}+T}^{t_i+T} e^{(\Omega_i + \Gamma_i \Theta_i)(t_i + T - \tau)} d\tau \right)^{-1} e^{(\Omega_i + \Gamma_i \Theta_i)(t_i - t_{i-1})}$$

With this input, the exact estimation for the i-th state $w_i(t)$ is smoothly reached at time $t_i + T$ and, consequently, the overall estimation error becomes identically 0 for $t \geqslant t_N + T$. This simple variation of the solution proposed in Section 3.1 could be interesting to obtain smooth trajectories of the observer states.

Remark It is worth noting that both the impulsive solution of Section 3.1 and the non-impulsive one presented in this Section look suitable for being extended in order to cope with model uncertainties or unknown inputs exploiting the nominal finite-time convergence to realize a sort of adaptive model predictive observer.

3.4 Simulations

The estimation technique presented in sections 3.1 and 3.2 has been applied to the same exosystem of the simulations of the asymptotic observer (see chapter 2).

The initialization of the observer substates $\hat{w}_i(t)$ have been performed by randomly generating all the components in the interval $[-10, 10]$.

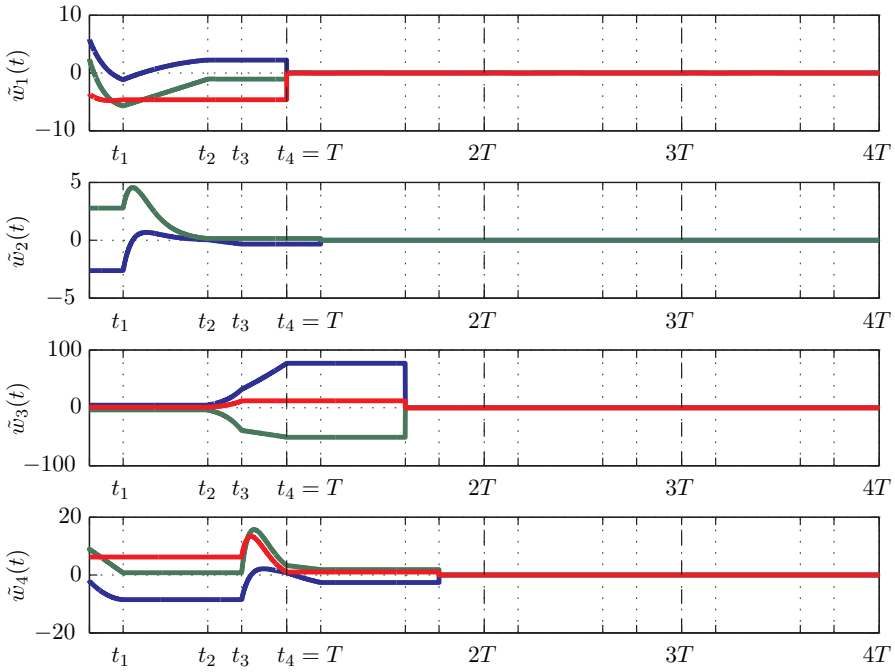

Figure 3.1: Impulsive observer. Evolution of the estimation errors $\tilde{w}_i(t)$ of the four subsystems

$$\begin{aligned}
\hat{w}_{01} &= \begin{pmatrix} -5.89 & -2.40 & 5.67 \end{pmatrix}^T \\
\hat{w}_{02} &= \begin{pmatrix} 3.62 & -0.78 \end{pmatrix}^T \\
\hat{w}_{03} &= \begin{pmatrix} 1.36 & 5.88 & -8.82 \end{pmatrix}^T \\
\hat{w}_{04} &= \begin{pmatrix} 2.06 & -8.99 & -1.69 \end{pmatrix}^T
\end{aligned} \tag{3.12}$$

The matrices Γ_i have been designed by taking into account only the conditions of proposition 3.1. In particular the matrix $(\Omega_3 + \Gamma_3\Theta_3)$ results to be non Hurwitz.

$$\begin{aligned}
\Gamma_1 &= \begin{pmatrix} 3 & 2.75 & 0 \end{pmatrix}^T & \Gamma_2 &= \begin{pmatrix} 5 & 6 \end{pmatrix}^T \\
\Gamma_3 &= \begin{pmatrix} -3 & 2.75 & -0.75 \end{pmatrix}^T & \Gamma_4 &= \begin{pmatrix} 6 & 11.75 & 7.5 \end{pmatrix}^T
\end{aligned} \tag{3.13}$$

The resulting evolution of the estimation errors $\tilde{w}_i(t)$ is depicted in figure 3.1. As stated in proposition 3.1, after $t = t_3 + T$ all the estimations $\hat{w}_i(t)$ exactly converge to $w_i(t)$ and the estimation error becomes 0. In figure 3.2 the estimation errors $\tilde{w}_i(t)$ of an

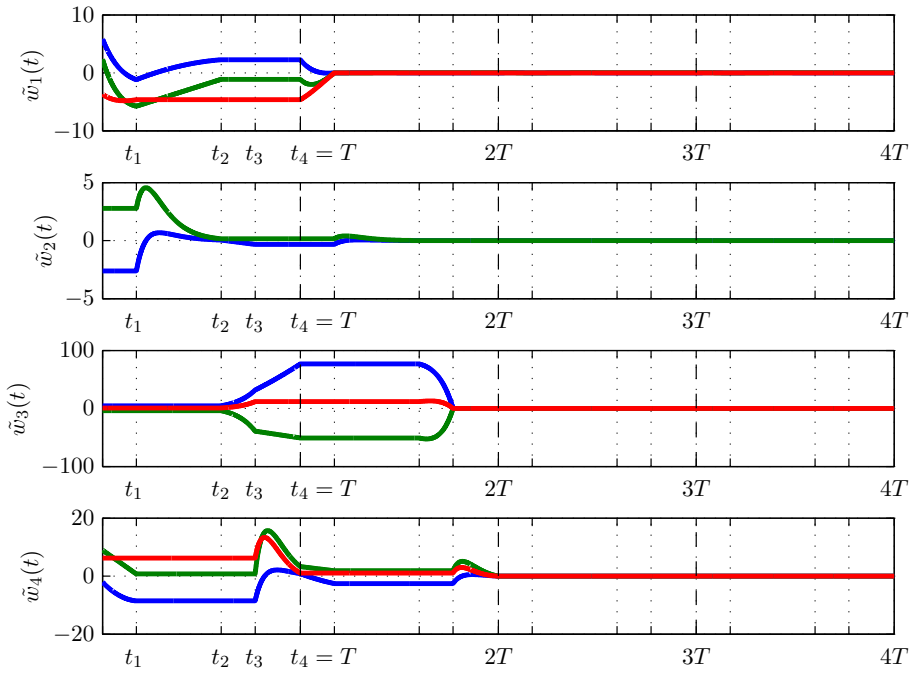

Figure 3.2: Non-impulsive observer. Evolution of the estimation errors $\tilde{w}_i(t)$ of the four subsystems

observer having the structure described in equation (3.10) is presented. The additional control input $u(t)$ has been defined as in equation (3.11).

Chapter 4

Control schemes for asymptotic tracking

This chapter illustrates two control schemes that achieve the asymptotic tracking of periodic references: a control scheme in which the observers that are described in previous chapters can successfully be used and a preliminary scheme based on the Internal Model Principle. The two schemes are compared and some preliminary results on the stabilization of the Internal Model based control are presented.

4.1 First control scheme: state trajectory generator

The first control scheme that is analyzed has been proposed by S. Devasia, B. Paden and C. Rossi in [DEVASIA 1997]. The main topic of their paper is how to generate a state trajectory x_d that guarantees the exact output tracking of a reference y_d on non-minimum phase switched linear plants. After providing the conditions for the solution of the synthesis problem, they consider on the same class of plants the problem of the asymptotic tracking of a reference y_d generated by a switched linear exosystem with unknown initial state. The solution of the asymptotic tracking problem involves the control scheme depicted in figure 4.1. This scheme has been considered as a first solution to the problem of the asymptotic tracking of references generated by exosystems having the parallel structure described in section 1.2.

4.1.1 Controller Structure

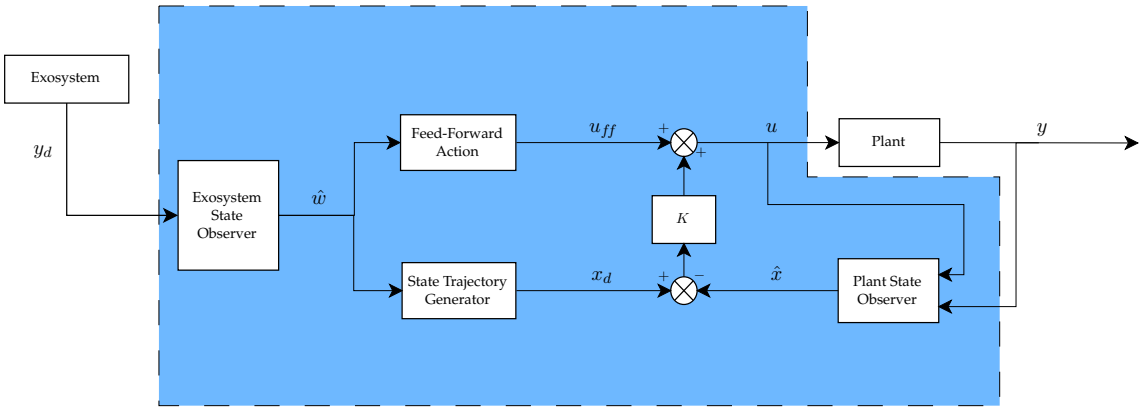

Figure 4.1: Control scheme for asymptotic tracking by Devasia, Paden, Rossi

The main components of the control scheme are:

1. an *observer* of the state of the exosystem;

2. a *state trajectory generator* that, taking as an input the estimation of the state of the exosystem, produces the trajectory that the state of the plant has to follow to ensure exact tracking;

3. a *linear feedback stabilizer* that makes the plant state to converge to the reference state trajectory.

In order to understand how this structure has been obtained and how each component is related with the others, it is profitable to first consider the problem of exact tracking of y_d on a generic LTI plant.

Denoting with r the relative degree of the plant, consider the plant (A, B, C) in *Brunovsky canonical form*:

$$\begin{cases} \dot{\xi}_1 = \xi_2 \\ \quad \dots \\ \dot{\xi}_{r-1} = \xi_r \\ \dot{\xi}_r = a_\xi \xi + b_\eta \eta + b_u u \\ \dot{\eta} = A_\eta \eta + B_\xi \xi \\ y = \xi_1 \end{cases} \tag{4.1}$$

where the $\eta \in \mathbb{R}^{n-r}$ represents the *zero dynamics* of the system. Suppose that the reference

to be tracked $y_d(t)$ is the output of the switched linear exosystems described in chapter 1:

$$\begin{cases} \dot{w}(t) = S_{\sigma(t)} w(t) & w(0) = w_0 \\ y_d(t) = q_{\sigma(t)} w(t) & \sigma(t) \in \{1, 2, \dots, N\} \end{cases} \tag{4.2}$$

In order to obtain the perfect tracking, i.e. impose that $y \equiv y_d$, $\forall t \geqslant t_0$, it is sufficient that the following conditions are satisfied:

i. initial conditions on ξ

$$\xi(t_0) = \mathcal{Q}_{\sigma(t_0)} w(t_0); \tag{4.3}$$

where

$$\mathcal{Q}_{\sigma(t)} = \begin{pmatrix} q_{\sigma(t)} \\ q_{\sigma(t)} S_{\sigma(t)} \\ q_{\sigma(t)} {S_{\sigma(t)}}^2 \\ \dots \\ q_{\sigma(t)} {S_{\sigma(t)}}^{r-1} \end{pmatrix}$$

ii. suitable control input $u(t)$

$$\begin{aligned} u(t) &= b_u^{-1} \Big(y_d^{(r)} - a_\xi \xi(t) - b_\eta \eta(t) \Big) = \\ &= b_u^{-1} \Big(q_{\sigma(t)} {S_{\sigma(t)}}^r w(t) - a_\xi \mathcal{Q}_{\sigma(t)} w(t) - b_\eta \eta(t) \Big) \end{aligned} \tag{4.4}$$

where $\eta(t)$ satisfies the following differential equation

$$\dot{\eta} = A_\eta \eta + B_\xi \xi \qquad \eta(t_0) = \eta_0$$

Since the state of the exosystem $w(t)$ is usually not available and the state of the plant $x = (\xi, \eta)^T$ cannot be arbitrarily assigned, the state $w(t)$ is replaced by its estimation $\hat{w}(t)$ and the condition on the initial states is asymptotically achieved by means of a state feedback control. The control input (4.4) is thus replaced by control input (4.5):

$$\begin{aligned} u(t) &= \underbrace{b_u^{-1} \Big(q_{\sigma(t)} {S_{\sigma(t)}}^r \hat{w}(t) - a_\xi \mathcal{Q}_{\sigma(t)} \hat{w}(t) - b_\eta \eta(t) \Big)}_{\textit{feed-forward action}} + \underbrace{K \Big(x_d(t) - x(t) \Big)}_{\textit{stabilizing action}} = \\ &= u_{ff}(t) + K \Big(x_d(t) - x(t) \Big) \end{aligned} \tag{4.5}$$

where x_d is the state trajectory that guarantees the exact tracking:

$$x_d(t) = \begin{pmatrix} \mathcal{Q}_{\sigma(t)} \hat{w}(t) \\ \eta(t) \end{pmatrix} \tag{4.6}$$

If, as it often happens in real world applications, the state of the plant is not available for feedback, it the pair (A, C) is observable a standard output feedback structure can be used instead by introducing an asymptotic observer of the state of the plant.

$$\begin{pmatrix} \dot{\hat{\xi}}(t) \\ \dot{\hat{\eta}}(t) \end{pmatrix} = A \begin{pmatrix} \hat{\xi}(t) \\ \hat{\eta}(t) \end{pmatrix} - L \left(y(t) - C \begin{pmatrix} \hat{\xi}(t) \\ \hat{\eta}(t) \end{pmatrix} \right)$$

The final control input considered by the scheme consequently is:

$$u(t) = b_u^{-1} \Big(q_{\sigma(t)} {S_{\sigma(t)}}^r \hat{w}(t) - a_\xi \mathcal{Q}_{\sigma(t)} \hat{w}(t) - b_\eta \hat{\eta}(t) \Big) + K \Big(x_d(t) - \hat{x}(t) \Big) \tag{4.7}$$

After the replacements that has been made ($w(t) \to \hat{w}(t)$, $x(t) \to \hat{x}(t)$,...), the scheme does not guarantee the exact tracking of y_d but its asymptotic tracking provided a suitable choice of matrices G_σ (convergence of $\hat{w}(t)$ to $w(t)$), L (convergence of $\hat{x}(t)$ to $x(t)$) and K (convergence of $\hat{x}(t)$ to $x_d(t)$).

Due to the particular cascade structure, the three feedback matrices G_σ, L and K can be separately designed. The overall stability can be easily verified from the stability of the single components.

To sum up we report the equations regulating all the components:

- Exosystem model: $\begin{cases} \dot{w}(t) = S_{\sigma(t)} w(t) & w(0) = w_0 \\ y_d(t) = q_{\sigma(t)} w(t) & \sigma(t) \in \{1, 2, \dots, N\} \end{cases}$;
- Plant model: $\begin{cases} \dot{x}(t) = Ax(t) + Bu(t) & x(0) = x_0 \\ y(t) = Cx(t) \end{cases}$;
- Asymptotic observer of the exosystem: $\dot{\hat{w}}(t) = S_{\sigma(t)} \hat{w}(t) - G_{\sigma(t)} (y_d - q_{\sigma(t)}) \hat{w}(t)$
- State trajectory generator: $x_d(t) = \begin{pmatrix} \mathcal{Q}_{\sigma(t)} \hat{w}(t) \\ \eta(t) \end{pmatrix}$;
- Feedforward action: $u_{ff}(t) = b_u^{-1} \Big(q_{\sigma(t)} {S_{\sigma(t)}}^r \hat{w}(t) - a_\xi \mathcal{Q}_{\sigma(t)} \hat{w}(t) - b_\eta \eta(t) \Big)$;
- Control Input: $u(t) = u_{ff}(t) + K(x_d(t) - \hat{x})$;
- Asymptotic observer of the plant: $\dot{\hat{x}}(t) = A\hat{x}(t) - L\left(y - C\hat{x}(t)\right)$

4.1.2 Comparison with the Internal Model Control

At a first glance, this scheme may appear an Internal Model control scheme since it includes both a component capable to generate the control input that guarantees the exact

tracking and a component deputed to ensure the asymptotic convergence of overall control system. Nevertheless, it is not a "pure" Internal Model control scheme since the Internal Model Unit is outside the control loop and is not fed by the tracking error. As a consequence, this scheme has not the intrinsic robustness properties to some kind of parameters uncertainties of the classic control schemes based on the Internal Model Principle.

In the path towards a general assessment of Switched Linear Internal Model approach, the Devasia, Paden and Rossi's control scheme has been considered as a preliminary solution. Its main advantages with respect to a "pure" Internal Model solution are the possibility to directly use the results about observers presented in chapters 2 and 3 and the fact that the design of stabilizing unit is much more simpler. Moreover, this control scheme is also important because it shares a fundamental issue with the Internal Model control. In fact the problem of designing a state trajectory generator requires to study the problem of *zero dynamics* and, in particular, to extend to the switching case the so-called *Regulator Equations*.

4.1.3 State trajectory generator: the Differential Sylvester Equation

In classic regulation theory in which LTI exosystems are considered (see [FRANCIS 1977], [BASILE 1992] or [ISIDORI 2003]), a necessary condition for asymptotic tracking is that the *zero dynamics* $\eta(t)$ are a static linear combination of the exosytem state $w(t)$.

$$\eta(t) = \Pi w(t), \qquad \eta(t_0) = \Pi w(t_0) \tag{4.8}$$

The Π satisfies the following *Algebraic Sylvester Equation* (*regulator equation*).

$$-\Pi S + A_\eta \Pi + B_\xi Q = 0 \tag{4.9}$$

If the non-resonance conditions on the eigenvalues of A_η and S are satisfied, the Sylvester equation has an unique solution and the initialization of *zero dynamics* η_0 is predetermined. The control input $u(t)$ and the plant state trajectory $x(t)$ become linear combinations of $w(t)$

$$u(t) = b_u^{-1}(qS^r - a_\xi Q - b_\eta \Pi) w(t) \qquad x(t) = \begin{pmatrix} Q \\ \Pi \end{pmatrix} w(t)$$

If the exosystem is time-variant the static relation (4.8) is no longer a necessary condition and may even produce unacceptable zero dynamics trajectories. In particular, considering the case of the switching exosystems of chapter 1 a common Π for all the system generally does not exist and a piecewise constant $\Pi_{\sigma(t)}$ that switches among the N solutions of the Algebraic Sylvester equations originating from the N subsystems may lead

to discontinuous zero dynamics. In order to cope with this problem, pursuing the idea of [DEVASIA 1997] and [ZHANG 2006], a possible relaxation is to allow a *time-variant* linear dependency between $w(t)$ and $\eta(t)$.

$$\eta(t) = \Pi(t)w(t) \tag{4.10}$$

The matrix $\Pi(t)$ is a solution of the following *Differential Sylvester Equation* (DSE):

$$\dot{\Pi}(t) = -\Pi(t)S_{\sigma(t)} + A_\eta \Pi(t) + B_\xi \mathcal{Q}_{\sigma(t)} \tag{4.11}$$

with initial condition $\Pi(t_0) = \Pi_0$ such that $\eta_0 = \Pi_0 w_0$.

The solution $\Pi(t)$ is *absolutely continuous* and *almost everywhere differentiable* for every initial condition Π_0 (see [FILIPPOV 1988]). In fact, being $S_{\sigma(t)}$ and $\mathcal{Q}_{\sigma(t)}$ piecewise constant with finite switches in finite time, the Switching Differential Sylvester Equation satisfies the *Carathéodory Conditions*.

The condition $\eta_0 = \Pi_0 w_0$ may lead to an infinite number of compatible initial conditions depending on the dimensions of the exosystem and of the plant. There is indeed a set of compatible $\Pi(t)$ that guarantees the exact tracking and this fact represents an additional degree of freedom with respect to classic regulation theory where the initial condition is predetermined.

By introducing the matrix $\Pi(t)$ the control input described by equation 4.4 can be written as a function of exosystem state $w(t)$

$$u(t) = b_u^{-1}\Big(q_{\sigma(t)} {S_{\sigma(t)}}^r w(t) - a_\xi \mathcal{Q}_{\sigma(t)} w(t) - b_\eta \Pi(t)\Big) w(t) \tag{4.12}$$

If the state of the plant $x(t) = \begin{pmatrix} \xi(t) \\ \eta(t) \end{pmatrix}$ is unavailable for feedback the convergence properties of Differential Sylvester Equation become fundamental. In [ZHANG 2006] Serrani and Zhang analyze the case of a DSE with continuous periodic coefficients and, in particular, their focus is on the research of periodic solutions. They provide the conditions for which the DSE admits a unique periodic solution and they show that, under these conditions, all the solutions asymptotically converge to the periodic solution. This result cannot be directly applied to our case due to the switching characteristics of $S_{\sigma(t)}$ and $B_\xi \mathcal{Q}_{\sigma(t)}$. Nevertheless, it is reasonable that a similar result holds also for the switching case even if a theoretical proof is not yet available. This conjecture is supported by the simulative results reported in next section.

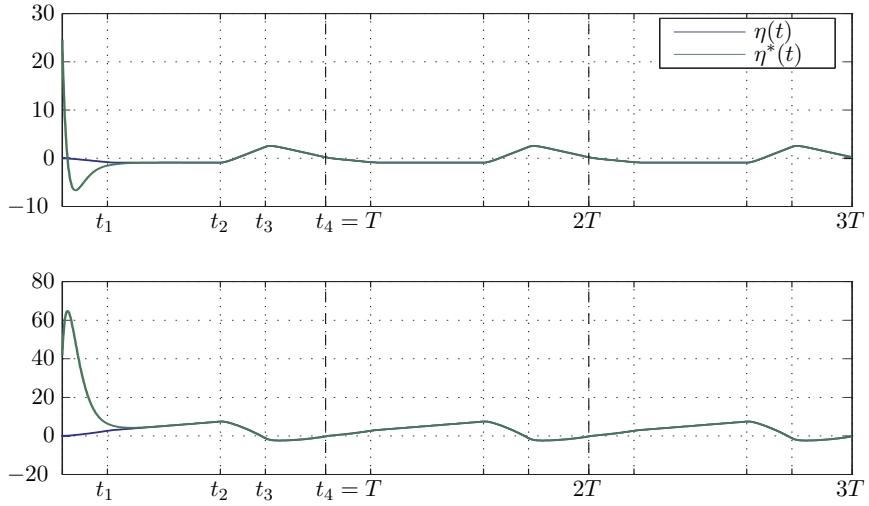

Figure 4.2: Test on convergence of $\Pi(t)$: trajectories of the two componenents of $\eta(t)$ and $\eta^*(t)$

4.1.4 Simulations

In order to show the use of the Differential Sylvester Equation, the first control scheme has been tested on a stable, minimum-phase plant (A, B, C) with relative degree $r = 2$. The reference and the considered exosystem modle are the same of the tests on Asymptotic Observers and Finite time observers.

The plant is described by the following matrices (the plant is in Brunowski canonical form):

$$A = \begin{pmatrix} 0 & 1 & 0 & 0 \\ -3 & -17 & -26 & -6 \\ 1 & -4 & -12 & -1 \\ 0 & 10 & 20 & 0 \end{pmatrix} \quad B = \begin{pmatrix} 0 \\ 1 \\ 0 \\ 0 \end{pmatrix} \quad C = \begin{pmatrix} 1 \\ 0 \\ 0 \\ 0 \end{pmatrix}^T \tag{4.13}$$

The matrix $\Pi(t)$ is online calculated by numerically solving the *Differential Sylvester Equation*.

The stability properties of the DSE have been previously tested by comparing the zero dynamics $\eta(t)$ generated by:

$$\dot{\eta}(t) = A_\eta \eta(t) + B_\xi \xi = \begin{pmatrix} -12 & -1 \\ 20 & 0 \end{pmatrix} \eta(t) + \begin{pmatrix} 1 & -4 \\ 0 & 10 \end{pmatrix} \begin{pmatrix} q_\sigma w \\ q_{\sigma(t)} S_{\sigma(t)} w \end{pmatrix} \qquad \eta(t_0) = \eta_0 \tag{4.14}$$

and the zero dynamics $\eta^*(t)$ obtained from $\eta^*(t) = \Pi(t)w(t)$ where the initial conditions of the DSE has been randomly generated. The evolution of $\eta(t)$ and $\eta^*(t)$ is depicted in

figure 4.2. Since $w(t)$ is a T-periodic function, the fact that $\eta^*(t)$ converges to T-periodic trajectory $\eta(t)$ confirms that the matrix $\Pi(t)$ converges to a T-periodic solution of the DSE.

The gains G_i of the asymptotic observer of the exosystem state has been calculated by applying the algorithm of proposition 2.7 and are reported in eq. (4.15).

$$\begin{aligned} G_1 &= \begin{pmatrix} 15 & 74 & 120 & 0 & 0 & 0 & 0 & 0 & 0 & 0 & 0 \end{pmatrix}^T \\ G_2 &= \begin{pmatrix} 0 & 0 & 0 & 9 & 20 & 0 & 0 & 0 & 0 & 0 & 0 \end{pmatrix}^T \\ G_3 &= \begin{pmatrix} 0 & 0 & 0 & 0 & 0 & 15 & 74 & 120 & 0 & 0 & \end{pmatrix}^T \\ G_4 &= \begin{pmatrix} 0 & 0 & 0 & 0 & 0 & 0 & 0 & 0 & 15 & 74 & 120 \end{pmatrix}^T \end{aligned} \tag{4.15}$$

The resulting tracking error is reported in figure 4.3.

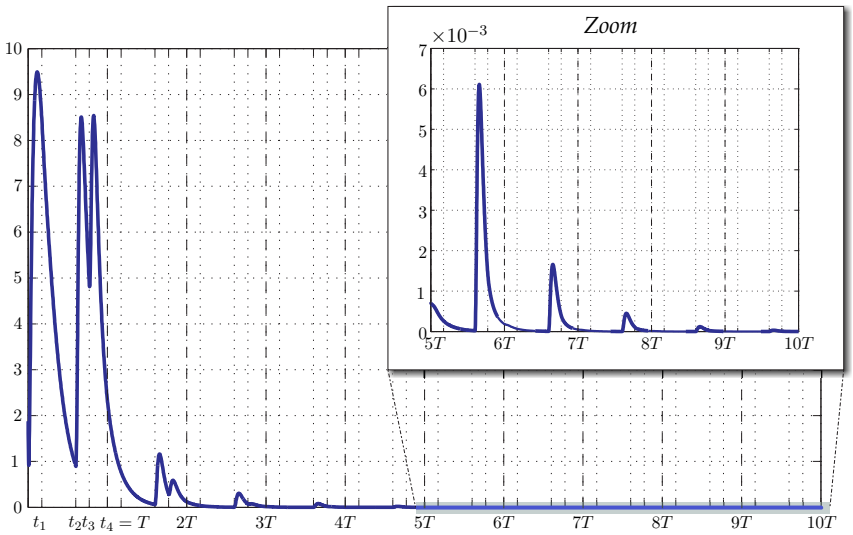

Figure 4.3: Simulations on the Devasia, Paden Rossi's control scheme: tracking error.

4.2 Second control scheme: preliminary SLIM control

The two main components of an Internal Model based control are the Internal Model Unit, deputed to generate a reference that guarantees the exact tracking, and the Stabilization Unit, deputed to stabilize the system. The main difference with the first scheme that has been analyzed in this chapter is that, in the Internal Model control, the Internal

model unit is inside the control loop. This makes more robust the control scheme with respect to plant uncertainties and exosystem uncertainties but on the other hand makes far more complicate the design of stabilization unit than in first control scheme.

A first attempt to provide a suitable design pattern for the stabilization unit has been done by extending the results on asymptotic stability of the observer that has been presented in chapter 2. The asymptotic observer in fact can be considered as an Internal model controller made by the cascade connection of a trajectory generator and a stabilization unit.

$$\begin{aligned} e(t) &= y_d(t) - y(t) && \text{(tracking error)} \\ u_{st} &= G_{\sigma(t)} e(t) && \text{(stabilizing action)} \\ \dot{\hat{w}}(t) &= S_{\sigma(t)} \hat{w}(t) + u_{st} && \text{(trajectory generator)} \\ y(t) &= q_{\sigma(t)} \hat{w}(t) \end{aligned} \tag{4.16}$$

The main idea is, that if the plant is sufficiently fast with respect to the reference to be tracked, the asymptotic observer of the exosystem state can be used as an Internal Model Controller without losing the stability properties. The feedback loop including the plant can be considered a perturbed system with respect to the simple asymptotic observer and the stability properties of the Internal Model control scheme can be inferred with singular perturbations-like arguments.

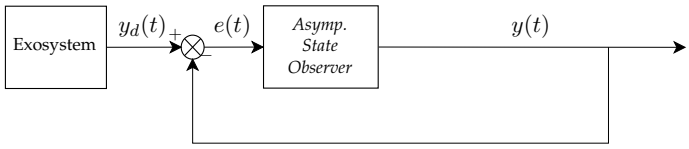

(a) Non perturbed system: classic asymptotic state observer

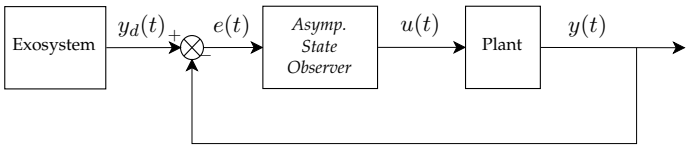

(b) Perturbed system: preliminary Internal Model Control

Figure 4.4: The main idea of the preliminary SLIM scheme.

4.2.1 Stability results involving Singular Perturbations techniques

Suppose that the plant is a first order LTI system:

$$\dot{y}(t) = \frac{1}{\varepsilon} y(t) + bu(t) \tag{4.17}$$

where the time constant $\varepsilon \ll T$ and T is the period of the reference $y_d(t)$.

By considering the asymptotic observer of the exosystem state as Internal Model Controller, the overall system is described by the following equation (see figure 4.2):

$$\begin{cases} \dot{w}(t) = S_\sigma w(t) \\ y_d(t) = q_\sigma w(t) \end{cases} \Big\} \textit{exosys.}$$
$$\begin{cases} \dot{\hat{w}}(t) = S_\sigma \hat{w}(t) - G_\sigma(y(t) - y_d(t)) \\ u(t) = \bar{q}_\sigma \hat{w}(t) \end{cases} \Big\} \textit{observ.} \qquad (4.18)$$
$$\varepsilon \dot{y}(t) = y(t) + bu(t) \qquad \textit{plant}$$

where the output matrix of the observer $q_{\sigma(t)}$ has been replaced by the matrix $\bar{q}_{\sigma(t)}$

$$\bar{q}_{\sigma(t)} = \frac{1}{b} q_{\sigma(t)} + \frac{\varepsilon}{b} q_{\sigma(t)} S_{\sigma(t)} \qquad (4.19)$$

in order to compensate the plant effects at steady state.

Since the parameter ε is assumed to be very small with respect to T, the equations (4.18) exhibit the standard form of a *singular perturbation problem* (see for example [KHALIL 2001, Ch. 11]) where the plant dynamics represent the fast dynamics while the controller dynamics represent the slow dynamics. For $\varepsilon = 0$ the equations of the standard Asymptotic observer of the exosystem state are obtained.

Unfortunately the standard singular perturbation theory cannot be directly applied to this stabilization problem since the quasi steady-state behavior $y = q_{\sigma(t)}\hat{w}$ is not continuous. Similarly to what happens for the stability of the Differential Sylvester Equation, an extension of the singular perturbation theory to the switching case is currently in development. The simulative results presented in next section can be considered an early confirmation that this extension can successfully be performed.

4.2.2 Simulations

The same asymptotic observer of chapter 2 has been used as a Switched Internal Model Control on the following first order system:

$$\dot{y}(t) = -30y + 30u \qquad \varepsilon = \frac{1}{30} \simeq 0.033 \qquad (4.20)$$

The resulting tracking error is depicted in figure 4.5: the system result to be asymptotic stable. The value of $\varepsilon = 0.033$ is near to the stability limit: in fact by choosing a plant with $\varepsilon = 0.04$, the overall system become unstable.

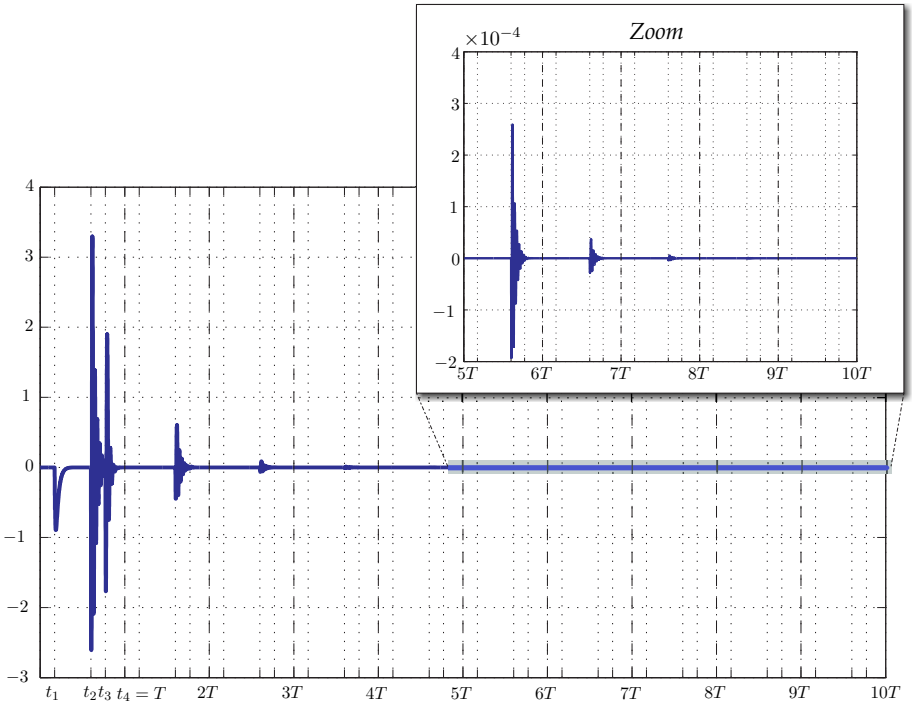

Figure 4.5: Simulations on the preliminary SLIM control scheme: tracking error.

Chapter 5

Preliminary sensitivity analysis

One of the main features that are expected from SLIM control is its reduced sensitivity to additive disturbances on the output with respect to other control schemes. In this chapter a comparison with the sensitivity properties of Repetitive Learning Control is carried out on a simple case study.

In previous chapters, many aspects of the SLIM control approach has been investigated. Nevertheless, a general design procedure for a SLIM controller in not yet available and, in particular, the path towards a general theory of the stabilization for this class of Internal Model controllers appears to be very involved. In order to motivate further efforts toward a general theory for SLIM controllers, we have looked for some examples where the proposed method enlightens good robustness properties with respect to other IMP-based approaches, since it is probably the most important feature expected for the SLIM method.

In this chapter a simple case study is used to compare qualitatively the robustness properties of the SLIM control solution with respect to a standard Repetitive Learning Control (RLC) one. The RLC has been chosen among the other existing solutions because it is the most widespread method for asymptotic tracking of periodic signals.

Since, at the moment, the only design pattern for a "pure" SLIM control that guarantees the asymptotic stability is to use an asymptotic observer on "sufficiently fast" LTI plants (see section 4.2), a LTI SISO plant with no zero-dynamics and sinusoidal disturbances superimposed on the controlled output has been considered. The standard Bode diagram of the sensitivity of the RLC has been compared with a suitably defined sensitivity harmonic response of the SLIM scheme.
It is worth noting that in designing the RLC and the SLIM solutions, the focus has been on guaranteeing the stability, "minimizing" the action of the stabilizing unit. This choice has been taken in order to enlighten mainly ("only", ideally) the intrinsic sensitivity proper-

ties of the different internal model units of the two approaches. In fact, a general qualitative rule for feedback control says that "while the stability is preserved, the higher the control gain is, the better the disturbance rejection will be". In other words, whatever the adopted IMP-scheme is, the action of the stabilizing unit affects relevantly the overall sensitivity features, therefore, in the proposed investigation, it has to be minimized.
Bearing in mind these considerations, a qualitative index for evaluating the sensitivity is how close to one (0dB) it is for all the disturbances which cannot be cancelled by the adopted IM unit. This kind of comparison is significant because in practical design, for both of the considered solutions, the final disturbance sensitivity can be addressed with an additional control loop, and the proposed investigation enlighten how critical its design is, owing to the intrinsic sensitivity properties of RLC and SLIM solutions.

The chapter is organized as follows. In Section 5.1, the considered case study is presented and stabilization of RLC and SLIM schemes is discussed. In Section 5.2, the definition of the sensitivity harmonic response is introduced for the SLIM scheme, which is linear, but not time-invariant. In Section 5.3, the simulation results are reported and discussed.

5.1 Case study

The reference

The periodic reference that has been considered for the case study is the same that has be used for previous simulations. Its trajectory is depicted in figure 1.1 and its SLIM exosystem model is described by equations (2.20), (2.21) and (2.22). It is a differentiable function with period $T = 5.83s$ ($f = 0.17Hz$) made up of three branches of parabola and a straight line and, therefore, its spectrum has an infinite number of harmonics.

The plant

In order to enlighten the restrictions imposed by Bode Integral constraints on sensitivity (see [GOODWIN 2000, Ch. 9]) only LTI systems with relative degree $r \geqslant 2$ have been considered for the case study. Since the singular perturbations approach that has been used in section 4.2 can be easily extended to higher order systems but may encounter some problems if zero dynamics are present, a LTI system with two poles and no zeros has been chosen. Both the poles have been placed at least one decade far from the principal harmonic of the reference ($f = 0.17Hz$). The resulting plant transfer function $G(s)$ is:

$$G(s) = \frac{5 \cdot 10^4}{(s + 10^2)(s + 5 \cdot 10^2)} \tag{5.1}$$

The SLIM controller

Following the ideas of preliminary SLIM controller presented in section 4.2, an asymptotic observer of the exosystem state has been used as an Internal Model controller. The stabilization matrices Γ_i^T have been calculated in order to place the eigenvalues of $\Omega_i + \Gamma_i\Theta_i$ $(i = 1, 3, 4)$ in $\{-1.5, -2, -2.5\}$ and the eigenvalues of $\Omega_2 + \Gamma_2\Theta_2$ in $\{-1.5, -2\}$.

$$\Gamma_1 = \Gamma_3 = \Gamma_4 = \begin{pmatrix} 6 & 11.75 & 7.5 \end{pmatrix} \quad \Gamma_2 = \begin{pmatrix} 3.5 & 3 \end{pmatrix} \tag{5.2}$$

The stability of SLIM controller has been tested by performing 100 simulations with random initial conditions and by checking the convergence of asymptotic observer state $\hat{w}(t)$ to $w(t)$ and of the plant state $x(t)$ to the state trajectory $x^*(t)$ that ensures the exact tracking. The evolution of the norm of the four tracking errors $\tilde{w}_i(t) = \hat{w}_i(t) - w_i(t)$ obtained in one of these simulations is depicted in figure 5.1. As for all the simulations the system has turned out to be stable, the asymptotic stability can be reasonably be inferred.

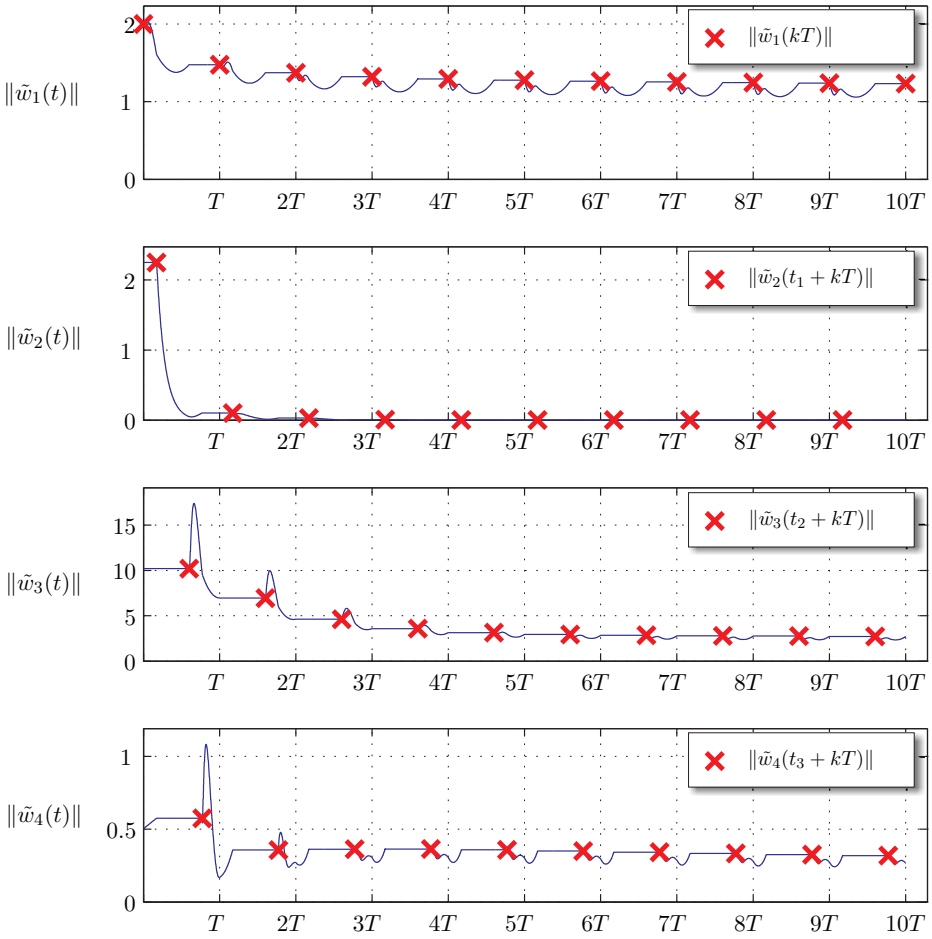

Figure 5.1: Stabilization of SLIM controller: convergence of the state of the controller

The repetitive learning controller

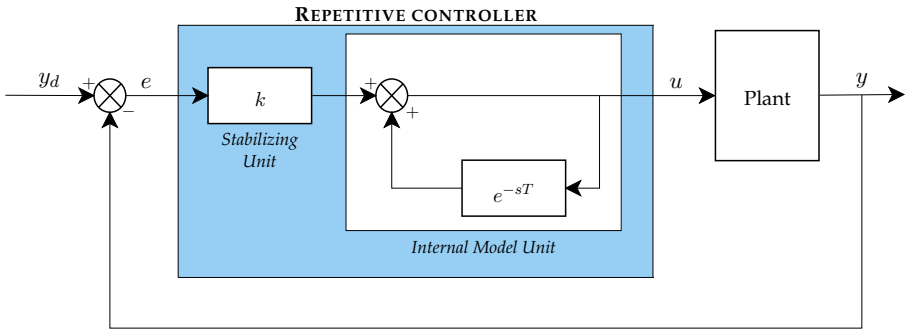

Figure 5.2: Repetitive Learning Controller structure

The structure of the repetitive controller considered for the case study is depicted in figure 5.2. The stabilization unit is a simple static gain that can be used to make the sensitivity function as close as possible to one (0 dB) while preventing the system to become unstable. The value for k chosen for the case study is $k = 0.1$. The resulting transfer function of the Repetitive Controller is:

$$R(s) = \frac{0.1}{1 - e^{-sT}} \tag{5.3}$$

5.2 The $\mathcal{L}_\infty$ gain sensitivity function

As the SLIM controller is a *time-variant system*, the classical analysis tools for the LTI systems such as the sensitivity transfer function cannot be used for the comparison with the RLC. However, an approximated sensitivity analysis on the SLIM controller can be carried out by exploiting the linearity and the asymptotic stability of the system.

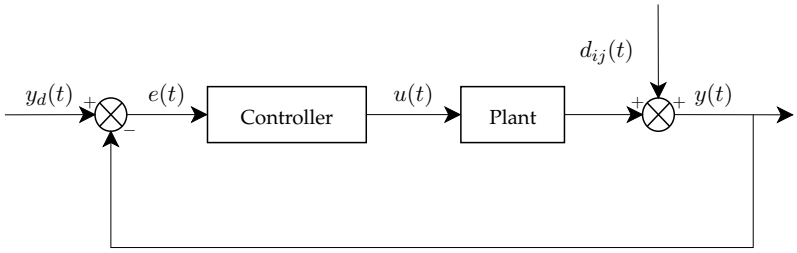

Figure 5.3: Sensitivity measurement

A sort of sensitivity function can be expermentally calculated by means of simulations. Let the output on the SLIM controller scheme be perturbed by a sinusoid $d_{ij}(t) = \sin(2\pi f_i t + \varphi_j)$ as depicted in figure 5.3. Since the overall system is asymptotic stable and

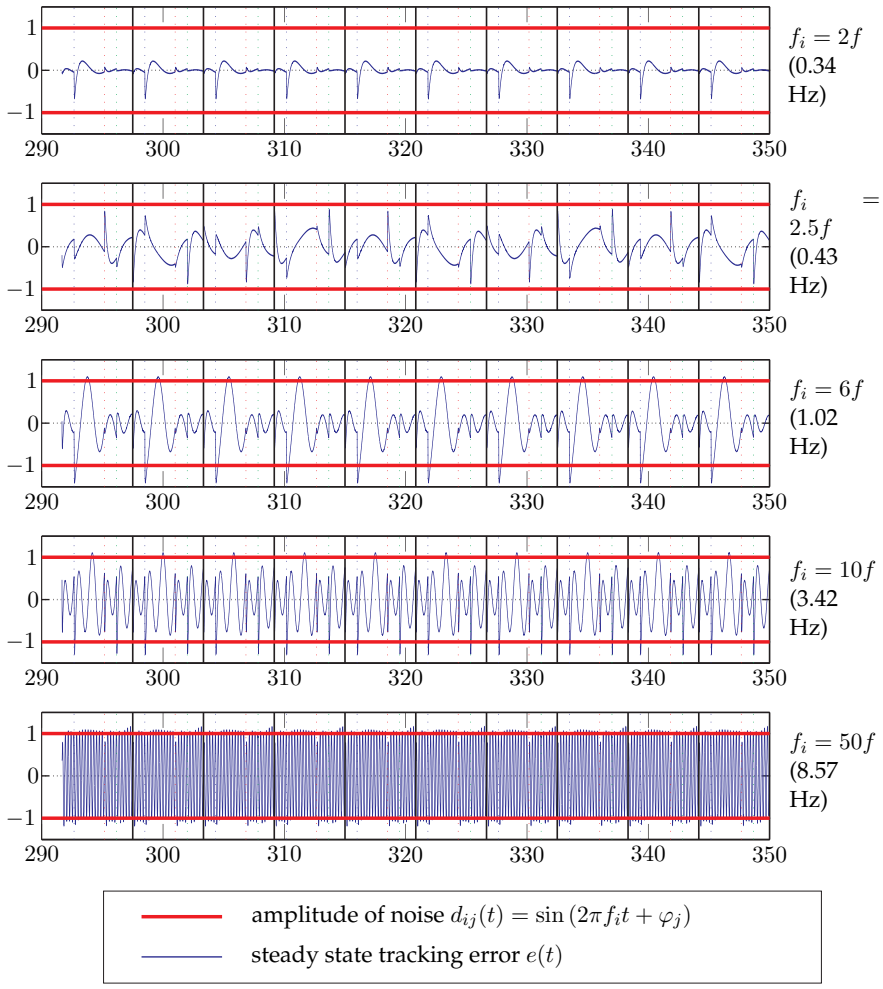

Figure 5.4: $\mathcal{L}_\infty$ Gain calculation: for each phase φ_j, the partial $\mathcal{L}_\infty$ gain $\gamma(f_i, \varphi_j)$ is calculated as $\frac{1}{2}\|e(t)\|_\infty$

the time-varying matrices $q(t)$ and $g(t)$ are limited, the system is also BIBO stable. Therefore, if the noise frequency f_i and the system frequency $f = \frac{1}{T}$ are commensurable, the system admits a periodic steady state whose period depends on the ratio $\frac{f_i}{f}$. The ratio between the $\mathcal{L}_\infty$-norm of steady state tracking error $e(t)$ and the $\mathcal{L}_\infty$-norm of the noise $d_{ij}(t)$ (i.e. the amplitude of the sinusoid) can be considered as a sensitivity Input-to-output gain $\gamma(f_i)$ (see for example [KHALIL 2001]).

The gain $\gamma(f)$ represents a sort of "worst case" sensitivity function. For example, let the additive noise on the output be the sum of three sinusoids having respectively amplitude a_1, a_2, a_3. The tracking error $e(t)$ will certainly be bounded by $2(a_1\gamma(f_1) + a_2\gamma(f_2) + a_3\gamma(f_3))$

The calculation of an "experimental" $\mathcal{L}_\infty$ Gain Sensitivity function for the case study has been performed by feeding the system with a set of 50 sinusoids having frequencies between $\frac{1}{70}f$ and $4000f$ ($2.4 \cdot 10^{-3}Hz \leqslant f_i \leqslant 686Hz$). The reaching of steady state condition has been evaluated with a test on the periodicity of the output. Since the gain $\gamma(f)$ depends on the phase φ_j, the simulation has been iterated 10 times for each frequency $\bar{f}_i$ by chosing 10 different input phases $\varphi_j = 0, \frac{\pi}{5}, \frac{2\pi}{5}, \ldots, \frac{9\pi}{5}$. The resulting $\gamma(f_i)$ have been then calculated as the maximum of the ten partial $\gamma(f_i, \varphi_j), j = 1, \ldots, 10$.

5.3 Simulation results

The comparison between the sensitivity function of RLC and the $\mathcal{L}_\infty$-gain sensitivity function of the SLIM controller is presented in figure 5.5. The SLIM $\mathcal{L}_\infty$-gain sensitivity function has been calculated as stated in section 5.2 whereas the RLC sensitivity function has been simply calculated as

$$S(f) = \left| \frac{1}{1 + \frac{0.1}{1-e^{-j2\pi fT}} \cdot \frac{50000}{(j2\pi f+100)(j2\pi f+500)}} \right| \tag{5.4}$$

.

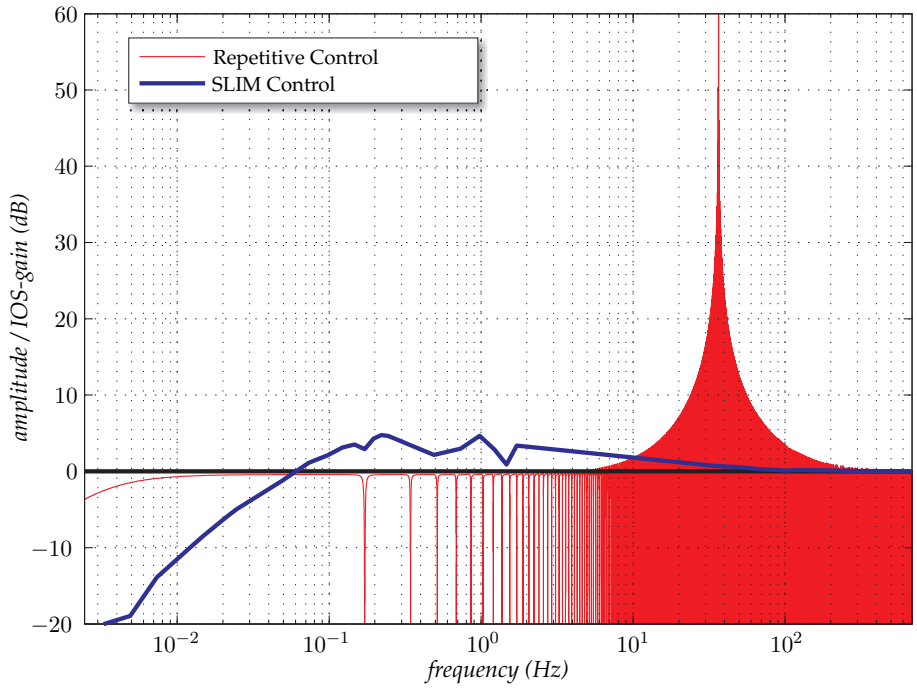

Figure 5.5: Comparison between RLC sensitivity function and SLIM controller IOS-gain sensitivity function

As expected, the RLC sensitivity function is very high at some frequencies (esp. between 30 Hz and 60 Hz) reaching a maximum of 60 dB versus a maximum of 5 dB for the SLIM controller. However, owing mainly to the spikes at switching instants (see figure 5.2), the SLIM performances are poorer than RLC ones between 0.1 and 10 Hz. These performances can be improved by introducing a mechanism that reduces the effects of the open-loop integration of the noise in the "rewinding" phase. One of the more promising techniques to fulfill this objective is to concatenate the subsystems thus using the information on the last active state to correct the initial state of the following time interval.

Part II

Applications of the Internal Model Principle

Chapter 6

Diamond Booster Quadrupole

An interesting application of the classic Internal model principle is the control of the Diamond Booster Quadrupole where a sinusoidal reference of amplitude variable in the range $[2A - 200A]$ has to be tracked with high precision.

Recent advances in many fields as medicine, chemistry, electronics and nano-technologies have promoted the design and construction of many third generation synchrotron radiation facilities at the intermediate energies of 2.5-3.5 GeV worldwide. Synchrotron radiation is an extremely intense and coherent light beam emitted when charged particles traveling close to the speed of the light are bent by a magnetic field generated by multipole magnets as dipoles, quadrupoles and sextupoles. The design and control of Power Supplies (PSs) feeding the magnets have to match two main specifications: an high accuracy in current tracking (due to the requirements on the magnetic fields) and a Power Factor (PF) close to the unit (due to high power involved).

Two classical solutions for variable currents Power Supplies are the direct connection between the booster magnets and the local electricity distribution by means of a transformer and the "White Circuit", which adopts an inductive/capacitive resonant scheme. The first one was early considered, for example, for the DIAMOND Synchrotron [MARKS 1996], Didcot, Oxfordshire and for the booster of BESSY II, Berlin [BURKMANN 1998] but was soon discarded in both cases because of its large costs. The second solution is utilized to empower the booster of the aforementioned BESSY II, and the one of SSRL, Stanford [HETTEL 1991].

In the last decade the availability of fast high-power switching devices has dramatically increased, permitting to consider different type of topologies for high power applications and revaluating the "Switch Mode technology". The "Switch-Mode technology" is a multilevel architecture made up of a series and/or parallel connection of many lower power modules. This solution is well established for ring magnets PSs with required

constant current [GRIFFITHS 2002, BELLOMO 2004], whereas it is the most innovative architecture for booster magnet PSs in which variable current are expected.

A breakthrough for the "Switch Mode" was the solution proposed by Jenni and his coauthors [IRMINGER 1998] for the Swiss Light Source (SLS). Its success made the switching solution the first choice for the synchrotron manufacturing companies as DIAMOND Ltd Company [DIA]. Another company that has already developed a similar solution for its booster dipole Power Supply is CANDLE, Yerevan, Armenia [CAN].

The SLS control solutions of [IRMINGER 1998] were shown in latter works: [JENNI 2002, JENNI 1999]. In particular, [JENNI 2002] describes the features of a digital PI regulator for current control where the aim is to ensure a good tracking for a biased sine-wave current reference. This PI solution represents the digital version of the widespread analog controllers already presented in literature [BELLOMO 2004]. The digital solution is becoming widespread because it allows the implementation of more complex and sophisticated control algorithms able to ensure good reference tracking, robustness to parameters variations from thermal effects and aging, and less sensitivity to noise. For instance, in [PETT 1996] and [KING 1999] Pett and his coauthors adopt a modern RST approach and a digital PII plus feed-forward action to comply with a requirement of an accuracy of 1 ppm (part per million).

The other problem that control has to face with is to get a Power Factor close to the unit. The requirement of a variable current running through the magnet involves an exchange of reactive energy between the magnet system and the Power Supply. Without counter measures, this leads to a strong pulsation on the DC-link capacitor voltage. An high distorted current is drawn into the mains and an high Power Factor can not be achieved. To cope with this problem in [IRMINGER 1998] 12-pulse bridges and buck converters, properly controlled by means of a pole placement, are inserted [JENNI 1999].

Although definitively interesting, the solutions proposed in [JENNI 2002] and in [JENNI 1999] leave open problems that have to be faced. The digital PI solution of [JENNI 2002] is a simple approach that can be substituted by more modern algorithms while in [JENNI 1999] the ultimate goal of a constant current flow from the mains is not achieved.

Aim of this chapter is to present an advanced control strategy for a particular kind of quadrupole magnet Power Supply. The case of the booster quadrupole magnet power converter of the DIAMOND synchrotron radiation facility under construction at the Harwell Chilton Science Campus, Didcot, has been considered [DOBBING 2006]. The Power Supply adopted in this case-study exploits a switch mode solution. Very high accuracy in the tracking of the desired current reference is reached by means of a digital internal model-based controller. The circuit and the control architecture of the front-end system is carefully considered. In particular, to achieve an high Power Factor, the task of the input section is twofold: to guarantee low harmonic distortion of the current drawn from the

line and to avoid low frequency components (usually referred to as subharmonics"), related to the quadrupole magnet oscillating current. In order to comply with these requirements, 12-pulse bridges and booster circuits are adopted. In particular, dimensioning and control design of the booster controller effectively allows to fulfill the requirement of constant input power from the line, while stationary oscillations are imposed to the magnet. For this purpose, confined oscillatory behavior imposed to the DC-link voltage of the booster stage plays a key role.

The chapter is organized as follows. In Section 6.1, the overall system is described: the control requirements, the structure of the adopted Power Supply and the features of the input and output section. In Sections 6.3 and 6.2, motivations which lead to the adopted control design approaches are deeply discussed and the proposed control solutions are presented. Simulation results are depicted in Section 6.4.

6.1 Control Specification and System Analysis

6.1.1 Control Specification

Control specifications concern the following topics.

i. Current reference. The magnet has to track a sinusoidal biased current bounded within the range $2A - 200A$ expressed as:

$$i^*_{lm}(t) = I_0 + (I_{AC}\sin(2\pi f_r t) + I_{AC}) \tag{6.1}$$

with $I_0 = 2A$, I_{AC} variable from $0A$ to $99A$ and $f_r = 5Hz$. An accuracy equal to $\pm 50ppm$ of the rated current, i.e. a current tracking error smaller than $10mA$, is required.

ii. The Power Supply topology has to adopt a switching solution. This requirement calls for a specification on the current ripple accuracy; a limit of $\pm 10ppm$ of the rated current, i.e. $2mA$, is demanded.

iii. The connection between Power Supply and mains has to be characterized by a Power Factor close to the unit and low current distortion.

6.1.2 System Analysis

The Power Supply architecture, depicted in Fig. 6.1, consists of an input section and an output one connected with the magnet load, Z_l. A current sharing topology is implemented by three modules, each one exploiting an AC/DC rectifier, a booster converter

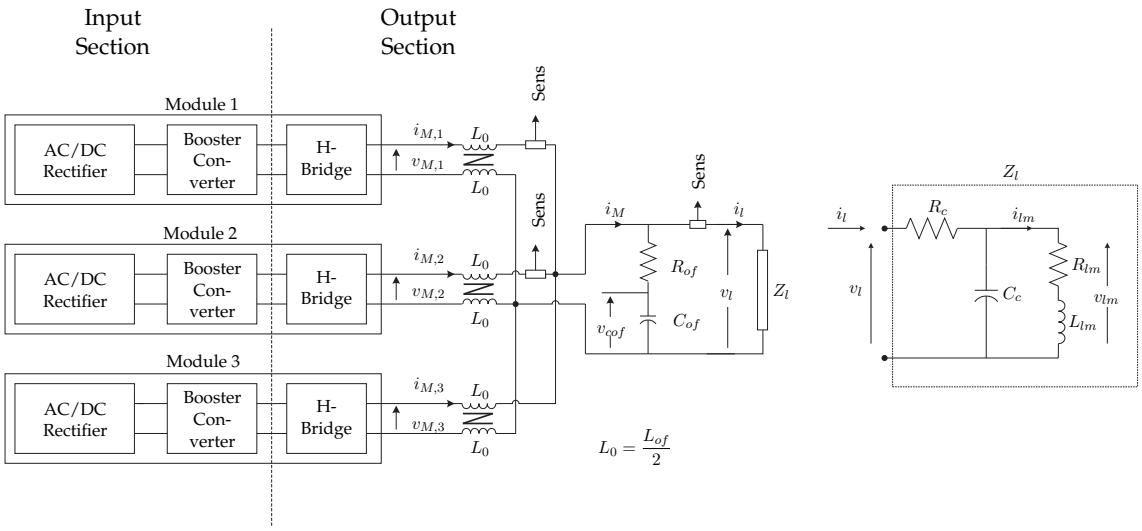

Figure 6.1: Power supply scheme.

and an H-Bridge. The sum of the three output currents is filtered by an output filter connected to the magnet load and composed by the inductors L_{of}, the capacitor C_{of} and the resistor R_{of}.

Input Section

To ensure a good Power Factor, the distortion of mains current and voltage waveforms and the displacement between mains current vector and mains voltage vector have to be as low as possible. AC/DC rectifiers exploiting a 12-pulse bridge in their front-end can fulfill this need. Three devices are used instead of a unique one in order to avoid parasitic currents and to ensure galvanic isolation. The electrical scheme of Fig. 6.2 sketches the main features of the converters. In ideal conditions the voltage $v_{if,i}$ delivered by this device is constant and ripple free as well as the currents running through the inductances L_{if}. Such type of current ensures correct operation both for the rectifiers and the transformer and the distortion of the currents $i_{A,i}$, $i_{B,i}$ and $i_{C,i}$ is kept small. Conversely, when the ripple of the current $i_{if1,i}$ and $i_{if2,i}$ is appreciable, the distortion of the mains currents grows. In the worst case the ripple is such that the current flowing trough the diodes reaches negative values turning them off. Hence a worse Power Factor has to be tolerated.

The capacitor C_{if} cannot be directly connected to the output section since the current reference to be tracked calls for an energy exchange between the magnet and the Power Supply that, without counter measures, leads to a strong pulsation of the C_{if} voltage and a considerable ripple on the current $i_{if1,i}$ and $i_{if2,i}$. To cope with this problem every module is endowed with a booster converter (see Fig. 6.1) whose architecture is sketched

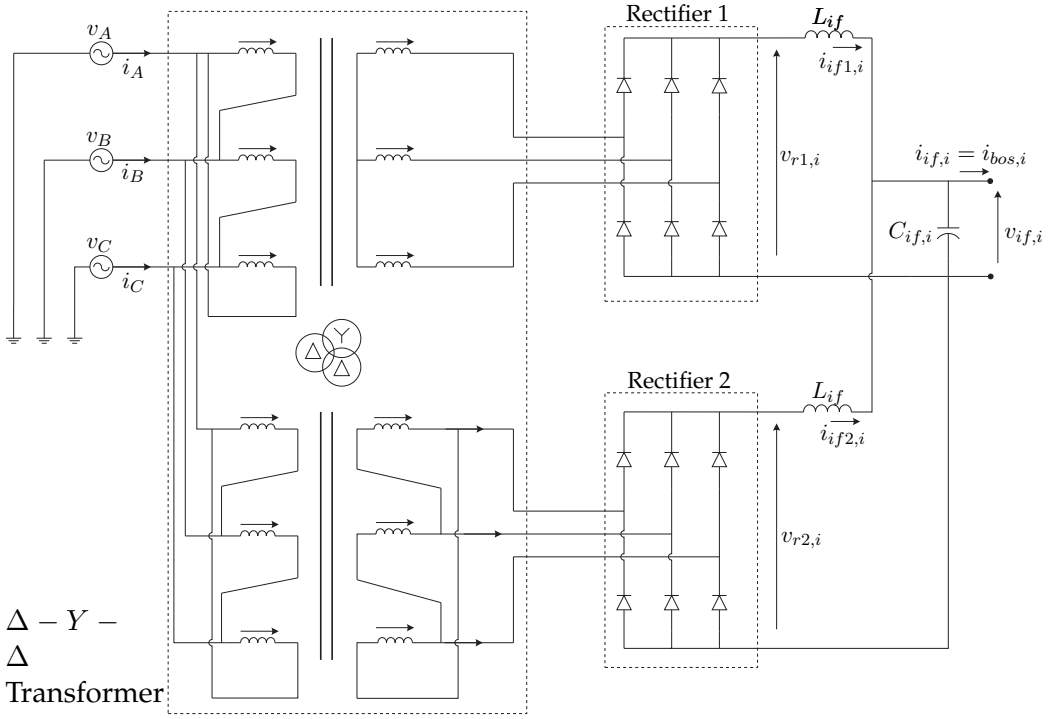

Figure 6.2: i-th module: AC/DC rectifier electrical scheme.

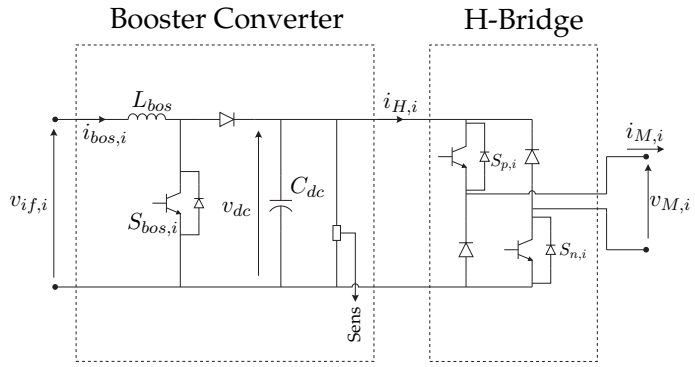

Figure 6.3: i-th module: Booster Converter and H-bridge scheme.

in Fig. 6.3. The converter task is twofold:

i. to keep the current $i_{bos,i}$ flowing trough the booster inductance of the i-th module constant in order to comply with the Power Factor specification as explained above;

ii. to control the oscillations of the DC-link voltage in order to keep $v_{dc,i}$ bounded within a safe range $[V^*_{min}, V^*_{max}]$. In fact, V^*_{max} cannot be overrun to respect capacitor physical constraints. Moreover, a minimal voltage level is necessary to drive the load current.

With respect to the buck topology, exploited for example in [JENNI 1999], the booster one has a lower voltage level on the rectifier, on the input filter and on the converter itself, thus allowing the adoption of more standard power switches.

The input section, made up of AC/DC rectifier, input filter and booster converter, is modeled as follows. Let v_{r1}, v_{r2} be the voltages and i_{if1}, i_{if1} be the currents at the end of the AC/DC rectifier[1]. The equations of the input filters made by the two inductances $L_{if,i}$ and the capacitor C_{if} are.

$$\begin{aligned} v_{if,i} &= v_{r1,i} - L_{if}\frac{d\,i_{if1,i}}{dt} = v_{r2,i} - L_{if}\frac{d\,i_{if2,i}}{dt} \\ i_{if1,i} + i_{if2,i} &= C_{if}\frac{d\,v_{if,i}}{dt} + i_{bos,i} \end{aligned} \tag{6.2}$$

or, alternatively, in state space form:

$$\frac{d}{dt}\begin{bmatrix} i_{if1,i} \\ i_{if2,i} \\ v_{if,i} \end{bmatrix} = \begin{bmatrix} 0 & 0 & -\frac{1}{L_{if}} \\ 0 & 0 & -\frac{1}{L_{if}} \\ \frac{1}{C_{if}} & \frac{1}{C_{if}} & 0 \end{bmatrix} \begin{bmatrix} i_{if1,i} \\ i_{if2,i} \\ v_{if,i} \end{bmatrix} + \begin{bmatrix} \frac{1}{L_{if}} & 0 \\ 0 & \frac{1}{L_{if}} \\ 0 & 0 \end{bmatrix} \begin{bmatrix} v_{r1} \\ v_{r2} \end{bmatrix} + \begin{bmatrix} 0 \\ 0 \\ -\frac{i_{bos,i}}{C_{if}} \end{bmatrix} \tag{6.3}$$

The i-th booster can be modeled as follows:

$$\begin{aligned} v_{if,i} &= L_{bos}\frac{di_{bos,i}}{dt} + (1-\rho_i)v_{dc,i} \\ (1-\rho_i)i_{bos,i} &= C_{dc}\frac{dv_{dc,i}}{dt} + i_{inH,i} \end{aligned} \tag{6.4}$$

Its state space representation is:

$$\frac{d}{dt}\begin{bmatrix} i_{bos,i} \\ v_{dc,i} \end{bmatrix} = \begin{bmatrix} 0 & -\frac{(1-\rho_i)}{L_{bos}} \\ \frac{(1-\rho_i)}{C_{dc}} & 0 \end{bmatrix} \begin{bmatrix} i_{bos,i} \\ v_{dc,i} \end{bmatrix} + \begin{bmatrix} \frac{v_{if,i}}{L_{bos}} \\ -\frac{i_{inH,i}}{C_{dc}} \end{bmatrix} \tag{6.5}$$

where:

[1]The relations between output voltages and currents $v_{r1,2}$, $i_{if1,2}$ and input three-phase voltages and currents are omitted since they follows from standard results on AC/DC converters (see for example...).

- $i_{bos,i}$, the current running through the booster inductance, is the first state variable;
- $v_{dc,i}$ the DC-link voltage, is the second state variable;
- ρ_i, the modulation index of the switch $S_{bos,i}$, is the input variable;
- $v_{if,i}$ is the voltage delivered by the AC/DC rectifier;
- $i_{inH,i}$ is the current flowing towards the H-bridge.

Output Section

Every module adopts a two quadrant H-bridge (positive and negative voltages, positive currents) in its outer section (see Fig. 6.3). This kind of implementation has a drawback: the switching behavior generates a current ripple that has to be damped. This is usually done introducing an output filter after the H-bridge. In this project, besides the filter, a current sharing and optimal interleaving technique have been added to improve overall performances [CHANG 1995].

Let write the output currents (see Fig. 6.1) as:

$$\begin{aligned} i_{M,i}(t) &= I_{M,i} + \Delta i_{M,i}(t) \quad \text{with } i \in \{1,2,3\} \\ i_M(t) &= i_{M,1} + i_{M,2} + i_{M,3} = I_M + \Delta i_M(t) \end{aligned} \tag{6.6}$$

where $I_{M,i0}$ and I_{M0} represent the mean values while $\Delta i_{M,i}(t)$ and $\Delta i_M(t)$ the current ripples. Using an optimal interleaving among N modules, the module commands are staggered in phase of $2\pi/N$. The resulting equivalent frequency of $\Delta i_M(t)$ is N times the frequency of $\Delta i_{M,i}(t)$ yielding a less stringent output filter dimensioning. Moreover, the split of the total current into N paralleled converters reduces by N times each module current allowing the use of more standard, faster and cheaper switches.

The model of the outer section can be obtained as follows. The voltage and current equations of the i-th module are:

$$\begin{aligned} v_{M,i} &= u'_{M,i}\, v_{dc,i} \\ i_{inH,i} &= u'_{M,i}\, i_{M,i} \quad \text{with } i \in \{1,2,3\} \end{aligned} \tag{6.7}$$

where $u'_{M,i}$ is the modulation index belonging to the set $[-1,1]$. The input filter voltages and currents are expressed as:

$$\begin{aligned} v_{M,i} &= L_{of}\frac{d\, i_{M,i}}{dt} + v_l \quad \text{with } i \in \{1,2,3\} \\ v_l &= v_{cof} + R_{of}C_{of}\frac{d\, v_{cof}}{dt} \end{aligned} \tag{6.8}$$

Load Model

Bending effects of the electron beam, focusing and defocusing, are achieved by means of a set of magnets connected through a cable. The electrical model of the load has to capture the different behaviors coming out both at high and low frequencies. A simpler representation is chosen since the current reference has only two components: a continuous component and a sinusoidal one at 5 Hz. The load equivalent circuit Z_l takes into account the load impedance R_{lm} and L_{lm} and the cable characterization R_c and C_c. The final load model is:

$$\begin{aligned} v_l &= R_c i_l + v_{lm} \\ v_{lm} &= R_{lm} i_{lm} + L_{lm} \frac{di_{lm}}{dt} \\ i_l &= i_{lm} + C_c \frac{dv_{lm}}{dt} \end{aligned} \tag{6.9}$$

The final state space representation can be obtained coupling the output section equations (6.8) and the load model relations (6.9):

$$\begin{aligned} \dot{\mathbf{x}}_{\mathbf{out}} &= \mathbf{A}_{\mathbf{out}}\, \mathbf{x}_{\mathbf{out}} + \mathbf{B}_{\mathbf{out}}\, \mathbf{v}_{\mathbf{M}} \\ i_l &= \mathbf{C}_{\mathbf{out}}\, \mathbf{x}_{\mathbf{out}} \end{aligned} \tag{6.10}$$

where:

$$\mathbf{x}_{\mathbf{out}} = \begin{bmatrix} i_{M,1} & i_{M,2} & i_{M,3} & i_{lm} & v_{of} & v_c \end{bmatrix}^T$$

$$\mathbf{v}_{\mathbf{M}} = \begin{bmatrix} v_{M,1} & v_{M,2} & v_{M,3} \end{bmatrix}^T$$

$$\mathbf{A}_{\mathbf{out}} = \begin{bmatrix} \alpha & \alpha & \alpha & 0 & \frac{\alpha}{R_{of}} & \frac{\alpha}{R_c} \\ \alpha & \alpha & \alpha & 0 & \frac{\alpha}{R_{of}} & \frac{\alpha}{R_c} \\ \alpha & \alpha & \alpha & 0 & \frac{\alpha}{R_{of}} & \frac{\alpha}{R_c} \\ 0 & 0 & 0 & -\frac{R_{lm}}{L_{lm}} & 0 & \frac{1}{L_{lm}} \\ \beta R_c & \beta R_c & \beta R_c & 0 & -\beta & \beta \\ \kappa R_{of} & \kappa R_{of} & \kappa R_{of} & -\frac{1}{C_c} & \kappa & -\kappa \end{bmatrix}$$

$$\mathbf{B}_{\mathbf{out}} = \begin{bmatrix} \frac{1}{L_{of}} & 0 & 0 \\ 0 & \frac{1}{L_{of}} & 0 \\ 0 & 0 & \frac{1}{L_{of}} \\ 0 & 0 & 0 \\ 0 & 0 & 0 \\ 0 & 0 & 0 \end{bmatrix}$$

$$\mathbf{C_{out}} = \begin{bmatrix} 1 - R_c\gamma & 1 - R_c\gamma & 1 - R_c\gamma & 0 & \gamma & -\gamma \end{bmatrix}$$
$$\gamma = \frac{1}{R_c + R_{of}}, \quad \alpha = -\frac{\gamma R_c R_{of}}{L_{of}}$$
$$\beta = \frac{\gamma}{C_{of}}, \quad \kappa = \frac{\gamma}{C_c}$$

It is worth noting that the current balance is not intrinsically guaranteed due to the asymmetry of the modules. Therefore a suitable control has to be provided.

6.2 Internal Model Current Control

The choice of an internal model approach for the power supply control is strictly related to the high accuracy requirements and to the requested interleaving coordination of the current sharing topology. In this section, the main features of this controller are deeply analyzed.

The control objective is twofold:

i. the current flowing in the load magnet has to track asymptotically the sinusoidal reference (6.1) with a steady-state error lower than 50 ppm;

ii. currents drawn from each module of the proposed topology have to be equal.

The first control objective can be pursued by means of an high-gain/large-bandwidth controller with sufficiently large gain at the frequencies where the reference harmonic content is relevant (0Hz, 5Hz). This solution is generally realized using an analog hysteresis current controller for each module of the proposed structure with a supervising controller. The second control objective is guaranteed imposing equal references to each module. Anyway, it is well known that hysteresis solutions could generate unpredictable converter switching sequences, weakening the interleaving technique effects and leading to high current ripples [U-97]. A digital implementation of PID controllers could be exploited as well but, owing to the high gain requirements and unless complicated lag network are added, the resulting controller will have a large bandwidth forcing a very small sampling time.

As a final result, an internal model based solution is clearly the preferable one because

- it is simple (no compensation network is needed) and suitable for digital implementation;
- a small sampling time is not needed since the resulting bandwidth can be kept very narrow (this is admissible because no requirement on the convergence rate is present);

- it guarantees excellent performances in terms of asymptotic tracking.

6.2.1 System model and Control Design

The overall output section model represented by equations (6.10) take into account cable parasitic elements and dynamics related to capacitor C_{of}. However the effects of these elements are not relevant in the control frequency range so a simplified Linear Time-Invariant (LTI) model can be adopted in the control design, since internal model approach guarantees steady-state tracking robustness. The following simplified model represents the basic behavior of the Power Supply combined with the load.

$$\begin{aligned}
L_{of}\frac{di_{M,1}}{dt} &= v_{M,1} - L_{lm}\left(\frac{di_{M,1}}{dt}+\frac{di_{M,2}}{dt}+\frac{di_{M,3}}{dt}\right) - R_{lm}\left(i_{M,1}+i_{M,2}+i_{M,3}\right)\\
L_{of}\frac{di_{M,2}}{dt} &= v_{M,2} - L_{lm}\left(\frac{di_{M,1}}{dt}+\frac{di_{M,2}}{dt}+\frac{di_{M,3}}{dt}\right) - R_{lm}\left(i_{M,1}+i_{M,2}+i_{M,3}\right)\\
L_{of}\frac{di_{M,3}}{dt} &= v_{M,3} - L_{lm}\left(\frac{di_{M,1}}{dt}+\frac{di_{M,2}}{dt}+\frac{di_{M,3}}{dt}\right) - R_{lm}\left(i_{M,1}+i_{M,2}+i_{M,3}\right)\\
i_{lm} &= i_{M,1}+i_{M,2}+i_{M,3}.
\end{aligned} \tag{6.11}$$

The corresponding state space form is:

$$\frac{d}{dt}\begin{bmatrix} i_{M,1}\\ i_{M,2}\\ i_{M,3}\end{bmatrix} = -\frac{R_{lm}}{3L_{lm}+L_{of}}\mathbf{A^R_{out}}\begin{bmatrix} i_{M,1}\\ i_{M,2}\\ i_{M,3}\end{bmatrix} + \mathbf{B^R_{out}}\begin{bmatrix} v_{M,1}\\ v_{M,2}\\ v_{M,3}\end{bmatrix} \tag{6.12}$$

with:

$$\begin{aligned}
\mathbf{A^R_{out}} &= \begin{bmatrix} 1 & 1 & 1\\ 1 & 1 & 1\\ 1 & 1 & 1\end{bmatrix}, \quad \mathbf{B^R_{out}} = \begin{bmatrix} \delta & \zeta & \zeta\\ \zeta & \delta & \zeta\\ \zeta & \zeta & \delta\end{bmatrix}\\
\delta &= \frac{2L_{lm}+L_{of}}{3L_{lm}L_{of}+L_{of}^2}, \quad \zeta = -\frac{L_{lm}}{3L_{lm}L_{of}+L_{of}^2}
\end{aligned} \tag{6.13}$$

Let define $u_{M,i}$ as:

$$u_{M,i} = u'_{M,i}\frac{v_{dc,i}}{V^*_{max}} = \frac{v_{M,i}}{V^*_{max}} \tag{6.14}$$

where $u'_{M,i} \in [-1,1]$ is the modulation index of the i-th module.

According to the control objectives, the following coordinate transformation is introduced:

$$\begin{bmatrix} i_{lm}\\ i_{d1}\\ i_{d2}\end{bmatrix} = {}^{\mathbf{td}}\mathbf{T_{123}}\begin{bmatrix} i_{M,1}\\ i_{M,2}\\ i_{M,3}\end{bmatrix}, \begin{bmatrix} u_{Mt}\\ u_{d1}\\ u_{d2}\end{bmatrix} = {}^{\mathbf{td}}\mathbf{T_{123}}\begin{bmatrix} u_{M,1}\\ u_{M,2}\\ u_{M,3}\end{bmatrix},$$

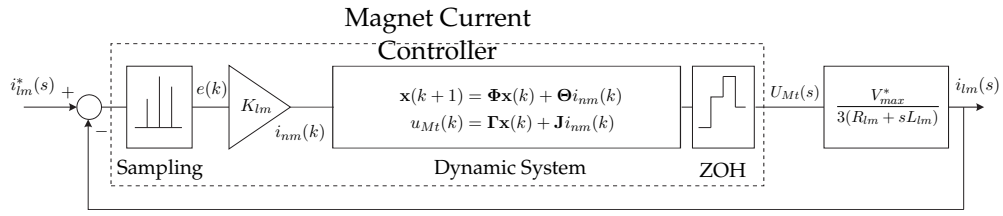

Figure 6.4: Load current controller and correspondent plant.

where:

$$^{\mathbf{td}}\mathbf{T_{123}} = \begin{bmatrix} 1 & 1 & 1 \\ 1 & -1 & 0 \\ 0 & 1 & -1 \end{bmatrix}$$

The resulting state space model is:

$$\frac{d}{dt}\begin{bmatrix} i_{lm} \\ i_{d1} \\ i_{d2} \end{bmatrix} = \begin{bmatrix} \frac{-3R_{lm}}{3L_{lm}+L_{of}} & 0 & 0 \\ 0 & 0 & 0 \\ 0 & 0 & 0 \end{bmatrix}\begin{bmatrix} i_{lm} \\ i_{d1} \\ i_{d2} \end{bmatrix} + \begin{bmatrix} \frac{V^*_{max}}{3L_{lm}+L_{of}} & 0 & 0 \\ 0 & \frac{V^*_{max}}{L_{of}} & 0 \\ 0 & 0 & \frac{V^*_{max}}{L_{of}} \end{bmatrix}\begin{bmatrix} u_{Mt} \\ u_{d1} \\ u_{d2} \end{bmatrix} \tag{6.15}$$

Neglecting L_{of} in the first row, since its value is definitively smaller than $3L_{lm}$ (see table 6.1) and exploiting the Laplace transformation, the final model adopted for the output section controller design is:

$$\begin{bmatrix} I_{lm}(s) \\ I_{d1}(s) \\ I_{d2}(s) \end{bmatrix} = \begin{bmatrix} \frac{V^*_{max}}{3(R_{lm}+sL_{lm})} & 0 & 0 \\ 0 & \frac{V^*_{max}}{sL_{of}} & 0 \\ 0 & 0 & \frac{V^*_{max}}{sL_{of}} \end{bmatrix}\begin{bmatrix} U_{Mt}(s) \\ U_{d1}(s) \\ U_{d2}(s) \end{bmatrix}$$

According to the above equations, the control indexes u_{Mt}, u_{d1} and u_{d2} are designed to control i_{lm}, i_{d1} and i_{d2} respectively by means of a digital implementation of the internal model principle.

Load Current Controller

the internal model based load current controller is made up of a digital dynamic system and a simple gain K_{lm} as sketched in Fig. 6.4. The digital dynamic system is designed as follows:

$$\begin{aligned} \mathbf{x}(k+1) &= \mathbf{\Phi x}(k) + \mathbf{\Theta} K_{lm} e(k) \\ u_{Mt}(k) &= \mathbf{\Gamma x}(k) + \mathbf{J} K_{lm} e(k) \end{aligned} \tag{6.16}$$

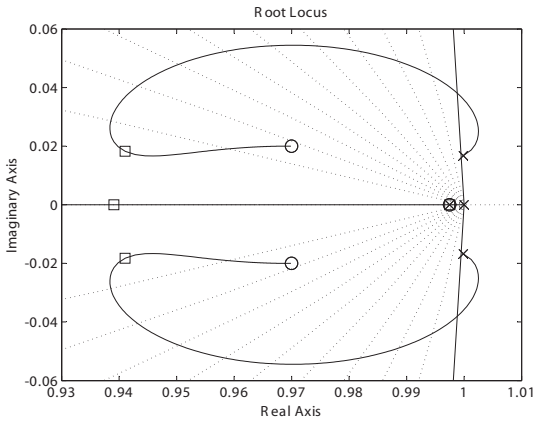

Figure 6.5: Root locus of the magnet current controller and its plant.

with:

$$
\begin{aligned}
& e(k) = i^*_{lm}(k) - i_{lm}(k) \\
& \mathbf{\Phi} = \begin{bmatrix} 1 & 0 & 0 \\ 0 & \cos(2\pi 5 T_s) & \sin(2\pi 5 T_s) \\ 0 & -\sin(2\pi 5 T_s) & \cos(2\pi 5 T_s) \end{bmatrix}, \qquad \mathbf{\Theta} = \begin{bmatrix} b_0 \\ b_1 \\ b_2 \end{bmatrix} \\
& \mathbf{\Gamma} = \begin{bmatrix} -1 & -1 & 0 \end{bmatrix}, \qquad \mathbf{J} = 1
\end{aligned} \tag{6.17}
$$

The matrix $\mathbf{\Phi}$ represents the digital internal model of the current reference: the term 1 in the first row is the model of the DC component I_0 while the other not null terms play the role of a digital oscillator with frequency $5Hz$. The value of $\mathbf{\Gamma}$ is chosen to guarantee the observability of the couple $(\mathbf{\Phi}, \mathbf{\Gamma})$ and $\mathbf{J}$ is the proportional part of the controller which ensures robustness.

Assume that the discrete time plant is obtained from the continuous one by means of a zero holder method discretization with sampling time equal to $0.533ms$ ($f_s = 1875Hz = 1/4f_{PWM}$). The zeros of the dynamic system transfer function are chosen to guarantee stability for the closed loop system. The first zero cancels the plant pole while the other two act like attractors for the imaginary poles of the controller ensuring stability. The controller gain is selected as $K_{lm} = 0.176$ and the corresponding poles of the closed loop system are marked with squares. The root locus of Fig. 6.5 is obtained. Then, the resulting $\mathbf{\Theta}$ is:

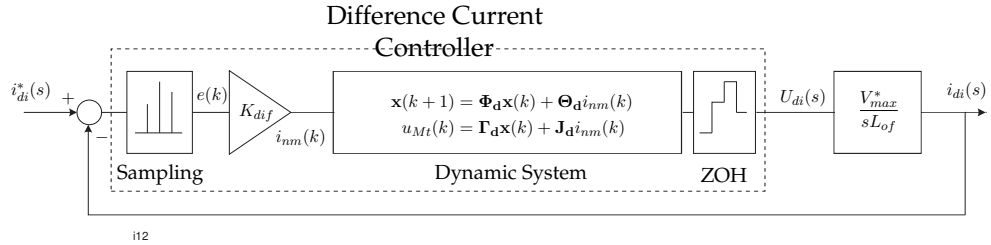

Figure 6.6: Difference current controller and correspondent plant.

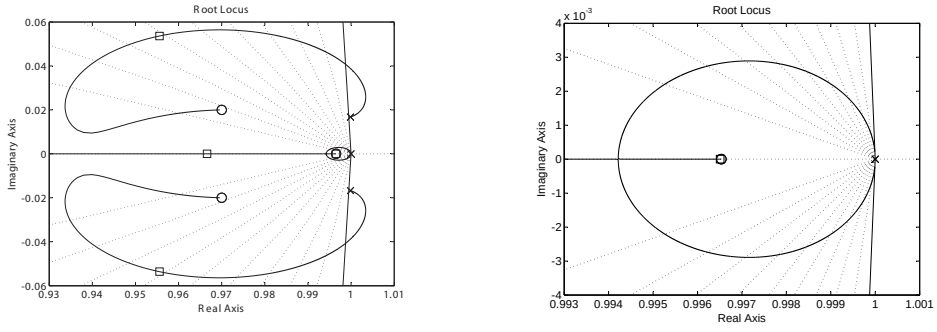

(a) Root locus

(b) Zoom of the root locus.

Figure 6.7: Root locus of the difference current controller and its plant.

$$z_{t1,2,3} = \begin{bmatrix} e^{(-\frac{R_{lm}}{L_{lm}}T_s)} \\ 0.97 + 0.02j \\ 0.97 - 0.02j \end{bmatrix} \Rightarrow \mathbf{\Theta} = \begin{bmatrix} -0.0117 \\ -0.0506 \\ -0.0692 \end{bmatrix} \tag{6.18}$$

In conclusion, the load current controller transfer function is:

$$G_c(z) = \frac{U_{Mt}(z)}{I^*(z) - I_{lm}(z)} = \frac{0.176(z - 0.9975)(z^2 - 1.94z + 0.9413)}{(z-1)(z^2 - 2z + 1)} \tag{6.19}$$

where $I^*(z)$ is the $\mathcal{Z}$-transform of the sampled magnet current reference.

Difference Current Controllers

the structure of the difference current controllers is the same of (6.16) with equal values for $\mathbf{\Phi_d}$, $\mathbf{\Gamma_d}$, $\mathbf{J_d}$ of the correspondent matrices. However, the different plants (Fig. 6.6) imply a different choice of the zeros of the controller transfer function and, consequently,

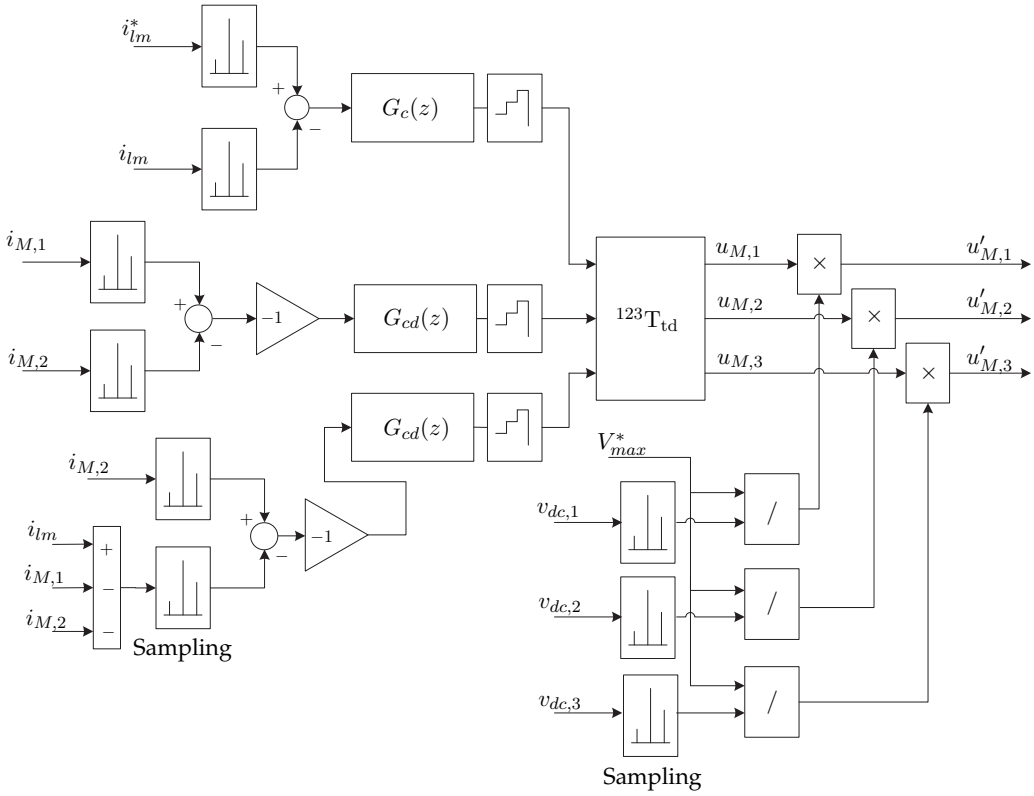

Figure 6.8: Current Controller.

of $\mathbf{\Theta_d}$ and K_{dif}:

$$z_{d1,2,3} = \begin{bmatrix} e^{(-\frac{R_{lm}+R_c}{L_{lm}}T_s)} \\ 0.97 + 0.02j \\ 0.97 - 0.02j \end{bmatrix} \Rightarrow \mathbf{\Theta_d} = \begin{bmatrix} -0.0160 \\ -0.0471 \\ -0.0726 \end{bmatrix} \tag{6.20}$$

The closed loop root locus is depicted in Fig. 6.7(a) and Fig. 6.7(b). The squares spot the system poles for the gain selected, $K_{dif} = 0.0039$. In the end, the difference current controller transfer functions are:

$$G_{cd}(z) = \frac{U_{di}(z)}{I_{di}(z)} = -\frac{0.00392(z - 0.9965)(z^2 - 1.94z + 0.9413)}{(z-1)(z^2 - 2z + 1)}, \quad i = 1, 2 \tag{6.21}$$

Remark 1. The control actions u_{d1} and u_{d2} should be equal to zero in ideal conditions, in fact current balancing control is inserted only to cope with asymmetries of the power modules.

Remark 2. The $u_{M,i}$ commands imposed by the controllers have to be transformed in modulation indexes for the interleaving PWM of the H-bridge switches. This task is quite critical since, as stated in section 6.1, the $v_{dc,i}$ have relevant oscillations owing to exchange of reactive power with the load magnet.

The final version of the internal model controller, implemented in suitable digital cards, is depicted in Fig 6.8. Its design takes into account that the values directly sensed are i_{lm}, $i_{M,1}$ and $i_{M,2}$ (see Fig. 6.1) and that the modulation indexes delivered to the PWM modulators have to be $u'_{M,i}$ and not $u_{M,i}$.

6.3 Cascade Booster Controller

The control systems of the booster converters have to fulfil two main objectives:

- to comply with the requirement on the Power Factor (see Section 6.1)
- to keep the DC-link voltage oscillations inside a safe range

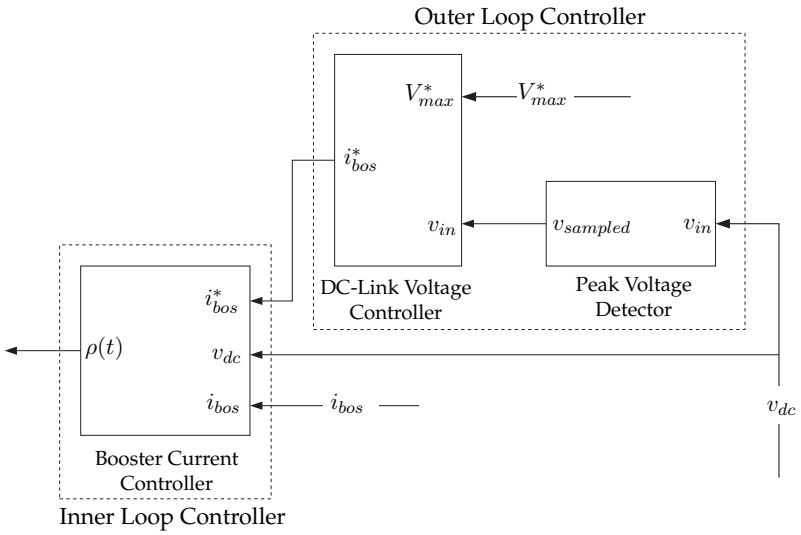

Figure 6.9: Architecture of the DC-link controllers.

The booster converter equations (6.22) that follow are obtained by elaborating (6.5) and (6.7):

$$\begin{aligned} \frac{d\,v_{dc,i}}{dt} &= -\left(\frac{i_{M,i}v_{M,i}}{C_{dc}}\right)\frac{1}{v_{dc,i}} + \frac{(1-\rho_i)}{C_{dc}}i_{bos,i} \\ \frac{d\,i_{bos,i}}{dt} &= -\frac{(1-\rho_i)}{L_{bos}}v_{dc,i} + \frac{v_{if,i}}{L_{bos}} \end{aligned} \tag{6.22}$$

This system is clearly a nonlinear underactuated system. It is a nonlinear system due to the presence of the term $1/v_{dc,i}$ and of the product between the control input ρ_i and the state $[v_{dc,i} \quad i_{bos,i}]^T$; it is underactuated because there are one input, ρ_i, and two control targets, $v_{dc,i}$ and $i_{bos,i}$.

Another important feature of the booster converter is the term $\frac{v_{M,i}i_{M,i}}{C_{dc}}$. As discussed in the previous Section, the internal model-based controller ensures the asymptotic convergence of each module output current $i_{M,i}$ to $i^*_{lm}/3$ and of the total current i_{lm} to i^*_{lm}. The single module voltage $v_{M,i}$ can be computed through (6.11) and therefore $\frac{v_{M,i}i_{M,i}}{C_{dc}}$, although time-variant, is asymptotically known and periodic with period equal to $T_r = 1/f_r$. Bearing in mind all these system features, the booster controllers are designed using a cascade configuration (see Fig. 6.9).

6.3.1 Outer Loop Controller

The Outer Loop Controller (OLC) is designed to control the maximum value of DC-link voltage trajectory, meanwhile allowing $v_{dc,i}$ to freewheel under this value.

This fact has two consequences. On the one hand, when the maximum value of the

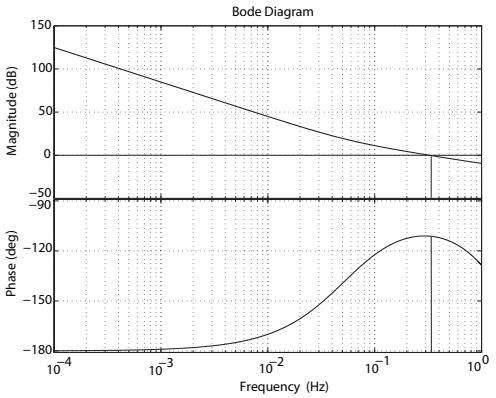

Figure 6.10: Bode diagram of the plant controlled by OLC.

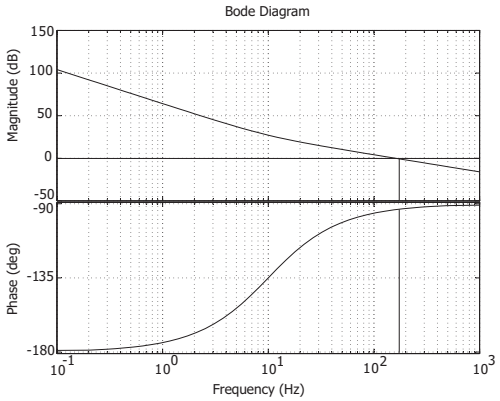

Figure 6.11: Bode Diagram of the plant controlled by ILC.

DC-link voltage is under control, a suitable dimensioning of the DC-link capacitors ensures bounded oscillations inside a safe range $[V^*_{min}, V^*_{max}]$ even in the worst case, i.e. when the load draws the maximum current from the DC-link. On the other hand the control of the maximum value of $v_{dc,i}$ without taking into account its whole dynamics can be simply pursued introducing a PI controller whose equilibrium state is pointed out by a continuous control action, $i_{bos,i}$, ensuring a good Power Factor, as asserted in Section 6.1.

The architecture of the OLC consists of two blocks: a peak voltage detector and a DC-link voltage controller (Fig. 6.9). The former device detects the maximum value of the voltage trajectory over the previous 200 ms time window. The obtained value is elaborated by the latter device as follows. First of all, the model of the maximum value of $v_{dc,i}$ has to be introduced. From (6.22) is straightforward to obtain:

$$C_{dc}\frac{1}{2}\frac{d}{dt}\left(v^2_{dc,i}\right) = \left(v_{if} - L_{bos}\frac{d\, i_{bos,i}}{dt}\right) i_{bos,i} - i_{M,i}v_{M,i} \tag{6.23}$$

This equation represents the power balance of the i-th booster: the left hand is the power on the capacitor C_{dc}, the right hand is the sum of the power flowing inside the booster, the power stored inside the inductance L_{bos} and the power flowing into the H-bridge (a losses free bridge is assumed). Integrating (6.23) over a time window equal to $T_r = 1/f_r = 200$ ms and assuming that the current running through L_{bos} is constant for the

period taken into account, the following relation is obtained:

$$\begin{aligned}\frac{C_{dc}}{2}\int_{kT_r}^{(k+1)T_r}\frac{d}{dt}\left(v_{dc,i}^2\right)dt &= \frac{C_{dc}}{2}\left(v_{dc,i}^2(k+1)-v_{dc,i}^2(k)\right)= \\ &= E_c(k+1)-E_c(k)= \\ &= \Delta E_{in}(k+1,k)-\Delta E_{L_{bos}}(k+1,k)-\Delta E_{out}(k+1,k)\end{aligned} \tag{6.24}$$

where:

$$\begin{aligned}\Delta E_{in}(k+1,k) &= \int_{kT_r}^{(k+1)T_r} v_{if}\,i_{bos}dt \simeq T_r\bar{v}_{if}\,i_{bos,i}(k) \\ \Delta E_{L_{bos}}(k+1,k) &= \int_{kT_r}^{(k+1)T_r} L_{bos}\frac{d\,i_{bos,i}}{dt}i_{bos,i}dt = \\ &= \frac{1}{2}L_{bos}\left(i_{bos,i}^2(k+1)-i_{bos,i}^2(k)\right) \\ \Delta E_{out}(k+1,k) &= \int_{kT_r}^{(k+1)T_r} i_{M,i}v_{M,i}dt\end{aligned} \tag{6.25}$$

$\bar{v}_{if}$ is the mean value of v_{if} over a period. Equation (6.24) is an energy balance and, properly rearranged, yields to the discrete time model of $v_{dc,i}$. The current reference (6.1) is periodic and therefore the voltage $v_{dc,i}$ oscillates with the same frequency at steady-state. On the other hand, during the transient the time interval between two consecutive peaks varies from a minimum of 0 ms and 400 ms. Since the mean value between these two bounds is 200 ms, the best choice for the sampling time of the discrete model is equal to 200 ms as well. Then, being kT_r and $(k+1)T_r$ the instants when the $v_{dc,i}$ reaches its maximum value, the following expression can be achieved:

$$\begin{aligned}(v_{dc,i}^{max}(k+1))^2 = (v_{dc,i}^{max}(k))^2 + \frac{2}{C_{dc}}\Bigg(&T_r\bar{v}_{if}i_{bos,i}(k)+ \\ &-\frac{1}{2}L_{bos}\left(i_{bos,i}^2(k+1)-i_{bos,i}^2(k)\right)+ \\ &-\int_{kT_r}^{(k+1)T_r} i_{M,i}v_{M,i}dt\Bigg)\end{aligned} \tag{6.26}$$

Linearizing the above model with an initial point equal to V_{max}^*, the discrete time model

of the maximum value of $v_{dc,i}$ is:

$$\begin{aligned} v_{dc,i}^{max}(k+1) = v_{dc,i}^{max}(k) + \frac{1}{C_{dc}}\Bigg(& T_r \frac{\bar{v}_{if}}{V_{max}^*} i_{bos,i}(k) + \\ & - \frac{1}{2}\frac{L_{bos}}{V_{max}^*}\left(i_{bos,i}^2(k+1) - i_{bos,i}^2(k)\right) + \\ & - \frac{1}{V_{max}^*}\int_{kT_r}^{(k+1)T_r} i_{M,i} v_{M,i} dt \Bigg) \end{aligned} \tag{6.27}$$

The term $\frac{1}{2}\frac{L_{bos}}{V_{max}^*}\left(i_{bos,i}^2(k+1) - i_{bos,i}^2(k)\right)$ is negligible with respect to $T_r \frac{\bar{v}_{if}}{V_{max}^*} i_{bos,i}(k)$ since in steady state condition $i_{bos,i}(k) \simeq i_{bos,i}(k+1)$. The last term is a disturbance that has to be rejected.

In the end the discrete time model of the maximum voltage of the DC-link is:

$$v_{dc,i}^{max}(k+1) = v_{dc,i}^{max}(k) + \frac{1}{C_{dc}}\left(T_r \frac{\bar{v}_{if}}{V_{max}^*} i_{bos,i}(k) - d_{i_{inH,i}}(k, k+1)\right) \tag{6.28}$$

Defining the voltage error:

$$\tilde{v}_{dc,i}(k) = v_{dc,i}^{max}(k) + V_{max}^* \tag{6.29}$$

the following plant is obtained:

$$\tilde{v}_{dc,i}(k+1) = \tilde{v}_{dc,i}(k) + \frac{1}{C_{dc}}\left(T_r \frac{\bar{v}_{if}}{V_{max}^*} i_{bos,i}(k) - d_{i_{inH,i}}(k, k+1)\right) \tag{6.30}$$

To stabilize this system and to reject the mean value of the disturb $d_{i_{inH,i}}(k, k+1)$, a simple proportional-integral controller is designed:

$$R_{OLC}(z) = \frac{I_{bos,i}^*(z)}{\tilde{V}_{dc,i}(z)} = -\left(k_p^{dc} + T_r \frac{k_i^{dc}}{z-1}\right) \tag{6.31}$$

where the operator z is related to a sample frequency equal to $T_r = 1/f_r = 0.2$ s. The control variable delivered by the regulator is the current reference $i_{bos,i}^*$ that will be tracked by the Intenal Loop Controller. The parameters of Table 6.1 are considered and the gains of the regulator are set equal to $k_i^{dc} = 16.5 \cdot 10^{-3}$ and $k_p^{dc} = 49.6 \cdot 10^{-3}$. The values of k_i^{dc} and k_p^{dc} are selected to keep the fastest dynamics of the open loop far from $f_r = 5Hz$ and to obtain a satisfactory phase margin of about 70^0 at a frequency near to $0.3Hz$: Fig. 6.10.

6.3.2 Inner Loop Controller

The aim of the ILC is to track the desired current reference generated by the OLC. To perform this task a simple PI controller with a PWM modulator is designed as follows.

The inductor behavior is described by the equation:

$$L_{bos}\frac{di_{bos,i}}{dt} = v_{if} - (1-\rho_i)v_{dc,i}$$

where ρ_i is the modulation index of the switch $S_{bos,i}$. Defining:

$$\rho_i = 1 - \frac{v_{if}}{v_{dc,i}} + \frac{1}{v_{dc,i}}\hat{\rho}_i$$

and the current error:

$$\tilde{i}_{bos,i} = i_{bos,i} - i^*_{bos,i}$$

the plant to be controlled is:

$$\frac{d\tilde{i}_{bos,i}}{dt} = \frac{1}{L_{bos}}\hat{\rho}_i - \frac{di^*_{bos,i}}{dt}$$

and the following PI control is exploited:

$$R_{ILC}(s) = \frac{\hat{P}_i(s)}{\tilde{I}_{bos,i}(s)} = -\left(k_p^{idc} + \frac{k_i^{idc}}{s}\right) \tag{6.32}$$

The corresponding discrete time version is obtained by means of a Forward Euler method with sampling frequency f_s.

The parameters of Table 6.1 are considered and the modulation index ρ_i is performed by a simple PWM modulator with frequency f_{PWM}. The gains $k_p^{idc} = 5.0329$ and $k_i^{idc} = 316.23$ are tuned to obtain the desired phase margins of 86.4^0 at frequency $161Hz$: Fig. 6.11.

6.3.3 Capacitor Design

Key point of the Power Supply design is the dimensioning of the DC-links. Their correct behavior does not depend on the voltage trajectories but only on the boundedness of voltages $v_{dc,i}$ between an upper value V^*_{max} and a lower value V^*_{min}. V^*_{max} cannot be overrun to respect capacitor physical constraints and V^*_{min} has to ensure the possibility of driving the current on the load. Moreover, if $v_{dc,i}$ becomes too small, modulation indexes $u'_{M,i}$ bigger than one could be requested thus introducing saturation phenomena. The formerly designed OLCs and ILCs keep under control the maximum values of $v_{dc,i}$.

The values of C_{dc} are obtained balancing the energies when the maximum current is drawn from the load. In this way, when references with smaller I_{AC} have to be tracked, the energy exchanged between the magnet and the capacitors C_{dc} is reduced and the oscillations of the DC-link voltages are reduced too. So, the minimum $v_{dc,i}$ value is greater than V^*_{min}.

Now assume that losses on the whole outer section are compensated by the power delivered by the booster converters and that the power stored in the active elements of the cable and in the output filter is negligible. So, the energy balance can be done taking into account only the DC-link capacitors and the magnet equivalent inductor. The energy stored in the magnet in the charging half period of the sinusoidal i_{lm} can be calculated as:

$$\Delta E_{L_{lm}} = \int_{-T_r/4}^{T_r/4} i_{lm}(t) L_{lm} \frac{di_{lm}(t)}{dt} dt = \frac{1}{2} L_{lm} ({I_{max}}^2 - {I_{min}}^2) \tag{6.33}$$

where i_{lm} is approximated with i_{lm}^* with $I_{AC} = 99A$ and $T_r = 1/f_r$. Let $\hat{C}_{dc} = 3C_{dc}$ be the parallel of the three capacitors. In the same time interval the energy delivered by the three modules is:

$$\Delta E_{\hat{C}_{dc}} = \int_{-T_r/4}^{T_r/4} v_{dc}(t) \hat{C}_{dc} \frac{dv_{dc}(t)}{dt} dt = \frac{1}{2} \hat{C}_{dc} ({V_{max}^*}^2 - {V_{min}^*}^2) \tag{6.34}$$

Given the values of V_{max}^* and V_{min}^*, the value of $\hat{C}_{dc}$, and therefore of C_{dc}, is straightforward.

The previous procedure yields useful results for the dimensioning of the DC-link capacitors. However it is worth to mention that this type of results is a little rough and should be refined through simulative or experimental tests.

6.4 Simulation Results

Extensive simulations were carried out to test the adopted control strategies. The overall system has been considered and the parameters of Table 6.1 were assumed. First of all, the performances of the internal model current controller are discussed and its effectiveness demonstrated. Then, the cascade booster controller is analyzed.

Table 6.1: Parameters for Booster Quadrupole Magnet Power Converter.

Parameters	Values	Units	Parameters	Values	Units
R_{lm}	0.496	Ω	V_{max}^*	600	V
L_{lm}	105	mH	V_{min}^*	510	V
R_c	0.187	Ω	f_s	1875	Hz
C_c	16	nF	f_{PWM}	7500	Hz
R_{of}	12.5	Ω	C_{if}	5	mF
C_{of}	350	μF	L_{if}	10	mH
L_{of}	10	mH	V_{FD}	0.9	V
C_{dc}	16	mF	V_{line}	294	V
L_{bos}	5	mH			

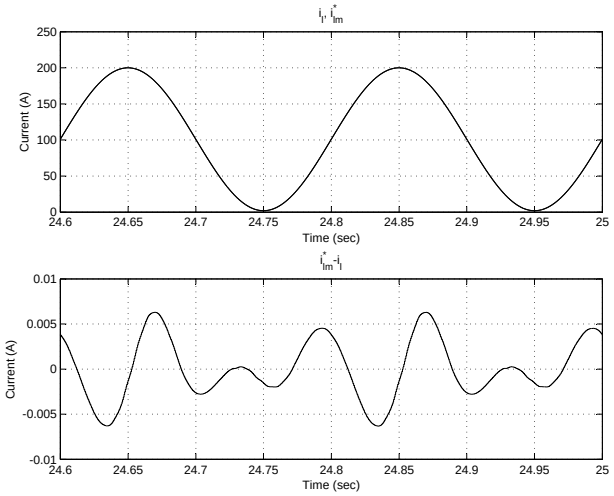

Figure 6.12: Magnet current, reference current and current error.

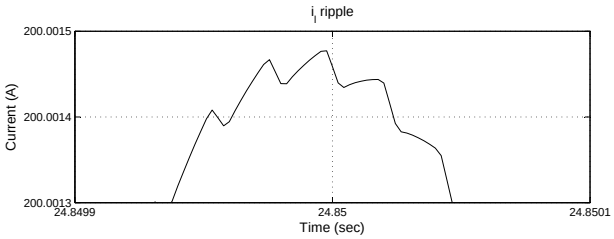

Figure 6.13: Current ripple.

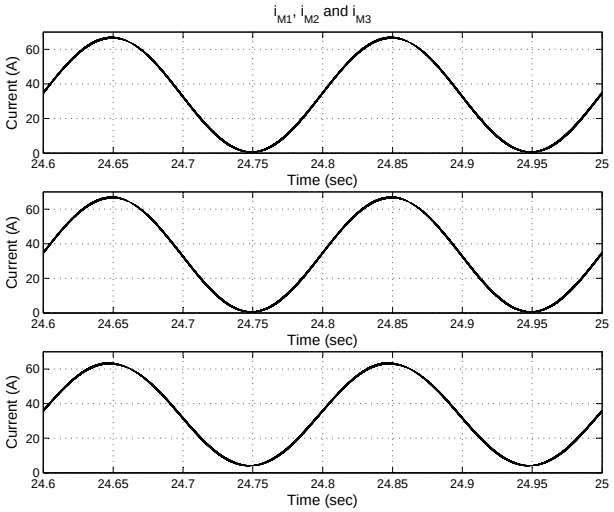

Figure 6.14: Currents of the modules.

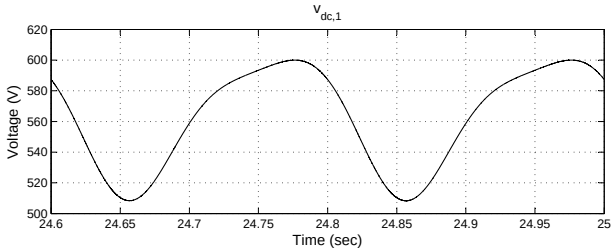

Figure 6.15: Trajectory of the $v_{dc,1}$.

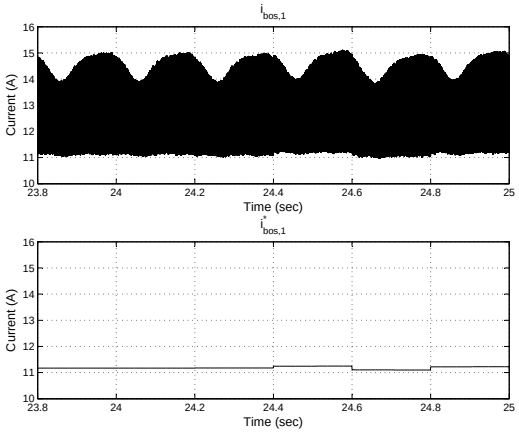

Figure 6.16: Trajectory of the $i_{bos,1}$ and $i^*_{bos,1}$.

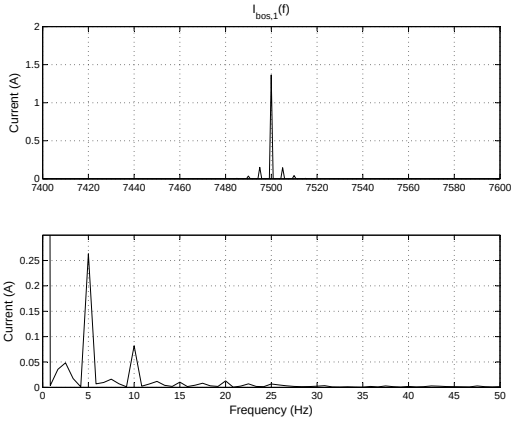

Figure 6.17: Fourier analysis of $i_{bos,1}$.

The proposed results refer to a simulation in full output power (i.e. the reference current is the maximum allowable, $I_{AC} = 99$A). The current reference, the load current i_l and the current tracking error are shown in Fig. 6.12. Thanks to the internal model based control the tracking of the current is very good. Error is kept below the admissible limit of 10mA as requested by the control specification 1), in 6.1.1. The satisfaction of the requirement of a ripple equal or less 2mA is shown in Fig. 6.13. The currents of the three modules are depicted in Fig. 6.14. It is possible to appreciate that the currents i_{M1} and i_{M2} are definitively similar. The current i_{M3} is slightly different since it is not directly sensed and a small current is drawn into C_{of}.

The DC-link voltage trajectory of the 1-st module is shown in Fig. 6.15. The maximum value of $v_{dc,1}$ is close to the maximum value V^*_{max} as expected while the minimum value of the oscillations is approximately 508V and the requirements on the upper and lower bounds of the safe voltage range are substantially satisfied.

The value of the DC-link capacitance C_{dc} needs further analysis. As asserted in 6.3.3 the algorithm for the dimensioning of the DC-link is a little rough and has to be tuned by means of simulations. Considering the specifications stated in 6.1.1, the value of I_{max}

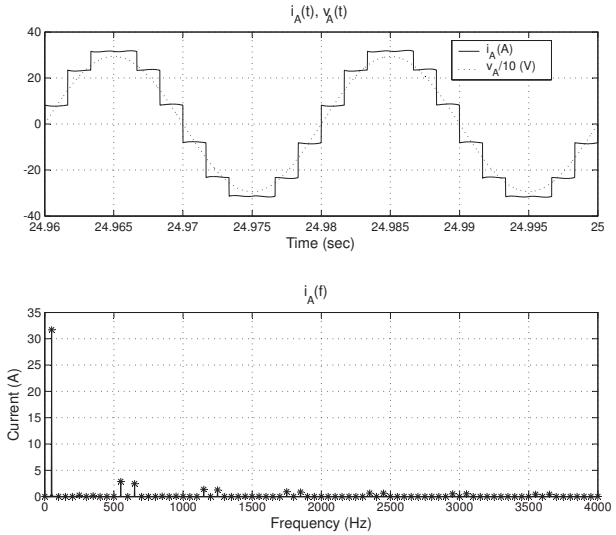

Figure 6.18: Mains current and voltage. Fourier analysis of i_A

and I_{min} are respectively $200A$ and $2A$ in full output power conditions. Adopting the values of V^*_{max} and V^*_{min} of Table 6.1, a C_{dc} value of $14mF$ is computed through (6.33) and (6.34). Simulations highlighted that C_{dc} value has to be increased to take into account the reactive power of output filter and cables. A slightly larger value of $16mF$ are selected. Similar results are obtained for the 2-nd and 3-rd module.

The $i_{bos,1}$ and its reference $i^*_{bos,1}$, delivered by the OLC, are sketched in Fig. 6.16. The OLC control objective of null error and constant output is not reached because of the approximations introduced: the $i^*_{bos,1}$ reference denotes a tiny residual oscillation less of 0.4%. Anyway, this oscillation can be tolerated. The Fourier analysis of $i_{bos,1}$ (Fig 6.17) denotes a main continuous component of $12.86A$ and two spurious harmonics.

Finally, the analysis of the Power Factor is reported. The mains voltage and current of phase A are depicted in Fig. 6.18. Analogous results can be shown for the phases B and C. The dominant component of the mains current is the 5Hz fundamental (second picture of Fig. 6.18). The values of the mains voltages and currents yield the following Power Factor for the connection between the Power Supply and the line:

$$PF = \frac{P_{in}}{(\mathbf{v}^{rms})^{\mathbf{T}}(\mathbf{i}^{rms})} = 0.988 \tag{6.35}$$

where:

$$\mathbf{v}^{rms} = \begin{bmatrix} v_A^{rms} \\ v_B^{rms} \\ v_C^{rms} \end{bmatrix}, \quad \mathbf{i}^{rms} = \begin{bmatrix} i_B^{rms} \\ i_B^{rms} \\ i_C^{rms} \end{bmatrix} \tag{6.36}$$

Hence, requirement 3) of 6.1.1 is substantially fulfilled and a PF close to the unit is

achieved.

Chapter 7

CNAO Storage Ring Dipole Magnet Power Converter 3000A / ±1600V

The control of the CNAO Storage Ring Dipole Magnet Power Converter is the application that inspired the SLIM control. In this chapter the control problem is presented and the control scheme that is currently implemented on the machine is illustrated.

A synchrotron machine, capable to accelerate either light ions or protons, will be the basic instrument of the CNAO (Centro Nazionale di Adroterapia Oncologica), the medical center dedicated to the cancer therapy, that is under construction in Pavia (Italy). The machine complex consists of one proton-carbon-ion linac that will accelerate the particles till the energy of 7 MeV/u. An injection line will transport them to the synchrotron ring where the injected particles will be accelerated and extracted with an energy ranging from 60 to 250 MeV for protons and from 120 to 400 MeV/u for carbon ions.

Protons and light ions are advantageous in conformal hadrontherapy because of three physical properties. Firstly, they penetrate the patient practically without diffusion. Secondly, they abruptly deposit their maximum energy density at the end of their range, where they can produce severe damage to the target tissue while sparing both traversed and deeper located healthy tissues. Thirdly, being charged, they can easily be formed as narrow focused and scanned pencil beams of variable penetration depth, so that any part of a tumor can accurately and rapidly be irradiated. Thus, a beam of protons, or light ions, allows highly conformal treatment of deep-seated tumors with millimeter accuracy.

This chapter is organized as follows. In the first part Power supply specifications are given. In the second part the system topology is faced, while in the third one control design is described. Finally, in the last part, simulations results are reported.

Three phase, 50 Hz input mains voltage	15,000 V $\pm$ 10%
Maximum Output Current	3,000 A
Maximum Output Voltage	$\pm$1,600 V
Maximum Output Power	$>$ 5 MVA
Load Inductance	199.1 mH
Load Resistance (cables included)	79.24 mΩ
Current Setting and Control Range	0.5 to 100% f.s.
Normal Operating Range (N.O.R.)	0.5 to 100 % f.s.
Current Setting Resolution	$< \pm 5 \times 10^{-6}$
Current Reproducibility	$< \pm 2.5 \times 10^{-6}$ f.s.
Current Readout Resolution	$< \pm 5 \times 10^{-6}$ f.s.
Residual Current Ripple (peak to peak) in N.O.R	$< \pm 5 \times 10^{-6}$ f.s.
Linearity Error $[(I_{set} - I_{out})/I_{set}]$	$< \pm 5 \times 10^{-6}$ f.s.
Ambient Temperature	0 to +40 C
Current Stability ($\Delta I/I_{set}$ over the normal operating range)	$< \pm 5 \times 10^{-6}$

Table 7.1: Specification for power supply

7.1 Power Supply Specification

The CNAO synchrotron ring is equipped with sixteen bending dipole magnets, plus one off line dipole magnet used for magnetic field measurements. In order to drive the particles to the required energy, the magnets must follow a predetermined cycle (see figure 7.1).

It consists of 7 parts:

- a starting bottom level, that is about the 5% of the maximum current level;
- a current/field ramp-up till the injection level, in a fixed time;
- a flat-bottom level (depending on the particle type) during which the particles are injected into the ring;
- a current/field ramp-up till the extraction level, in a fixed time;
- a flat-top level (depending on the particular therapy cycle the patient must be subject to) during which the slow extraction takes place and the particles are extracted

from the ring; this level does not necessarily coincides with the maximum current level;

- a ramp-up till the maximum field/current value, for a correct magnet "standardization"; no particles are in the ring during this phase of the cycle;
- a ramp-down to the starting bottom level.

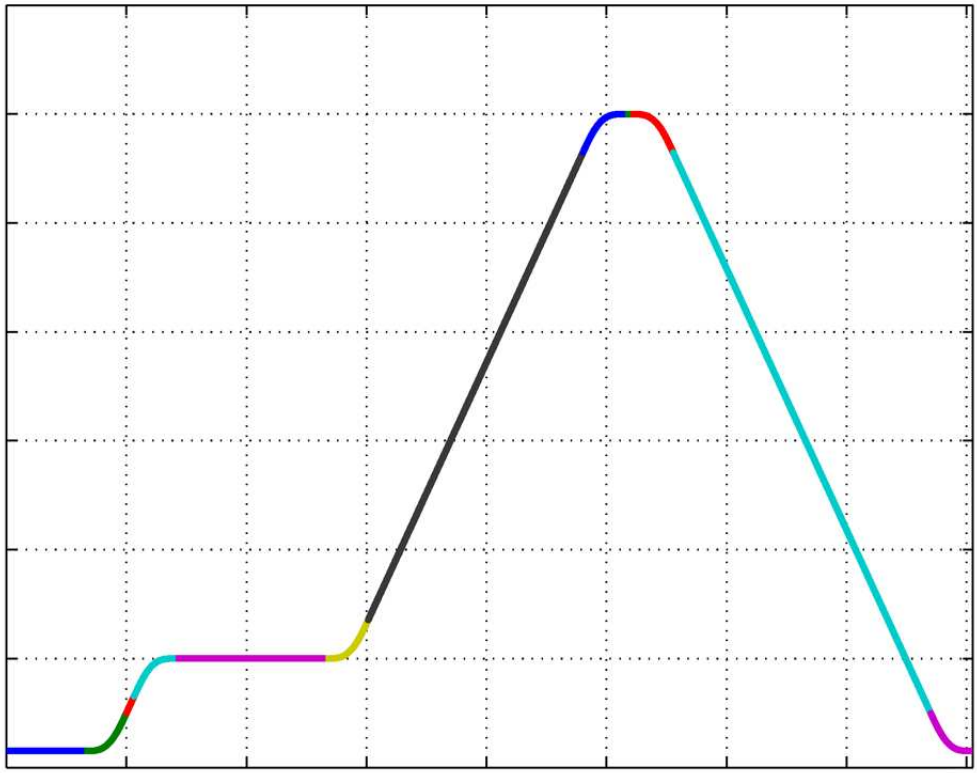

Figure 7.1: Magnets cycle

To achieve the above magnets behavior, the power supply has to satisfy some tight constraints. In particular, it has to track very high current references (maximum output current of 3000 A) with tracking error smaller than 5 ppm with respect to full scale (see table 7.1 for the complete power supply specification).

7.2 Topology

The stringent specification on CNAO synchrotron ring power supply includes two key requirements: high load current and small ripple and tracking error with respect to the

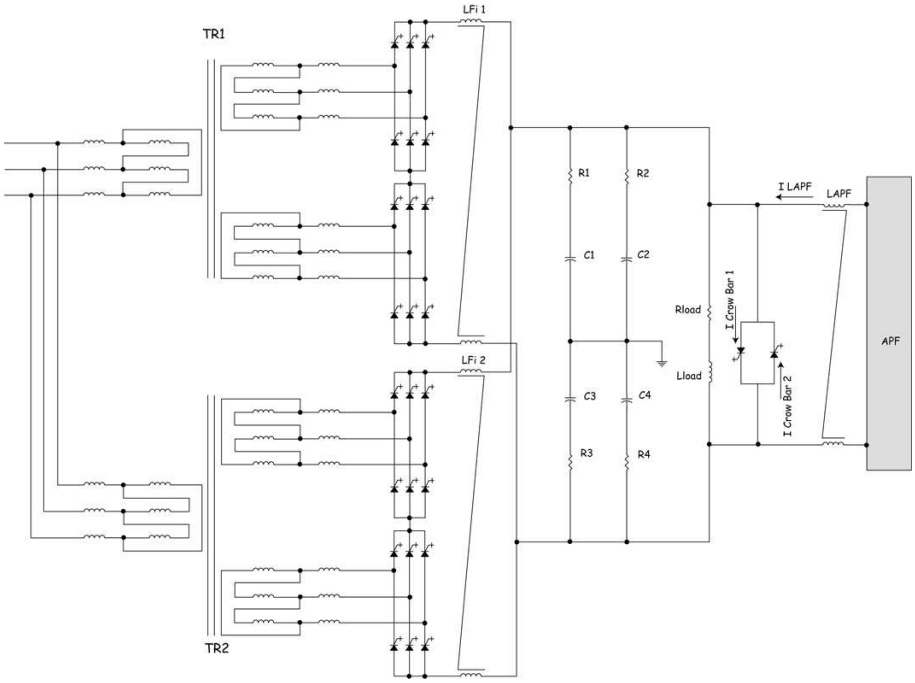

Figure 7.2: Topology of CNAO synchrotron power supply

specified reference.

The high requested current can be supplied by a thyristors-based power converter (in particular a twenty-four pulses SCR rectifier); nowadays, thyristors are the only controllable power device capable to work properly in so high current and voltage conditions. Unfortunately, they introduce high ripple in low load current conditions and their bandwidth is very small. Therefore, the small tracking error requirement cannot be satisfied using a twenty-four pulses SCR rectifier alone. The adopted solution consists in adding an Active Power Filter (APF) which cooperates with the 24-pulses rectifier in order to improve the tracking error capability of the system when the current reference is small or rapidly variable.

A first power converter design was characterized by a series connection between the APF and the 24-pulses rectifier. This choice required the addition of a transformer for the necessary APF DC-link electrical insulation: otherwise in the case of APF not inserted, the APF DC-link would be charged indefinitely. The series solution was soon discarded because the saturation of transformer complicated the control structure. In final power converter topology (fig. 7.2) a parallel connection has been preferred for the APF: in this way no additional transformer is needed and control structure is simpler. Moreover, using a suitable reconfigurable control, the parallel connected APF can be disconnected when necessary without mining the system stability.

In summary, the main components present in CNAO power supply topology are: a

24-pulse SCR-rectifier; an IGBT-based Active Power Filter; a digital control system (implemented on DSP and FPGA) controlling the 24-pulses and the APF output currents; a very accurate DCCT sensor (specifically designed for this application); a protection system (crow-bar) to discharge the load stored energy on the load itself.

7.2.1 Twenty-four pulse rectifier

The twenty-four pulse SCR-rectifier is made up of two Δ_{ext}-Δ_{ext}-Δ_{ext} three-phase transformers, four six pulse thyristor bridges and a suitable passive low-pass filter. The primary windings of the transformers are parallel connected, consequently the nominal primary voltage is 15 kV, that is the voltage of medium voltage distribution network that power all the CNAO structure. The secondary windings are series connected. The requested output voltage of each secondary winding can be easily calculated given the maximum output voltage of the power converter V_{max} and the voltage drops in transformers and HV/MV line $V_{linedrop}$. The specification's worst case has been considered, that is a -10% on primary nominal voltage:

$$V_{2(rms)} = \frac{V_{linedrop}}{2} + \frac{1}{0.9}\left(\frac{|V_{max}|}{2} \cdot \frac{\pi}{3\sqrt{2}}\right) \cong 690V$$

The low-pass filter dimensioning is performed to compensate the maximum load voltage ripple that is reached for a firing angle $\alpha = 90°$ of the thyristor bridge. In this case the output voltage waveform is a sawtooth with amplitude peak to peak of 976 V at frequency of 600 Hz. A LPF with resonance frequency of 145 Hz, $A_{db} = -24$ dB at $f = 1200$ Hz and $A_{db} = -35.5$ dB at $f = 2400$ Hz is chosen. The resulting inductors, capacitors and resistors parameters are:

$$\begin{aligned} L_{Fi1} = L_{Fi2} &= 3.2\,\mathrm{mH} \\ C_1 = C_3 &= 1.2\,\mathrm{mF} \\ C_2 = C_4 &= 300\,\mu\mathrm{F} \\ R_1 = R_3 &= 0.7288\,\Omega \\ R_2 = R_4 &= 25\,\mathrm{m}\Omega \end{aligned}$$

7.2.2 Active Power Filter

The APF is built by four modules series connected, each module being a four quadrant full bridge. The main stage of each module is a six pulses IGBT rectifier with a low pass filter whose resonance frequency is 70 Hz.

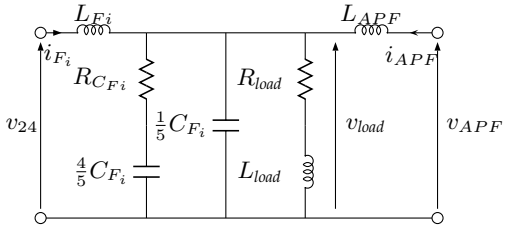

Figure 7.3: Simplified equivalent electrical circuit of the plant

The sizing of DC-link capacitor is estimated assuming that the output current in the worst case can be approximated to a ramp with a slope of 267A/s for $T_{ramp} = 300$ ms. Hence, balancing the involved energies, the DC-link capacitance is:

$$C_{DC} = 4\frac{2E_{DC}}{(4.4V_{DC} + \Delta V)^2 - (4.4V_{DC})^2} = 15\,\mathrm{mF}$$

where $V_{DC} = 444$V is the nominal DC-link voltage of each module and $E_{DC} = 688J$ is the energy that has to be stored in DC-link in the worst case.

As in twenty-four pulse rectifier, considering the voltage drop on APF lines $V_{linedrop}$, the nominal secondary output rms voltage can be calculated:

$$V_{2APF(rms)} = \frac{\pi V_{DC}}{3\sqrt{2}} + V_{linedrop} = 346\mathrm{V}$$

7.3 System model and Control Design

The aim of the control system design is to develop a closed loop control system suitable to be implemented on a DSP board. The design of the control system in the discrete time plays a fundamental role to satisfy the tight specification on CNAO power supply. To assure enough safety margin on the control system reliability, a sample period T_s=100μs has been chosen, i.e. a frequency of 10 kHz. Moreover, plants and regulators have been discretized using the ZOH method.

The design of a good control algorithm needs a previous modelling phase. In figure 7.3 a simplified electrical equivalent circuit of the plant is presented: from a control point of view the series connected dipole magnets constitute a single load with resistance (including cables) $R_{load} = 79.24$ mΩ and inductance $L_{load} = 199.1$ mH.

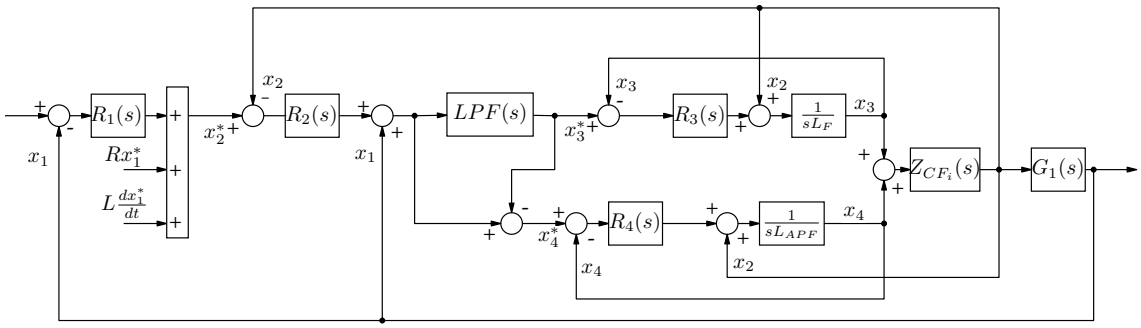

Figure 7.4: Structure of Cascade controller

Assuming the following state variables:

$$x_1 = i$$
$$x_2 = v_{load}$$
$$x_3 = i_{LF}$$
$$x_4 = i_{APF}$$
$$x_5 = v_{C1}$$

and the following controlled variables:

$$u_1 = v_{24}$$
$$u_2 = v_{APF}$$

the state space equation of the system is defined as follows:

$$\dot{\mathbf{x}} = A\mathbf{x} + B\mathbf{u}$$

where

$$\mathbf{x} = [x_1, x_2, x_3, x_4, x_5]^T,$$
$$\mathbf{u} = [v_{24}, v_{APF}]^T,$$

$$A = \begin{bmatrix} -\frac{R_{load}}{L_{load}} & \frac{1}{L_{load}} & 0 & 0 & 0 \\ -\frac{5}{C_{Fi}} & -\frac{5}{C_{Fi}R_{CFi}} & \frac{5}{C_{Fi}} & \frac{5}{C_{Fi}} & \frac{5}{C_{Fi}R_{CFi}} \\ 0 & -\frac{1}{L_{Fi}} & 0 & 0 & 0 \\ 0 & -\frac{1}{L_{APF}} & 0 & 0 & 0 \\ 0 & \frac{5}{4C_{Fi}R_{CFi}} & 0 & 0 & -\frac{5}{4C_{Fi}R_{CFi}} \end{bmatrix},$$

$$B = \begin{bmatrix} 0 & 0 \\ 0 & 0 \\ \frac{1}{L_{Fi}} & 0 \\ 0 & \frac{1}{L_{APF}} \\ 0 & 0 \end{bmatrix}.$$

Denoting with $i^* = x_1^*$ the reference for the current running through the magnets, the goal of the CNAO controller is to generate the right controlling input $\mathbf{u}$ able to track i^* with a maximum error equal to ± 0.015 A.

The developed solution is a cascade controller (see figure 7.4). It is composed by three nested loops, with the inner one composed by other two parallel loops, that will be analyzed one by one in the next paragraphs.

7.3.1 Outer loop

The outer loop has to generate a correct reference $v_{load}^* = x_2$ for the intermediate loop when the reference i^* is given and the tracking error is computed. The considered plant, obtained by a simple voltages balance on the load, is:

$$\dot{x}_1 = \frac{1}{L}(x_2 - Rx_1).$$

Since the controller has to track a linearly growing current reference it must contain a double integrator. The controller zeros have been placed to ensure a bandwidth as large as required by the current error requirements with the assigned current references.

The resulting regulator is:

$$R_1(s) = \frac{10^{\frac{93}{20}}}{s^2}(1 + s\frac{L}{R}1.1)(1 + \frac{s}{2\pi 30})$$

The plant $G_1(s)$ and the regulator $R_1(s)$ transfer functions are discretized by means of the zero order hold method with sampling time $T_s = 10^{-4}$ sec. The Bode diagram of the resulting loop function is shown in fig. 7.5.

As the reference trajectory and the relation between the state variables x_1 and x_2 are well known, performance can be improved by adding a feedforward action, i.e. by adding to the output of $R_1(s)$ the sum $Rx_1^* + L\dot{x}_1^*$.

7.3.2 Intermediate loop

When the reference for the load voltage x_2^* is given, next step is to compute the amount of current that has to be drawn from the 24 pulse rectifier and from the APF. Applying

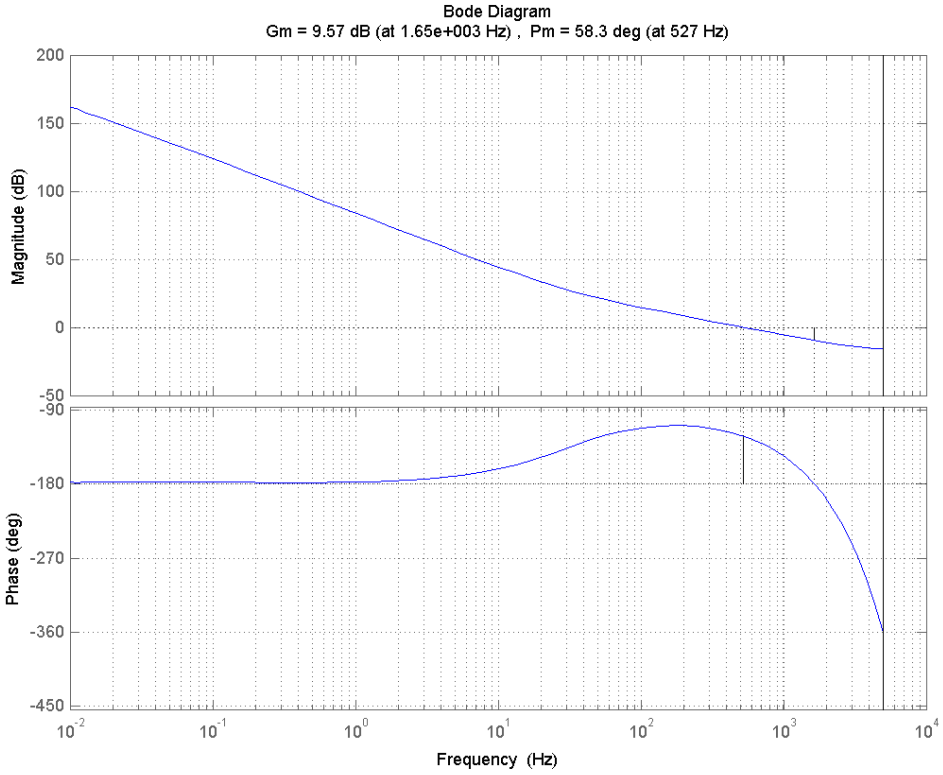

Figure 7.5: Bode diagram of outer loop regulator

Kirchoff's current law we obtain:

$$x_s = x_1 + x_{ZCFi} = x_3 + x_4$$

where x_{ZCFi} is the current flowing into the two branches in parallel with the load and the value the intermediate controller must generate, as x_1 is given.

So, the plant, in the Laplace domain, is:

$$G_2(s) = Z_{ZCFi}(s) = \frac{X_2(s)}{X_{ZCFi}(s)} = \\ = (R_{CFi} + \frac{4}{5sC_{Fi}})//(\frac{1}{5sCFi})$$

The discretized designed controller is:

$$R_2(z) = 0.89125$$

The Bode diagram of the loop function $R_2(z)G_2(z)$ is reported in fig. 7.6.

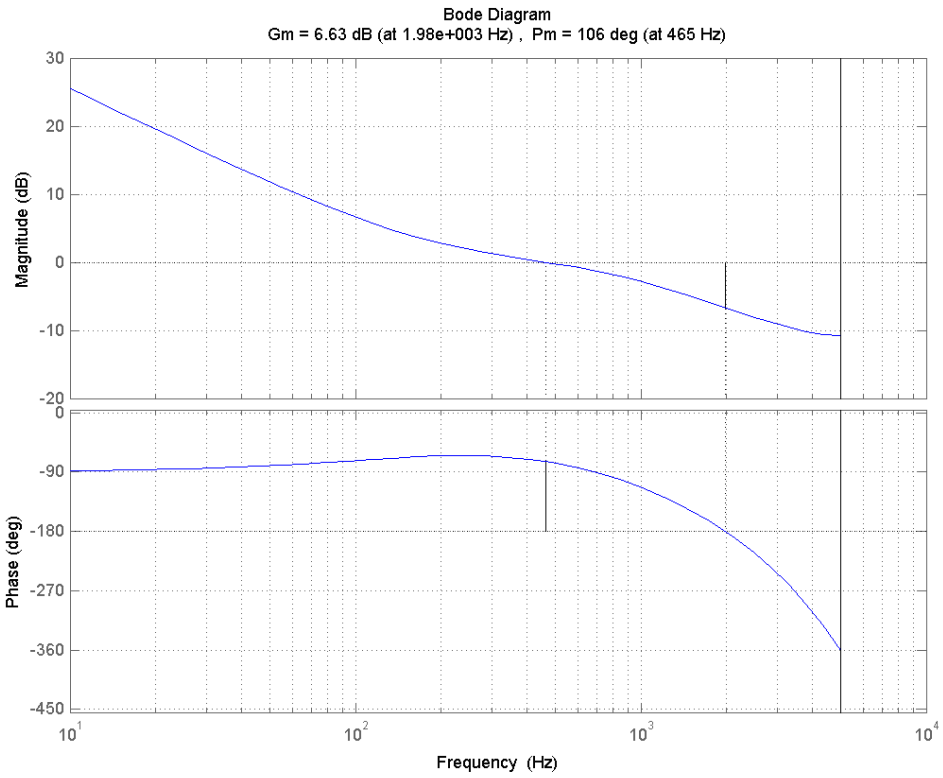

Figure 7.6: Bode diagram of intermediate loop regulator

7.3.3 Inner loops

The sum x_s between the actual value of x_1 and the computed value of x_{ZCFi} is the reference for the inner loop. However this current cannot be entirely supplied only by the 24 pulse rectifier due to its limited bandwidth . So, the separation between low frequency components, that will be tracked by the 24 pulse rectifier, and high frequency ones, that will be tracked by the APF, is required. This result is obtained by lowpassing the reference x_s^* with a 1^{st} order low pass filter, having cut frequency at 70 Hz:

$$LPF(z) = 48.327 * 10^{-5} \frac{(z + 0.9793)}{(z - 0.9691)^2}.$$

The LPF output will be x_3^*. Subtracting it from x_s, x_4^* is given too.

The system to be controlled by the 24 pulse rectifier controller is:

$$\dot{x}_3 = \frac{1}{L_{Fi}}(v_{24} - x_2)$$

Defining $\tilde{x}_3 = x_3 - x_3^*$, the controlling voltage v_{24} is given by:

$$V_{24} = X_2(z) - R_3(z)\tilde{X}_3(z)$$

where:

$$R_3(z) = 1.0042\frac{z - 0.9937}{z - 1}.$$

The Bode diagram of the resulting loop function is shown in fig. 7.7.

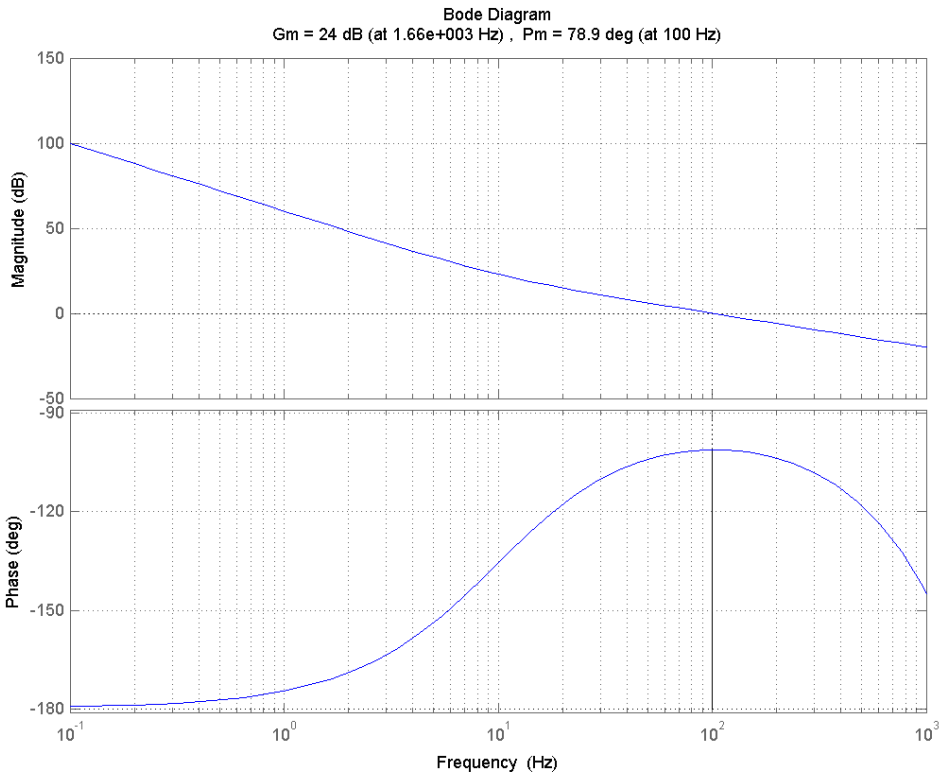

Figure 7.7: Bode diagram of 24 pulse rectifier loop

Similarly, for the Active Power Filter the system is:

$$\dot{x}_4 = \frac{1}{L_{APF}}(v_{APF} - x_2)$$

Defining $\tilde{x}_4 = x_4 - x_4^*$, the controlling voltage v_{APF} is given by:

$$V_{APF} = X_2(z) - R_4(z)\tilde{X}_4(z)$$

where:

$$R_4(z) = 1.3343\frac{z - 0.9813}{z - 0.9969}.$$

The Bode diagram of the resulting loop function is shown in fig. 7.8.

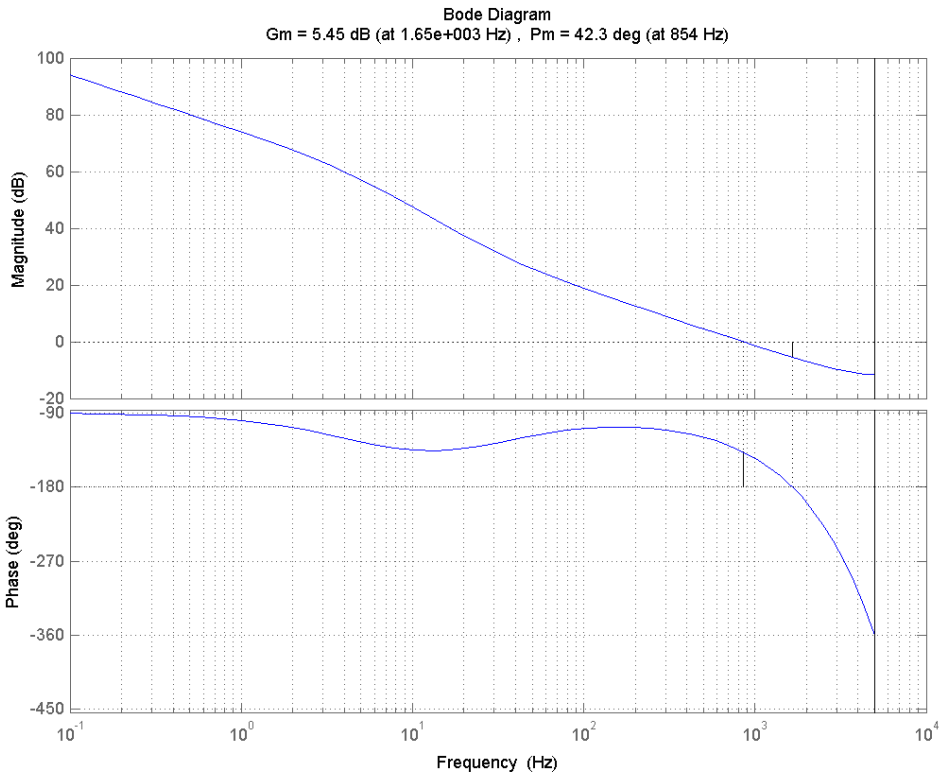

Figure 7.8: Bode diagram of APF loop

7.4 Simulations Results

To test the topology and the adopted control strategies, extensive simulations have been carried out using Matlab and Simulink.

A Simulink model of the system has been implemented using SimPowerElectronics components initialized with parameters of table 7.1. The system has been tested with the whole set of current references, each one made up of constants or ramps connected by 5th order polynomial curves with no discontinuities in the first and second derivative (see fig. 7.1). For simulation purposes, these analog signals have been approximated to 100 KHz sampled signals (ten times the digital controller operating frequency).

All the tests have been performed both in nominal V_{line} conditions and in critical

V_{line} conditions when input mains voltage can be either 110% or 90% of nominal value (respectively fig. 7.9 and 7.10). Finally a test with V_{line} equal to 90% the nominal value and a 5% load derating has been carried out (fig. 7.11).

Factory tests are scheduled before the end of 2006.

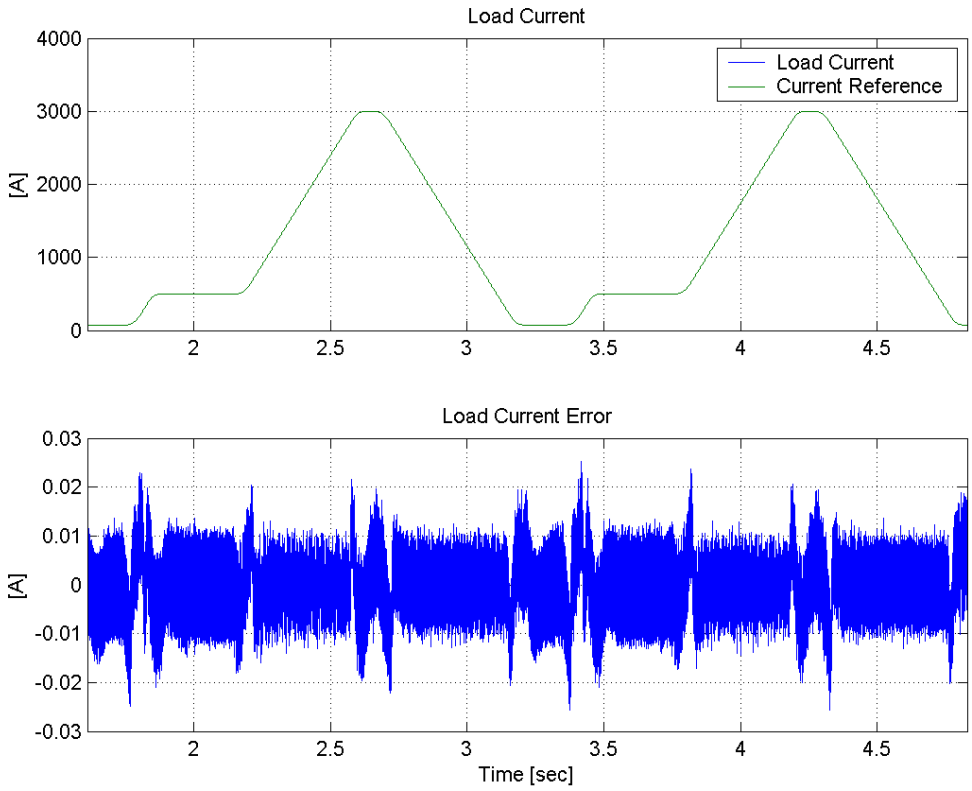

Figure 7.9: Total load current error (ripple and linearity error), case with V_{line} at 110%.

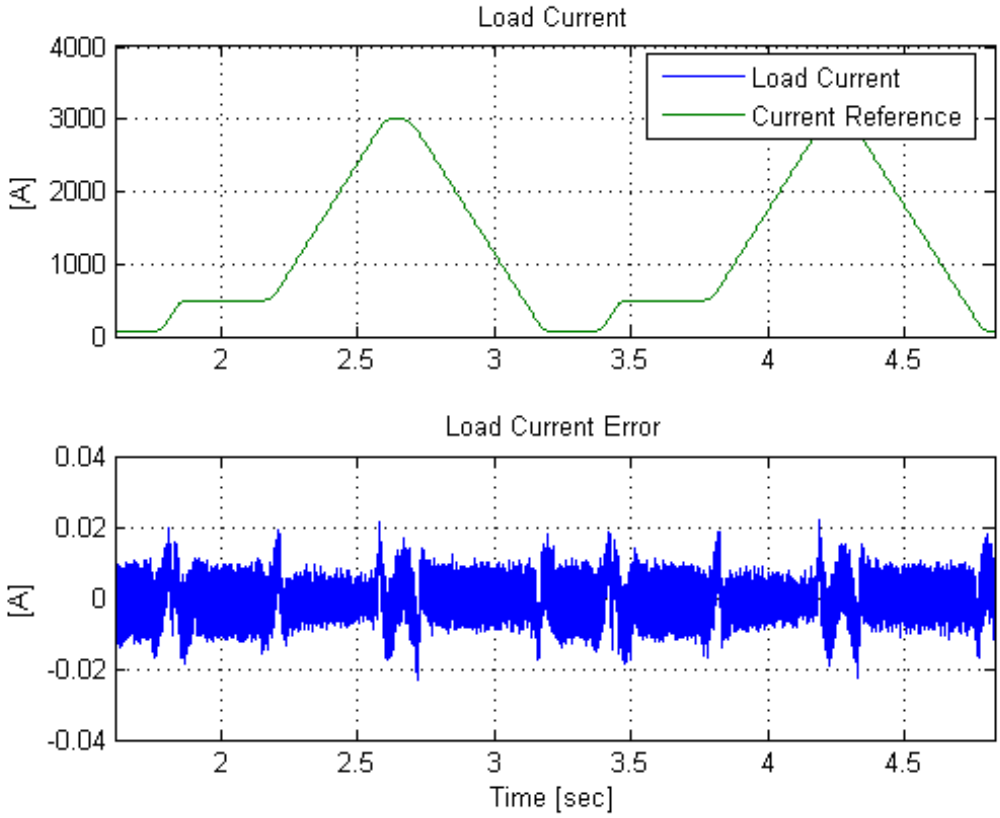

Figure 7.10: Total load current error (ripple and linearity error), case with V_{line} at 90%.

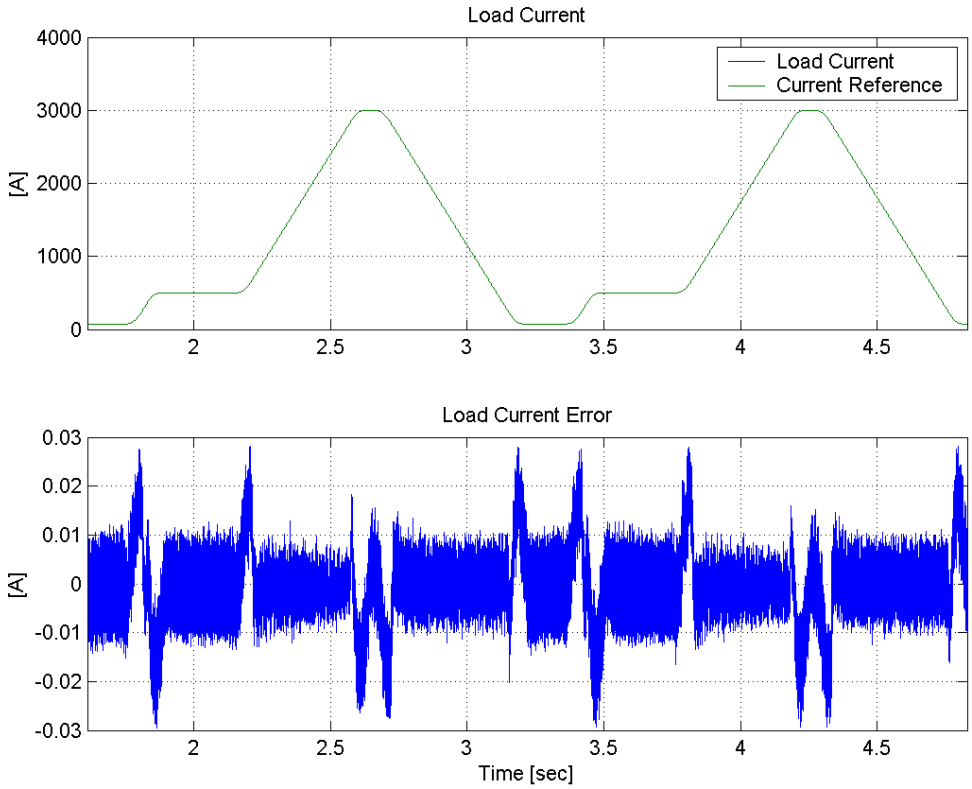

Figure 7.11: Total load current error (ripple and linearity error), case with V_{line} at 90% and 5% load derating.

Conclusions and Final Remarks

This work deals with a novel control approach based on the extension of Internal Model Principle to the case of periodic switched linear exosystems. This extension, motivated by the power electronics application described in chapter 7, has proven to be a challenging control problem mainly due to the fact that the observability properties of switched systems can change at switching instants. A final assessment of the so-called Switching Linear Internal Model (SLIM) approach is still not available but many preliminary results and, above all, the first analyses on the sensitivity performances, motivate further efforts towards the goal of a comprehensive design method.

The first issue concerning the SLIM control that has been tackled is the problem of synthesizing a periodic switched linear generator for a given periodic reference (chapter 1). A solution exhibiting a parallel structure has been provided and the problems connected with a minimization procedure of this solution has been described. The main asset of this solution is that its design procedure is very simple and can be applied to all the infinite-harmonics references considered for the SLIM approach whereas its more problematic drawback is its intrinsical partial observability and possible undetectability.

Due to its universal applicability, the parallel structure has been considered as the exosystem model in all the subsequent problems regarding the SLIM control. In chapter 2 a first step towards a general procedure for the stabilization of SLIM controller has been done by solving the problem of asymptotic observer of the exosystem state. Two different sufficient conditions for the asymptotic stability have been provided and if, on one hand, the first condition has been proved to be unfeasible, on the other hand, an effective design procedure based on the second condition has been illustrated.

The novel approach to obtain finite time convergence in the observers that has been developed in recent years by Allgöwer et al. has been successfully applied to asymptotic observer of the exosystem state (chapter 3). By exploiting the periodicity of state trajectory the original solution involving two asymptotic observer has been simplified by using a single switched observer. Both a finite-time observer exhibiting an impulsive behavior and a non impulsive observer have been described underlining the possible use of non impulsive solution for a model predictive-like estimation of unknown inputs.

The results on asymptotic observer of the exosystem state has been exploited in two

control schemes achieving the asymptotic tracking of infinite-harmonics periodic references on LTI systems (chapter 4). In particular the problem of the extension of the regulator equations to the switching case has been considered and some considerations on the convergence of the solutions of the Differential Sylvester Equation have been reported. A preliminary approach to the stabilization of SLIM controllers by exploiting the results on asymptotic observers has been illustrated in the second proposed control scheme. A singular perturbation formulation has been proposed to infer the stability of the controller for "sufficiently fast" LTI plants and, even no theoretical result are yet available, this approach is supported by simulations.

Since the general problem of stabilization for the SLIM approach seems very involved, a confirmation of the initial guess about better performances in terms of sensitivity to disturbances with respect to other control approaches was needed to motivate further efforts. A preliminary sensitivity analysis has been carried out in chapter 5 by using ad hoc tools to compare the sensitivity functions of a LTI controller (Repetitive Learning Control) and a time variant controller (SLIM control). The results of the simulations have confirmed the expectations on the sensitivity behaviour of the SLIM control with respect to the RLC and this fact motivates further researches to achieve a complete and comprehensive extension of the Internal Model principle to the switching case

From an applicative point of view, in this thesis two advanced control applications coming from the world of high energy physics have been presented. The Diamond Booster control, which has been described in chapter 6, is a classic application of the Internal Model Principle. An interesting problem that has been successfully solved in this applications is the control of DC-Link where, differently from many other power electronics applications, the voltage trajectory has not be imposed to be constant but has only been maintained inside safety bounds. In CNAO Storage Ring Dipole power supply a control guaranteeing a practical regulation of a infinite-harmonics reference within very strict error bounds have been provided. The SLIM control is expected to improve this performances and, at the same time, to reduce the control effort that in this case is considerable.

Future developments

Many open issues remain in the field of Switched Linear Internal Model control. The most important and urgent question that have to be solved certainly is the problem of stabilization. The first step in this direction may be the extension of the singular perturbations method to the switching case which would ensure the asymptotic stability on a class of LTI plants. Nevertheless once it would be achieved, this should not be considered a resolutive result since the frequential separation needed in this approach cannot

be achieved in all practical applications. Moreover, even the results on asymptotic observers that have been presented in chapter 2 cannot be considered a final mark because the proposed design procedure leads to very conservative observers that could considerably amplify the measurements noise. Since the second condition for asymptotic stability is only a sufficient condition, further researches for a less conservative result may be carried out.

A second topic that is closely related with the stabilization of the controller is the the study of the convergence properties of the Differential Sylvester Equation. In particular the results on Linear Periodic Systems have to be extended to the switching case and the non-minimum phase case have to be considered.

Besides the stabilization problem, another field in which many improvements can be carried out is the reduction of sensitivity to external disturbances. Only preliminary studies on the concatenation between the system have been effectuated and this seems a promising approach to cope with the problem of spikes at switching instants. Moreover the $\mathcal{L}_\infty$-gain function represent a very conservative estimation of the sensitivity of the system and more sophisticated tools may be considered.

Throughout this thesis the switching instants are supposed to be known and all the stability results are based on this hypothesis. In real world applications this need not be the case and an extension in this sense is certainly desirable. This problem has been tackled in the world of observers for switched systems and solutions involving Fault Detection techniques have been provided. Nevertheless, this "detector of switching instants" could complicate the stabilization problem since it intrinsically introduces a delay that should be taken into account.

Another open problem that has been briefly discussed in chapter 1 is the minimization of exosystem structure and the research of observable continuous-state switching realization. In general the system that defines the matrices for basis transformation is nonlinear due to the non-singularity condition and its solution is not straightforward. In the cases in which the system has not solution an higher order exosystem can be considered and the problem of determining the order of a minimum realization automatically raises.

Finally, when the stabilization problem will be solved, a comparison of the SLIM control with the exisisting control on the motivating example of CNAO storage ring dipole magnet power supply is desirable to enlighten the properties of the novel control approach.

Appendix A

Basic results on switched linear systems

This chapter briefly introduces some basic results on switched linear systems, with a particular concern on the topics related to stability and the controllability/observability using a Lyapunov approach.

In order to make the description of the SLIM control approach clearer and more fluent, some basic results on switched linear systems will be presented in this chapter.

A switched system is a dynamical system which consists of a finite set of subsystems and a rule that alternatively activate one subsystem of the set. Under the denomination of "Differential equations with Discontinuous Right-hand side", switched systems have been studied since the begin of twentieth century (see for example Carathéodory's works on uniqueness of the solution or the fundamental work of Filippov [FILIPPOV 1988]), anyway it is in the last two decades of the century that the interest in this class of systems exploded, originating an acceleration in the development of new techniques for analysis and synthesis and introducing these new results in applications.

In the last years the literature about switched systems has been growing up exponentially and many different frameworks have been proposed both for analysis and synthesis. A list of the more relevant contributions includes the Sliding Mode control ([UTKIN 1992]), the Stochastic Switching Systems ([BOUKAS 2005]), the "jump-flow" framework and the graphical convergence ([GOEBEL 2006]), the Multiple Lyapunov Functions approach ([BRANICKY 1998], [YE 1998b]). For a general overview on the topics related to the switched systems we refer to the recent books by Liberzon ([LIBERZON 2003]), Sun and Ge ([SUN 2005]) or Li, Soh and Wen ([LI 2005]).

The aim of this chapter is not to provide a comprehensive survey but to focus on the tools which are used in the theory of Switched Linear Internal model control. For this

reason some topics such as the Sliding Mode control and the stability under arbitrary switching will not be considered in the following although they very important in the world of switched system.

One last question that have to be mentioned before beginning our survey concerns the terminology. Many authors speak without distinction of "hybrid systems" and "switched systems" and this could be misleading in some cases. This ambiguity is probably due to the fact that switched systems have historically been the first hybrid systems to be studied. Anyway if one accepts the more general definition of hybrid system as "dynamical systems that inherently combines logical and continuous processes", it becomes clear that the set of switched systems is a proper subset of the set of hybrid systems. Although in this work this distinction will be maintained, we inform the reader that in some of the referenced papers the ambiguity still remains and that, in that cases, the term "hybrid system" is always a synonym of "switched system".

A.1 Switched Dynamical Systems

Although more general descriptions have been used (for example the concept of motions, see [YE 1998b]), a (continuous) switched system is usually described as:

$$\begin{aligned} \dot{x}(t) &= f_{\sigma(t)}\big(x(t), u(t)\big) \qquad x(0) = x_0 \\ y(t) &= h_{\sigma(t)}\big(x(t)\big) \end{aligned} \tag{A.1}$$

where $x(t) \in \mathbb{R}^n$ is the state, $u(t) \in \mathbb{R}^m$ is the input and $y(t) \in \mathbb{R}^p$ is the output. The function $\sigma(t) : \mathbb{R} \to \mathcal{P}$ is usually called *switching function* (or *switching rule*) and is a piecewise right-continuous function with values taken in the index set $\mathcal{P} = \{1, 2, 3, \ldots, N\}$.

In general, the switching function may depend on the time, its own past value, the state/output and/or possibly an external signal as well.

$$\sigma(t) = \varphi\big(t, \sigma(t^-), x(t), y(t), z(t)\big) \tag{A.2}$$

where $z(t)$ is an external signal produced by other devices. If $\sigma(t) = i$, then we say that the i-th subsystem is active at time t. It is clear that at any instant there is one (and only one) active subsystem.

The instants $t_0 < t_1 < \ldots < t_k < \ldots$ such that $\sigma(t_i^-) \neq \sigma(t_i)$ are called *switching instants* and the sequence of active indexes $[\sigma(t_0), \sigma(t_1), \ldots, \sigma(t_k), \ldots]$ is called *switching sequence*.

In order to prevent the occurring of phenomena like sliding modes and Zeno behavior that involve the concept of *differential inclusion*, the following assumption on $\sigma(t)$ is

required.

Assumption I *In a finite time interval $[\tau_1, \tau_2]$, the switching function $\sigma(t)$ has a finite number of switchings. That is*

$$\Delta T = \inf_k \{t_{k+1} - t_k\} > 0 \tag{A.3}$$

This fact guarantees that the solution of the switched system (A.1) does not require a Filippov solution but a simple Carathéodory solution.

When all the subsystems (f_k, h_k) are linear time-invariant systems, the system (A.1) is termed *switched linear system* and can be written as

$$\begin{aligned} \dot{x}(t) &= F_{\sigma(t)}x(t) + G_{\sigma(t)}u(t) \qquad x(0) = x_0 \\ y(t) &= H_{\sigma(t)}x(t) \end{aligned} \tag{A.4}$$

where F_k, G_k, H_k are linear mappings in appropriate spaces.

Even if most of the literature on switched systems is based on the hypothesis of that $x(t)$ is continuous, some authors consider systems with impulse effects (see [YE 1998a], [LI 2005], [XIE 2006], [GOEBEL 2006], [GU 2009]). In this framework the system becomes ($\sigma(t)$ is left-continuous):

$$\begin{aligned} \dot{x}(t) &= F_{\sigma(t)}x(t) + G_{\sigma(t)}u(t) \quad \text{when } \sigma(t^+) = \sigma(t) \\ \dot{x}(t^+) &= M_{\sigma(t)}x(t) + N_{\sigma(t)}u(t) \quad \text{when } \sigma(t^+) \neq \sigma(t) \\ y(t) &= H_{\sigma(t)}x(t) \end{aligned} \tag{A.5}$$

The presence of the so-called "*reset of the state*" (or *jumps* in Teel's framework), which is described by the second equation of (A.5), leads to more conservative results on stability with respect to standard switched systems. Since the current formulation of SLIM approach has the continuity of the state trajectories among its basic assumptions, the results on impulsive systems, though very significant, are not presented in this chapter.

A.2 Stability

The stability properties of a switched system Σ cannot be simply reduced to the stability properties of his subsystems but strongly depend also on the switching function. This following example ([BRANICKY 1998]) shows how two globally asymptotically stable systems can produce an unbounded trajectory when combined by means of a suitable switching law.

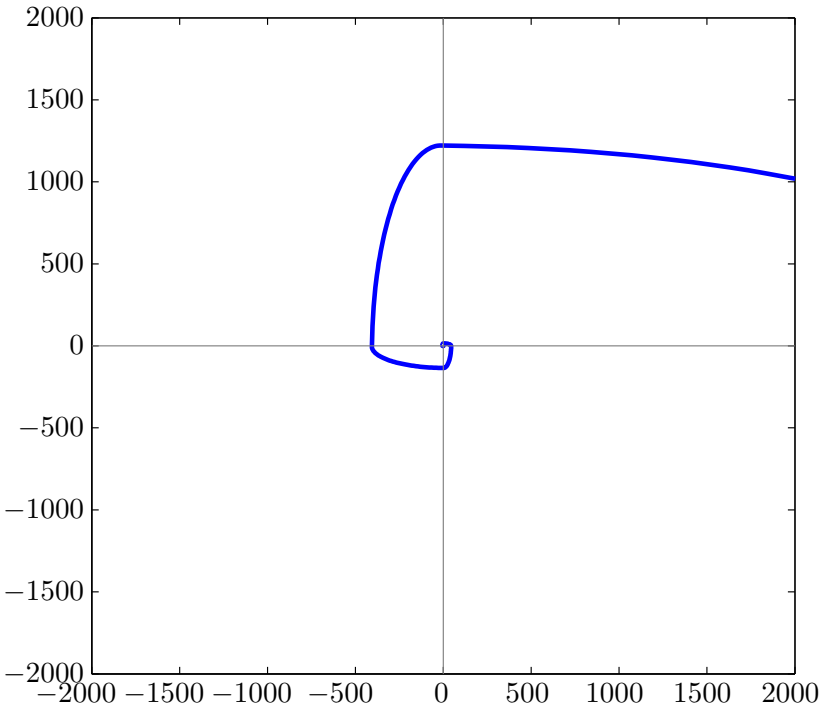

Figure A.1: State trajectory of Example 1.1

Example 1.1 (*Unstable trajectory of switched stable systems)*

$$\dot{x}(t) = A_{\sigma(t)}x(t) \qquad \textit{where } x(t) = \begin{pmatrix} x_1 \\ x_2 \end{pmatrix} \textit{ and } \sigma(t) \in \{1, 2\} \tag{A.6}$$

where

$$A_1 = \begin{pmatrix} -1 & 10 \\ -100 & -1 \end{pmatrix} \qquad A_2 = \begin{pmatrix} -1 & 100 \\ -10 & -1 \end{pmatrix} \qquad \sigma(t) = \begin{cases} 1 & \textit{when } x_1 x_2 \leqslant 0 \\ 2 & \textit{when } x_1 x_2 > 0 \end{cases}$$

The results on stability of switched systems may be classified depending on the nature of their switching function: completely known and periodic, completely known and a-periodic, arbitrary, with minimum dwell time and so on. In the following some of the more meaningful results on stability of switched systems will be illustrated maintaining this classification on their switching law.

A.2.1 Stability under known periodic switching

The early results on the stability of switched systems were obtained by Willems ([WILLEMS 1970]) in the ambit of switched periodic systems and then extended by Ezzine and Haddad ([EZZINE 1989]). Actually, the Willems theorem is a straightforward extension to switched systems of the well known condition on monodromy matrix used in periodic systems.

Theorem 1.2 (*Willems 1970, [*WILLEMS 1970*])* *Consider the periodic switching linear system described by the following equation.*

$$\begin{aligned} \dot{x}(t) &= F_{\sigma(t)}x(t) + G_{\sigma(t)}u(t) \qquad x(0) = x_0, \sigma(t) = \sigma(t+T) \\ y(t) &= H_{\sigma(t)}x(t) \end{aligned} \tag{A.7}$$

and denote with δt_i the time interval during which $\sigma(t) = i$ ($\sum_{i=1}^{N} \delta t_i = T$).

The null solution of (A.7) *is* uniformly asymptotically stable *if and only if the eigenvalues of the matrix*

$$\varphi(t_0 + T, t_0) = \prod_{i=N}^{1} \exp(F_i\, \delta t_i)$$

is Shur *(i.e. have all eigenvalues less than 1). It is unstable if at least one eigenvalue of this matrix has magnitude greater than 1.*

The necessary and sufficient condition found by Willems is not very useful when the target is to stabilize an unstable system since it does not depends directly on the stability parameters of the subsystems such as the eigenvalues.

For this reason, the extension of Ezzine and Haddad is preferable in stabilization problems, though it is only a sufficient condition.

Theorem 1.3 (*Ezzine and Haddad, [*EZZINE 1989*])* *The null solution of* (A.7) *is uniformly asymptotically stable if*

$$\sum_i \mu(F_i)\frac{\delta t_i}{T} < 0$$

where $\mu(F_i) = \max \lambda \left(\frac{F_i + F_i^T}{2}\right)$. The symbol $\lambda(A)$ denotes the spectrum of matrix A.

This sufficient condition exploits the *logarithmic norm* (or *measure of a matrix*) that was introduced in the Fifties separately by Lozinskij ([LOZINSKIJ 1958]) and Dahlquist ([DAHLQUIST 1959]).

Definition 1.4 *The* logarithmic norm *of a matrix A (*measure *of a matrix A) associated with*

the matrix norm $\|\cdot\|$ is defined by

$$\mu(A) = \lim_{\theta \to 0^+} \frac{\|I - \theta A\| - 1}{\theta}$$

In particular, when the associated norm is the euclidean one (2-norm), the logarithmic norm of matrix A becomes:

$$\mu_2(A) = \lim_{\theta \to 0^+} \frac{\|I - \theta A\|_2 - 1}{\theta} = \max \lambda \left(\frac{A + A^T}{2} \right)$$

It is important to note that, unlike theorem 1.2, theorem 1.3 does not rely on the periodicity of the system and therefore can be applied to general switched systems.

A.2.2 Stability under known switching

In the Twentieth century the Lyapunov theory has definitely been the most used technique to study the stability properties of dynamical systems. Anyway the sufficiency of Lyapunov criteria requires that, in order to demonstrate the stability of a system, a Lyapunov function for that system has to be found. In the case of switched systems the requirements on continuity and differentiability of the classical Lyapunov functions makes the research very difficult.

For this reason, since the end of the eighties, many authors ([PELETIES 1991], [WICKS 1994], [BRANICKY 1998], [YE 1998b], [WICKS 1998], [LIBERZON 1999a], [PETTERSSON 1996]) have extended the Lyapunov theory by using multiple Lyapunov-like functions concatenated together to produce a nontraditional (piecewise continuous and piecewise differentiable) Lyapunov function. The problem of finding the Lyapunov function in this way reduces to the research of a Lyapunov-like function for each subsystem and the check of some additional properties holding at the switching instants.

Since its advent the MLF technique has been the most used approach to study the stability of switched systems when the switching law is known. One of its more important features is that it can be used indifferently both for state-driven switching and for time-driven switching. Anyway in the case of time-driven switching, some authors ([CHENG 2004], [CHENG 2005]) recently returned to analyze the stability by using the properties of the norms and thus expanding the ideas of Ezzine and Haddad ([EZZINE 1989]).

In the following both the approaches will be presented.

Multiple Lyapunov Functions

From point of view of the switching law, the results that involves the so-called *Multiple Lyapunov Functions* do not assume the periodicity of switching function (as in theorem 1.2) but still postulate his perfect knowledge.

The systems that are considered in this approach are free nonlinear systems of the form

$$\dot{x}(t) = f_{\sigma(t)}x(t) \qquad x(0) = x_0 \tag{A.8}$$

where all the f_i are Lipschitz continuous mappings of $\mathbb{R}^n$ in $\mathbb{R}^n$. In this framework the switching law is usually represented as an *(anchored) switching sequence* Σ indexed by the initial state x_0.

$$\Sigma = \{x_0; (i_0, t_0), (i_1, t_1), \ldots, (i_k, t_k) \ldots\}, \qquad t_j \in \mathbb{R},\ i_j \in \mathcal{P} = \{1, 2, \ldots, N\} \tag{A.9}$$

Σ is such that $\sigma(t) = i_j$ for $t \in [t_j, t_{j+1}]$. The presence of initial state x_0 assures that the switching sequence can model both the case in which $\sigma(t)$ is a function of the time and the case in which $\sigma(t)$ is a function of the state.

Given a switching sequence Σ, the symbol $\Sigma|i = \left\{t_0^i, t_1^i, t_2^i, \ldots\right\}$ denotes the sequence of all the switching times in which the i-th subsystem is "turned on" or "turned off": the even terms of the sequence $(t_0^i, t_2^i, t_4^i, \ldots)$ represent the "switching on" instants and the odd terms $(t_1^i, t_3^i, t_5^i, \ldots)$ represent the "switching off" instants. Given a strictly increasing sequence of times $T = \{t_0, t_1, t_2, \ldots\}$, the *interval completion* of sequence T is defined as :

$$\mathcal{I}(T) = \bigcup_{j \in \mathbb{Z}^+} [t_{2j}, t_{2j+1}]$$

whilst the *even sequence* $\mathcal{E}(T)$ is the subsequence made up of all the even terms of T, $\mathcal{E}(T) = \{t_0, t_2, t_4, \ldots\}$. The solution of (A.8) corresponding to the switching sequence Σ will be denoted with the symbol $x_\Sigma(t)$.

The Multiple Lyapunov Functions approach is based upon the concept of *Lyapunov-like functions* ([PELETIES 1991], [BRANICKY 1994], [BRANICKY 1998]).

Definition 1.5 (*Lyapunov-like function*) *Given a sequence of strictly increasing times T in $\mathbb{R}$, a function $V(x) \in C^1[\mathbb{R}^n, \mathbb{R}^+]$ is called* Lyapunov-like *for trajectory $x(t)$ if:*

i. $\dot{V}\big(x(t)\big) \leqslant 0 \qquad$ *for* $t \in \mathcal{I}(T)$

ii. $V\big(x(t)\big)$ *is monotonically nonincreasing on* $\mathcal{E}(T)$

Remark The difference between a traditional Lyapunov function and a Lyapunov-like function is that, while a Lyapunov function is negative definite in the domain, a Lyapunov-like function may even be increasing outside $\mathcal{I}(T)$.

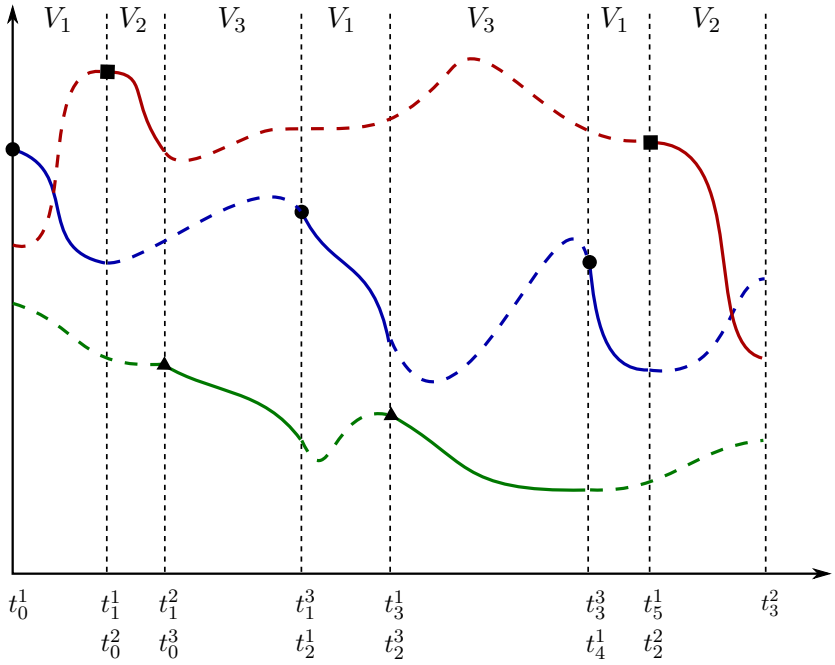

Figure A.2: Example of proposition 1.6. With respect to this particular switching law all the V_is are Lyapunov-like functions.

The concept of Lyapunov-like function is used by Branicky ([BRANICKY 1994], [BRANICKY 1998]) to demonstrate the following stability criterion.

Proposition 1.6 (*Branicky, [*BRANICKY 1994*])* *Consider a set of N positive definite functions V_i and a vector field $\dot{x}(t) = f_i x(t)$ such that $f_i(0) = 0$. Let $\mathcal{S}$ be the set of all the switching sequences associated with the system. If for each $\Sigma \in \mathcal{S}$ it holds that, for all i, V_i is a* Lyapunov-like function *for $x_\Sigma(t)$ over $\Sigma|i$, then the equilibrium $x = 0$ of the system* (A.8) *is* stable in the sense of Lyapunov.

Remark When the number of subsystems N is 1, the proposition 1.6 reduces to standard Lyapunov stability criterion.

In order to extend the Branicky's results, Hou, Michel and Ye introduced in the late nineties the concept *weak Lyapunov-like functions* ([HOU 1996], [YE 1998b]) in which the first property of Lyapunov-like functions is replaced by a less restrictive condition.

Definition 1.7 (*weak Lyapunov-like function*) *Given a sequence of strictly increasing times T in $\mathbb{R}$, a function $V(x) \in C^1\,[\mathbb{R}^n, \mathbb{R}^+]$ is called* weak Lyapunov-like *if:*

i. there exists an $h \in C(R^+, R^+)$ satisfying $h(0) = 0$ such that

$$V\big(x(t)\big) \leqslant h\Big(V\big(x(t_{2j})\big)\Big)$$

for all $t \in (t_{2j}, t_{2j+1})$ *and all* $j \in \mathbb{Z}^+$

ii. $V\big(x(t)\big)$ *is nonincreasing on* $\mathcal{E}(T)$

The sufficient condition of proposition 1.6 can be relaxed by requiring that the V_i are weak Lyapunov-like functions instead of Lyapunov-like functions.

Proposition 1.8 (*Hou-Michel-Ye, [*HOU 1996*])* *Consider a set of* V_i*s, a vector field* f_i *and a set* $\mathcal{S}$ *as in Proposition 1.6. If for each* $\Sigma \in \mathcal{S}$ *it holds that, for all* i, V_i *is a* weak Lyapunov-like function *for* $x_\Sigma(t)$ *over* $\Sigma|i$*, then the equilibrium* $x = 0$ *of the system* (A.8) *is* stable in the sense of Lyapunov.

Proposition 1.8 can be further extended by using multiple functions V_{ik} for each subsystem $\dot{x} = f_i x$ and by allowing that the condition $f_i(0) = 0$ does not hold only for all the vector fields f_i but only for a subset of f_i ([PETTERSSON 1996], [PETTERSSON 1997]).

In order to guarantee the *asymptotic stability* of the equilibrium point, Proposition 1.8 have to be enriched by a third condition thus obtaining the following proposition.

Proposition 1.9 (*Hou-Michel-Ye, [*HOU 1996*])* *If in addition to assumptions in Proposition 1.8, the following condition is satisfied for all the functions* V_i

$$\textit{iii. } DV_i\big(x(t^i_{2j})\big) \triangleq \frac{1}{t^i_{2j+2} - t^i_{2j}} \Big(V_i\big(x(t^i_{2j+2})\big) - V_i\big(x(t^i_{2j})\big) \Big) \leqslant -\varphi_i \left(\left\| x^i_{2j} \right\| \right)$$

for all $j \in \mathbb{Z}^+$, φ_i *of class* $\mathcal{K}$ *and where* $\Sigma|i = \{t^i_0, t^i_1, \ldots\}$*, then the equilibrium* $x = 0$ *of the system* (A.8) *is* asymptotically stable.

A different more restrictive condition for asymptotic stability can be found in [BRANICKY 1998] and [LIBERZON 1999a]: in that case the V_i are required to be decreasing in $\mathcal{I}(\Sigma_i)$ similarly to definition 1.5.

Stability analysis and stabilization of switched systems by using the properties of the norms

The recent results that exploits the properties of the norms and of the matrix exponentials are confined mainly to the world of linear switched systems with time-driven switching laws. Though their field of application is very small if compared to the Multiple Lyapunov Functions approach, these recent techniques are very important since they provide constructive methods for the stabilization both for systems with known switching functions and systems with dwell-time properties.

Consider the theorem 1.3. It is based on the so called *Coppel Inequality* ([COPPEL 1975, p. 41]).

Proposition 1.10 (*Coppel Inequality*) *Let $A(\cdot) : [t_0, +\infty) \to \mathbb{C}^{n\times n}$ be locally integrable. Then the solution of*

$$\dot{x}(t) = A(t)x(t) \qquad x(t_0) = x_0, \quad x_0 \in \mathbb{R}^n$$

satisfies the inequalities:

$$|x_0|\, e^{-\int_{t_0}^{t} \mu(-A(s))ds} \leqslant |x(t)| \leqslant |x_0|\, e^{\int_{t_0}^{t} \mu(A(s))ds} \tag{A.10}$$

where the symbol $\mu(A)$ represents the measure of matrix A, i.e.

$$\mu(A) = \lim_{\theta\to 0} \frac{\|I - \theta A\| - 1}{\theta} \tag{A.11}$$

The upper bound of the Coppel Inequality is very conservative and leads to conservative sufficient conditions (as, for example, theorem 1.3). If matrix A is Hurwitz and the system is *LTI*, the following upper bound on the transition matrix, which is well-known in System Theory can be exploited.

$$\left\|e^{At}\right\| \leqslant Me^{-\lambda t} \qquad \text{for some } \lambda > 0 \tag{A.12}$$

where $M = \|T_J\| \|T_J\|^{-1}$ and T_J is the matrix of generalized eigenvectors of A, i.e. $T_J^{-1}\Omega T_J = J$, where J is the Jordan canonical form of A.

By replacing the Coppel inequality with this bound in theorem 1.3, a novel sufficient condition for switched systems where all the subsystems are stable can be easily found.

The main work that has been done in the last years ([FANG 2002], [CHENG 2004], [CHENG 2005]) has been the estimation of the dependance of M from λ in presence of state feedback in order to obtain conditions for the stabilization. As it can be inferred from the references, the bound of equation A.12 is important both for known and for stochastic switching laws.

Proposition 1.11 (*Cheng et al., [CHENG 2004]*) *Consider two matrices $A \in \mathbb{R}^{n\times n}$ and $B \in \mathbb{R}^{n\times m}$ such that the pair (A, B) is controllable. Then for any $\lambda > 0$ there exist a matrix $K \in R^{m\times n}$ such that*

$$\left\|e^{(A+BK)t}\right\| \leqslant M\lambda^L e^{-\lambda t} \tag{A.13}$$

where $L = \frac{1}{2}(n-1)(n+2)$ and M is a constant that is independent from λ

The independence from λ is the key point for the stabilization. Roughly speaking since $\lim_{\lambda\to+\infty} M\lambda^L e^{-\lambda t} = 0$ for any L and M and being the pair (A, B) controllable, there certainly exists a matrix K for which the transition matrix between two switching instants is less than 1.

This is the rationale that is behind the following proposition that is included in this

section as a result deriving from 1.11 though it actually can be considered a result on systems with dwell-time (the frequency f is in certain way the reciprocal of dwell-time).

Proposition 1.12 *Consider the linear switching system of equation* (A.4)*. Let f the frequency of switching function $\sigma(t)$ defined as:*

$$f = \limsup_{t\to\infty} \frac{\{\textit{number of switches in [0,t]}\}}{t}$$

If all the pairs (F_i, G_i) is controllable then for a given positive number α, there exist a set of matrices $\{K_i : i = 1, \ldots, N\}$ such that for any frequency $f \leqslant \alpha$, the switched linear system (A.4) *is* exponentially stable *under the state feedback $u(t) = K_\sigma x(t)$.*

A.2.3 Stability of switched systems with dwell time

The results on stability that have been presented in the previous sections are based on the fundamental assumption of the perfect knowledge of the switching function $\sigma(t)$. However, in many applications the switching function is not a-priori known but there is rather a lower bound on the interval between two consecutive switchings which is usually called *dwell time* ([MORSE 1996], [HESPANHA 1999], [ZHAI 2000], [ISHII 2002], [DE PERSIS 2002], [MITRA 2004], [WIRTH 2005], [NI 2008]). Although the results about this class of systems are not directly used in the Switched Linear Internal Model control, the problem of the stabilization of the observer at first sight may look very similar especially to the case with stable and unstable sytems ([ZHAI 2000]). In order to emphasize the difference, a brief overview of the results on stability with dwell time will be provided in the following.

Consider a free switched linear system

$$\dot{x}(t) = A_{\sigma(t)} x(t) \tag{A.14}$$

where all the matrices A_i have negative eigenvalues. From standard results it follows that, for all i, there exist two positive numbers α_i and β_i such that:

$$\left| e^{A_i t} \right| \leqslant e^{\alpha_i - \beta_i t}$$

Let τ_D be a positive number satisfying

$$\tau_D > \sup_{i\in\mathcal{P}} \left\{ \frac{\alpha_i}{\beta_i} \right\}$$

and consider the set $\mathcal{S}[\tau_D]$ of all the switching functions with interval between consecutive discontinuities no smaller than τ_D (*dwell time*).

Proposition 1.13 (*Morse, [*MORSE 1996*])* *For any $\sigma(t) \in \mathcal{S}[\tau_D]$ the system* (A.14) *is* exponentially stable *with a decay rate β no larger than the decay rates β_i.*

In recent years the concept of *dwell time* has been losing popularity in favour of the less restrictive concept of *average dwell time* introduced by Hespanha and Morse ([HESPANHA 1999]). For each switching signal $\sigma(t)$ and each $t \geqslant \tau \geqslant 0$, let $N_\sigma(t, \tau)$ denote the number of switchings occurred in the open time interval (τ, t). For given N_0, $\tau_D > 0$, the symbol $\mathcal{S}_{ave}[\tau_D, N_0]$ denote the set of all the switching functions for which

$$N_\sigma(t, \tau) \geqslant N_0 + \frac{t - \tau}{\tau_D}$$

The constant τ_D is called the *average dwell time* and N_0 the *chatter bound*.

For the systems with average dwell time the proposition 1.13 can be extended in the following way.

Proposition 1.14 (*Hespanha-Morse, [*HESPANHA 1999*])* *If there exists a positive constant β_0 such that, for all $i \in \mathcal{P}$, the matrix $A_i + \beta_0 I$ is Hurwitz then for any $\beta \in [0, \beta_0)$ there exists a finite constant τ_D^* such that the system* (A.14) *is* exponentially stable *over $\sigma(t) \in \mathcal{S}_{ave}[\tau_D, N_0]$, with stability margin β, for any average dwell time $\tau_D \geqslant \tau_D^*$ and any chatter bound $N_0 > 0$.*

In the last decade, this result has been extended for example to nonlinear systems (the same [HESPANHA 1999] or [DE PERSIS 2002]) and to systems with stable and unstable subsystems ([HU 1999], [ZHAI 2000]) In the latter case the main idea to achieve the stability in the latter case is to require that the stable subsystems stay active longer than unstable ones. The ratio between "total activation time" of stable systems and "total activation time" of unstable systems depends on the exponential growth rates and decay rates of the subsystems.

A.3 Observers of Switched Systems

Besides the results on stability, another important thread that has been developed in the world of switched systems is that of the observers of the state. The first studies in this field me be considered those of Ackerson and Fu ([ACKERSON 1970]) that extended the work of Kalman to obtain an optimal observer for Markov Jumping discrete systems. Anyway, as well as for the other topics in switched systems, it was the last decade that the growing interest in this class of systems impressed a considerable acceleration in the research of general results both for linear and nonlinear systems.

Similarly to what happens for the stability, the contributions on the observers can be classified depending on the knowledge of the switching function: a-priori known, available for feedback, to be estimated as well as the continuous state.

In the current formulation of the SLIM approach the switching law is assumed to be a-priori known. The removal of this assumption by using the results on discrete state estimation will probably be one of the first improvements that will be implemented.

The more common approach that is used for the observers for switched systems is to design an asymptotic observer for each subsystem and then use the switching law of the system (that is either available for feedback or estimated by another observer) to select the observer of the active subsystem. Taking inspiration from the classical Luenberger results, the switched observer for the linear system of eq. (A.4) has the following structure.

$$\dot{\hat{x}}(t) = A_{\sigma(t)}\hat{w}(t) - L_{\sigma(t)}(y(t) - C_{\sigma(t)}\hat{x}(t)) \qquad \hat{x}(0) = \hat{x}_0 \tag{A.15}$$

Systems where the switching function is available for feedback

This observer structure is used for example in [CHEN 2004]. By introducing a dwell time condition on the switching function, the global asymptotic stability is guaranteed. In order to have the global exponential stability, a condition on the A_is similar to that of Theorem 1.3 is presented. Moreover additional conditions to guarantee the convergence when using a reduced observer or under arbitrary switching are provided.

The results about arbitrary switching, similarly to what happens in stability theory, is confined to switching signals having a finite number of switchings in finite time. In more recent papers ([CHAIB 2006]) this assumption is removed and observers for switched systems with sliding modes or zeno behaviors are considered.

Systems where the switching function has to be estimated

In the field of observers where the switching function is not available but has to be estimated, a fundamental work is represented by [BALLUCHI 2002]. The discrete state is estimated by using a *signatures generator* as in Fault Detection: a set of N Luenberger observers (one for each subsystem) working at the same time is considered and the discrete state is evaluated by comparing the norm of estimation errors with predetermined thresholds. The estimation of the value of $\sigma(t)$ is then used for selecting the right observer as in [CHEN 2004]. Similar conditions for the convergence are provided but, in this case, only practical convergence can be guaranteed due to the delay that is inherently introduced by the discrete state observer.

A common requirement to all the contributions that has been cited is that all the subsystems has to be at least detectable (in some cases the complete observability is required). Therefore, to the best of the author's knowledge, the asymptotic observer that is presented in chapter 2 is the first example of an asymptotic switched observer where this hypothesis is removed.

Bibliography

Switched Linear Internal Model Control

[ROSSI 2008a] C. ROSSI, A. TILLI, AND M. TONIATO. Asymptotic tracking of non-sinusoidal periodic references: a switched linear internal model approach. In *Proc. of 17th IFAC World Congress, July 6-11 2008*, p. 3895–3900, Seoul, South Korea, July 2008.

[ROSSI 2008b] C. ROSSI, A. TILLI, AND M. TONIATO. On the sensitivity of a switched linear internal model controller. In *Proc. 16th Mediterranean Conf. on Control & Automation, MED'08, June 23-25 2008*, p. 113–118, Ajaccio, France, June 2008.

[ROSSI 2009a] C. ROSSI, A. TILLI, AND M. TONIATO. Finite-time observers for a class of periodic switched linear systems, 2009. Submitted to the *48th IEEE CDC'09*, Shanghai, China, 16-18 December 2009.

[ROSSI 2009b] C. ROSSI, A. TILLI, AND M. TONIATO. A preliminary step towards the switched linear internal model control: the asymptotic observer problem, 2009. To be presented at the *10th ECC'09*, Budapest, Hungary, 23-26 August 2009.

Books on linear and non linear system theory

[BASILE 1992] G. BASILE AND G. MARRO. *Controlled and Conditioned Invariants in Linear System Theory*. Prentice Hall, 1992.

[COPPEL 1975] W. COPPEL. *Stability and Asymptotic Behavior of Differential Equations*. Heath, Boston, MA, 1975.

[GOODWIN 2000] G. C. GOODWIN, S. GREABE, AND M. SALGADO. *Control System Design*. Prentice Hall, 2000.

[ISIDORI 1995] A. ISIDORI. *Nonlinear Control Systems*. Springer Verlag, London, 3rd edition edition, 1995.

[KHALIL 2001] H. K. KHALIL. *Nonlinear Systems*. Prentice Hall, 2001.

[WILLEMS 1970] J. L. WILLEMS. *Stability Theory of Dynamical Systems*. Wiley Interscience Division, 1970.

Books on Switched Systems

[BOUKAS 2005] E.-K. BOUKAS. *Stochastic Switching Systems. Analysis and Design*. Birkhuser, 2005.

[FILIPPOV 1988] A. F. FILIPPOV. *Differential Equations with Discontinuous Righthand Sides*, vol. 18 of *Mathematics and Its Applications*. Kluwer Academic Publishers, Dordrecht, The Netherlands, 1988.

[LI 2005] Z. LI, Y. SOH, AND C. WEN. *Switched and Impulsive Systems. Analysis, Design and Applications*, vol. 313 of *Lecture Notes in Control and Information Sciences*. Springer, 2005.

[LIBERZON 2003] D. LIBERZON. *Switching in Systems and Control*. Birkhuser, Berlin, Germany, 2003.

[SUN 2005] Z. SUN AND S. S. GE. *Switched Linear Systems: Control and Design*. Springer, 2005.

[UTKIN 1992] V. I. UTKIN. *Sliding Modes in Control and Optimization*. Springer-Verlag, 1992.

Stability of Switched Systems

[BRANICKY 1994] M. BRANICKY. Stability of switched and hybrid systems. In *Proc. 33rd IEEE CDC'94, December 14-16, 1994*, vol. 4, p. 3498–3503, Lake Buena Vista, FL, USA, 14-16 Dec. 1994.

[BRANICKY 1998] M. BRANICKY. Multiple Lyapunov functions and other analysis tools for switched and hybrid systems. *IEEE Trans. Automat. Contr.*, vol. 43(4), p. 475–482, April 1998.

[CHENG 2004] D. CHENG, L. GUO, Y. LIN, AND Y. WANG. A note on overshoot estimation in pole placements. *Journal of Control Theory and Applications*, vol. 2(2), p. 161–164, 2004.

[CHENG 2005] D. CHENG, L. GUO, Y. LIN, AND Y. WANG. Stabilization of switched linear systems. *IEEE Trans. Automat. Contr.*, vol. 50(5), p. 661–666, 2005.

[DE PERSIS 2002] C. DE PERSIS, R. DE SANTIS, AND A. MORSE. Nonlinear switched systems with state dependent dwell-time. In *Proc. 41st IEEE CDC'02, December 10-13, 2002*, vol. 4, p. 4419–4424 vol.4, Las Vegas, NV, USA, Dec. 2002.

[FANG 2002] Y. FANG AND K. LOPARO. Stabilization of continuous-time jump linear systems. *IEEE Trans. Automat. Contr.*, vol. 47(10), p. 1590–1603, Oct. 2002.

[GOEBEL 2006] R. GOEBEL AND A. R. TEEL. Solutions to hybrid inclusions via set and graphical convergence with stability theory applications. *Automatica*, vol. 42(4), p. 573–587, 2006.

[GU 2009] Z.-Q. GU, H.-P. LIU, AND F.-C. LIAO. A Common Lyapunov Function for a Class of Switched Descriptor Systems. In *Proc. International Asia Conference on Informatics in Control, Automation and Robotics CAR '09*, p. 29–31, 2009.

[HESPANHA 1999] J. P. HESPANHA AND A. S. MORSE. Stability of switched systems with average dwell-time. In *Proc. 38th IEEE CDC'99, December 7-10 1999*, vol. 3, p. 2655–2660, Phoenix, AZ, USA, 7–10 Dec. 1999.

[HOU 1996] L. HOU, A. MICHEL, AND H. YE. Stability analysis of switched systems. In *Proc. 35th IEEE CDC'96, December 11-13, 1996*, vol. 2, p. 1208–1212, Kobe, Japan, 11-13 Dec. 1996.

[HU 1999] B. HU, X. XU, A. N. MICHEL, AND P. J. ANTSAKLIS. Stability analysis for a class of nonlinear switched systems. In *Proc. 38th IEEE CDC'99, December 7-10 1999*, vol. 5, p. 4374–4379, Phoenix, AZ, USA, 7–10 Dec. 1999.

[ISHII 2002] H. ISHII AND B. FRANCIS. Stabilizing a linear system by switching control with dwell time. *IEEE Trans. Automat. Contr.*, vol. 47(12), p. 1962–1973, Dec 2002.

[LIBERZON 1999a] D. LIBERZON AND A. MORSE. Basic problems in stability and design of switched systems. *IEEE Control Systems Magazine*, vol. 19(5), p. 59–70, Oct. 1999.

[MITRA 2004] S. MITRA AND D. LIBERZON. Stability of hybrid automata with average dwell time: an invariant approach. In *Proc. 43rd IEEE CDC'04, December 14-17, 2004*, vol. 2, p. 1394–1399 Vol.2, Paradise Island, Bahamas, Dec. 14-17 2004.

[MORSE 1996] A. S. MORSE. Supervisory control of families of linear set-point controllers Part I. Exact matching. *IEEE Trans. Automat. Contr.*, vol. 41(10), p. 1413–1431, Oct. 1996.

[NI 2008] W. NI, D. CHENG, AND X. HU. Minimum dwell time for stability and stabilization of switched linear systems. In *Proc. 7th World Congress on Intelligent Control and Automation WCICA 2008*, p. 4109–4115, 25–27 June 2008.

[PELETIES 1991] P. PELETIES AND R. A. DECARLO. Asymptotic stability of m-switched systems using lyapunov-like functions. In *Proc. of the American Control Conference, 1991*, p. 1679 – 84, Boston, MA, USA, 1991.

[PETTERSSON 1996] S. PETTERSSON AND B. LENNARTSON. Stability and robustness for hybrid systems. In *Proc. 35th IEEE CDC'96, December 11-13, 1996*, vol. 2, p. 1202–1207, Kobe, Japan, 11-13 Dec. 1996.

[PETTERSSON 1997] S. PETTERSSON AND B. LENNARTSON. Controller Design of Hybrid Systems. In *HART'97, March 26-28, 1997*, vol. 1201 of *Lecture Notes in Computer Science*, p. 240–254, Grenoble, France, Mar 1997.

[WICKS 1994] M. A. WICKS, P. PELETIES, AND R. A. DECARLO. Construction of piecewise Lyapunov functions for stabilizing switched systems. In *Proc. 33rd IEEE CDC'94, December 14-16, 1994*, vol. 4, p. 3492–3497, Lake Buena Vista, FL, USA, 14-16 Dec. 1994.

[WICKS 1998] M. A. WICKS, P. PELETIES, AND R. A. DECARLO. Switched controller synthesis for the quadratic stabilization of a pair of unstable linear systems. *Eur. J. Contr.,*, vol. 4p. 140–147, 1998.

[WIRTH 2005] F. WIRTH. A converse lyapunov theorem for switched linear systems with dwell times. In *Proc. 44th IEEE CDC-ECC '05, December 12-15, 2005*, p. 4572–4577, Dec. 2005.

[XIE 2006] G. XIE AND L. WANG. Stability and stabilization of switched impulsive systems. In *Proc. of the American Control Conference, 2006*, p. 6pp., 14-16 June 2006.

[YE 1998a] H. YE, A. MICHEL, AND L. HOU. Stability analysis of systems with impulse effects. *IEEE Trans. Automat. Contr.*, vol. 43(12), p. 1719–1723, Dec 1998.

[YE 1998b] H. YE, A. MICHEL, AND L. HOU. Stability theory for hybrid dynamical systems. *IEEE Trans. Automat. Contr.*, vol. 43(4), p. 461–474, April 1998.

[ZHAI 2000] G. ZHAI, B. HU, K. YASUDA, AND A. MICHEL. Stability analysis of switched systems with stable and unstable subsystems: an average dwell time approach. In *Proc. of the American Control Conference, 2000*, vol. 1(6), p. 200–204, Chicago, IL, USA, 28-30 June 2000.

Observers of Switched Systems

[ACKERSON 1970] G. ACKERSON AND K. FU. On state estimation in switching environments. *IEEE Trans. Automat. Contr.*, vol. 15(1), p. 10–17, Feb 1970.

[BALLUCHI 2002] A. BALLUCHI, L. BENVENUTI, M. D. D. BENEDETTO, AND A. L. SANGIOVANNI-VINCENTELLI. Design of Observers for Hybrid Systems. In *Proc. of the 5th Int. Workshop on Hybrid Systems: Computation and Control, HSCC 2002*, p. 76–89, Stanford, CA, USA, 25-27 March 2002.

[CHAIB 2006] S. CHAIB, D. BOUTAT, A. BENALI, J.-C. GUILLOT, AND J.-P. BARBOT. Observer Design for Linear Switched Systems : a Common Lyapunov Function Approach. In *Proc. IEEE International Conference on Control Applications CCA '06*, p. 361–366, 2006.

[CHEN 2004] W. CHEN AND S. MEHRDAD. Observer design for linear switched control systems. In *Proc. American Control Conference 2004*, vol. 6, p. 5796–5801 vol.6, 2004.

[EZZINE 1989] J. EZZINE AND A. HADDAD. Controllability and observability of hybrid systems. *Intern. Journal of Control*, vol. 49(6), p. 2045 – 2055, 1989.

Finite Time Observers

[DRAKUNOV 1995] S. DRAKUNOV AND V. UTKIN. Sliding mode observers. tutorial. In *Proc. 34th IEEE Conference on Decision and Control*, vol. 4, p. 3376–3378, 13–15 Dec. 1995.

[ENGEL 2002] R. ENGEL AND G. KREISSELMEIER. A continuous-time observer which converges in finite time. *IEEE Trans. Automat. Contr.*, vol. 47(7), p. 1202–1204, Jul 2002.

[HASKARA 1998] I. HASKARA, U. OZGUNER, AND V. UTKIN. On sliding mode observers via equivalent control approach. *International Journal of Control*, vol. 71(6), p. 1051 – 67, 1998.

[JAMES 1991] M. R. JAMES. Finite time observer design by probabilistic-variational methods. *SIAM Journal on Control and Optimization*, vol. 29(4), p. 954 – 967, 1991.

[MENOLD 2003] P. H. MENOLD, R. FINDEISEN, AND F. ALLGÖWER. Finite time convergent observers for nonlinear systems. In *Proc. 42nd IEEE Conference on Decision and Control*, vol. 6, p. 5673–5678, 9–12 Dec. 2003.

[MICHALSKA 1995] H. MICHALSKA AND D. MAYNE. Moving horizon observers and observer-based control. *IEEE Transactions on Automatic Control*, vol. 40(6), p. 995 – 1006, 1995.

[RAFF 2007a] T. RAFF AND F. ALLGÖWER. An impulsive observer that estimates the exact state of a linear continuous-time system in predetermined finite time. In *Proc. Mediterranean Conf. on Control & Automation MED '07*, p. 1–3, 27–29 June 2007.

[ZIMMER 1994] G. ZIMMER. State observation by on-line minimization. *International Journal of Control*, vol. 60(4), p. 595 – 606, Oct 1994.

Repetitive Learning Control

[CUIYAN 2004b] L. CUIYAN, Z. DONGCHUN, AND Z. XIANYI. Theory and applications of the repetitive control. In *Proc. SICE 2004 Annual Conference*, vol. 1, p. 27–34 vol. 1, 2004.

[HARA 1988] S. HARA, Y. YAMAMOTO, T. OMATA, AND M. NAKANO. Repetitive Control System: a New Type Servo System for Periodic Exogenous Signals. *IEEE Trans. Automat. Contr.*, vol. 33(7), p. 659–668, 1988.

Output Regulation

[BYRNES 2004] C. I. BYRNES AND A. ISIDORI. Nonlinear internal models for output regulation. *IEEE Trans. Automat. Contr.*, vol. 49(12), p. 2244–2247, Dec. 2004.

[BYRNES 2005] C. I. BYRNES, A. ISIDORI, L. MARCONI, AND L. PRALY. Nonlinear Output Regulation Without Immersion. In *Proc. 44th IEEE CDC'05 and ECC'05, December 12-15, 2005*, p. 3315–3320, Seville, Spain, Dec 2005.

[DAVISON 1976] E. DAVISON. The robust control of a servomechanism problem for linear time-invariant multivariable systems. *IEEE Trans. Automat. Contr.*, vol. 21(1), p. 25–34, Feb 1976.

[DEVASIA 1997] S. DEVASIA, B. PADEN, AND C. ROSSI. Exact-output tracking theory for systems with parameter jumps. *International Journal of Control*, vol. 67(1), p. 117–131, 1997.

[FRANCIS 1975] B. A. FRANCIS AND W. M. WONHAM. The internal model principle for linear multivariable regulators. *J. Appl. Math. Optimization*, vol. 2(2), p. 170–194, 1975.

[FRANCIS 1977] B. A. FRANCIS. The linear multivariable regulator problem. *SIAM J. Control*, vol. 15(3), p. 486–505, 1977.

[ISIDORI 1990] A. ISIDORI AND C. I. BYRNES. Output regulation of nonlinear systems. *IEEE Trans. Automat. Contr.*, vol. 35(2), p. 131–140, Feb. 1990.

[ISIDORI 2003] A. ISIDORI, L. MARCONI, AND A. SERRANI. *Robust Autonomous Guidance. An Internal Model Approach*. Advances in Industrial Control. Springer Verlag, London, 2003.

[MARCONI 2008] L. MARCONI AND R. NALDI. Aggressive control of helicopters in presence of parametric and dynamical uncertainties. *Mechatronics*, vol. 18(7), p. 381 – 389, 2008.

[SERRANI 2001] A. SERRANI, A. ISIDORI, AND L. MARCONI. Semi-global nonlinear output regulation with adaptive internal model. *IEEE Trans. Automat. Contr.*, vol. 46(8), p. 1178–1194, Aug. 2001.

[ZHANG 2006] Z. ZHANG AND A. SERRANI. The linear periodic output regulation problem. *Systems & Control Letters*, vol. 55(7), p. 518 – 529, 2006.

[ZHANG 2009] Z. ZHANG AND A. SERRANI. Adaptive robust output regulation of uncertain linear periodic systems. *IEEE Trans. Automat. Contr.*, vol. 54(2), p. 266–278, Feb. 2009.

General Power Supplies

[BELLOMO 2004] P. BELLOMO AND A. DE LIRA. SPEAR3 Intermediate DC Magnet Power Supplies. In *Proc. 9th European Particle Accelerator Coonference EPAC, 5-9 July 2004*, p. 1798–1800, Lucerne, July 2004.

[BURKMANN 1998] K. BURKMANN, G. SCHINDHELM, AND T. SCHEEGANS. Performance of the White Circuits of the BESSY II Booster Synchrotron. In *Proc. 6th European Particle Accelerator Coonference EPAC, 22-26 June 1998*, p. 2062–2064, Stockholm, Sweden, June 1998.

[GRIFFITHS 2002] S. GRIFFITHS, G. CHARNLEY, N. MARKS, AND J. THEED. A Power Converter Overview for the DIAMOND Storage Ring Magnets. In *Proc. 8th European Particle Accelerator Coonference EPAC, 3-7 June 2002*, p. 2472–2474, Paris, June 2002.

[HETTEL 1991] R. HETTEL, R. AVERILL, M. BALTAY, S. BRENNAN, C. HARRIS, M. HORTON, C. JACH, J. SEBEK, AND J. VOSS. The 10Hz Resonant Magnet Power Supply for SSRL 3GeV Injector. In *Proc. IEEE Particle Accelerator Coonference PAC, 10-14 June 1991*, p. 926–928, San Francisco, May 1991.

[IRMINGER 1998] G. IRMINGER, M. HORVAT, F. JENNI, AND H. BOKSBERGER. A 3Hz, 1MWpeak Bending Magnet Power Supply for the Swiss Light Source (SLS). Paul Scherrer Institut, nov 1998.

[JENNI 1999] F. JENNI, H. BOKSBERGER, AND G. IRMINGER. DC-Link Control for a 1MVA-3Hz Single Phase Power Supply. In *Proc. 30th Annual IEEE Power Electronics Specialists Conference, PESC 99., 27 June - 1 July 1999*, vol. 2, p. 1172–1176, Charleston, July 1999.

[JENNI 2002] F. JENNI, L. TANNER, AND M. HORVAT. A Novel Control Concept for Highest Precision Accelerator Power Supplies. In *Proc. 10th International POWER ELECTRONICS and MOTION CONTROL Conference EPE-PEMC, 9-11 September*, Cavtat & Dubrovnik, September 2002.

[KING 1999] Q. KING, I. BARNETT, D. HUNDZINGER, AND J. PETT. Developments in the High Precision Control of Magnet Currents for LHC. In *Proc. IEEE Particle Accelerator Coonference PAC, 29 March - 2 April 1999*, p. 3743–3745, New York, April 1999.

[MARKS 1996] N. MARKS AND D. POOLE. The Choice of Power Converter Systems for a 3GeV Booster Synchrotron. In *Proc. 5th European Particle Accelerator Coonference EPAC, 10-14 June 1996*, p. 2331–2333, Sitges, Spain, June 1996.

[PETT 1996] J. PETT, I. BARNETT, G. FERNQVIST, D. HUNDZINGER, AND J.-C. PERREARD. A Strategy for Controlling the LHC Magnet Currents. In *Proc. 5th European Particle Accelerator Coonference EPAC, 10-14 June 1996*, p. 2317–2319, Sitges, Spain, June 1996.

[U-97] U-97. Modelling, analysis and compensation of the current-mode converter.

Power Supplies for Synchrotrons

[CAN] The CANDLE web site. `http://www.candle.am/~TDA/`.

[CARROZZA 2006] S. CARROZZA, F. BURINI, ET AL. CNAO storage ring dipole magnet power converter 3000A / ± 1600V. In *Proc. 10th European Particle Accelerator Conference EPAC, 26-30 June 2006*, p. 2673–2675, Edinburgh, UK, Jun 2006.

[DIA] The DIAMOND web site. `http://www.diamond.ac.uk/`.

[DOBBING 2006] J. A. DOBBING, C. A. ABRAHAM, R. J. RUSHTON, F. CAGNOLATI, M. P. C. PRETELLI, L. SITA, G. FACCHINI, AND C. ROSSI. Diamond

booster magnet power converters. In *Proc. 10th European Particle Accelerator Conference EPAC, 26-30 June 2006*, p. 2664–2666, Edinburgh, UK, June 2006.

Current Sharing

[CHANG 1995] C. CHANG. Current ripple bounds in interleaved dc-dc power converters. In *Proc. International Conference on Power Electronics and Drive Systems, 21-24 Feb. 1995*, vol. 2, p. 738–743, 1995.

Other

[DAHLQUIST 1959] G. DAHLQUIST. *Stability and error bounds in the numerical integration of ordinary differential equations*, vol. 130. Trans. of the Royal Institute of Technology, 1959.

[FAHMY 1982] M. FAHMY AND J. O'REILLY. On eigenstructure assignment in linear multivariable systems. *IEEE Trans. Automat. Contr.*, vol. 27(3), p. 690–693, 1982.

[GUGGENHEIMER 1995] H. W. GUGGENHEIMER, A. S. EDELMAN, AND C. R. JOHNSON. A Simple Estimate of the Condition Number of a Linear System. *The College Mathematics Journal*, vol. 26p. 2–5, Jan. 1995.

[LOZINSKIJ 1958] S. M. LOZINSKIJ. Error estimate for numerical integration of ordinary differential equations, part i. *Izvestiya Vysshikh Uchebnykh Zavedenii. Matematika*, vol. 6p. 52–90, 1958. (in Russian).

Alla fine di questi tre anni di dottorato presso l'Università di Bologna mi guardo indietro e mi rendo conto di quante persone abbiano contribuito a far sì che questa esperienza diventasse una parte fondamentale della mia vita.

Innanzitutto voglio ringraziare le due persone che mi hanno accompagnato più da vicino in questi tre anni: Silvia *e* Luca. *Silvia mi è stata accanto fin dall'inizio di questa esperienza: il suo appoggio e la sua disponibilità ad ascoltarmi sono stati un filo conduttore di questo periodo in "trasferta" soprattutto nei momenti difficili. Mio fratello Luca mi ha ospitato e soppportato per tutto questo periodo: la sua generosità va di pari passo con le sue capacità in cucina. Insieme a loro voglio ringraziare anche il resto della mia* famiglia, *e in particolar modo i miei genitori, che non mi hanno mai fatto mancare il loro supporto malgrado mi vedessero solo nei fine settimana.*

Se ormai posso considerare Bologna una mia seconda casa è anche grazie a Susi, Stefania, Elisabetta *e* Gianna *che fin dai primi giorni hanno contribuito a farmi vivere un'atmosfera familiare.*

Gran parte del lavoro di questa tesi ha visto la luce grazie alle indicazioni e ai preziosi consigli del prof. Carlo Rossi *e dell'ing.* Andrea Tilli. *A loro va il mio più grande ringraziamento per avermi guidato in tematiche che per me erano del tutto nuove come i sistemi ibridi e l'elettronica di potenza. Inoltre voglio ringraziare anche il prof.* Patrizio Colaneri *del Politecnico di Milano per la sua disponibilità e per il suo aiuto che si è rivelato fondamentale.*

Poi vorrei ringraziare tutte le persone che in questi tre anni ho potuto conoscere al CASY e al DEIS. Prima di tutto Fabio Ronchi *che mi ha aiutato ad inserirmi velocemente in un progetto già avviato come CNAO e* Manuel Spera, *il cui contributo in gran parte del lavoro nell'ambito dell'elettronica di potenza è stato fondamentale; poi* Roberto Naldi, Riccardo Falconi, Gianluca Lucente, Andrea Paoli, Luca Gentili, Matteo Sartini, Gianni Borghesan, Andrea Pagani, Davide Samorì, Giovanni Cignali, Marcello Montanari, Alessandro Macchelli, Raffaella Carloni, Alberto Ghirotti, Lorenzo Marconi *e* Anna Scuncio. *La loro accoglienza e la loro amicizia dimostrata fin da subito sono state una componente fondamentale della mia esperienza bolognese.*

Padova, 16 Marzo 2009 *Manuel Toniato*